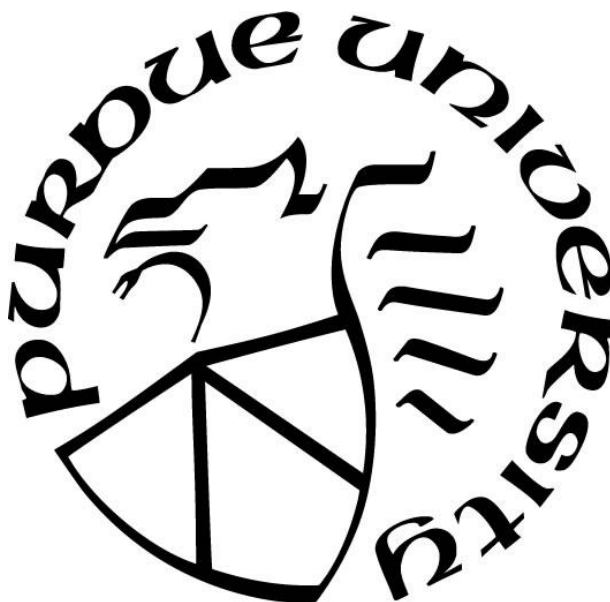# THE DESIGN, SYNTHESIS, AND APPLICATION OF A REFINED PHOTO-SWITCHABLE CYCLIC PEPTIDE SCAFFOLD FOR BETA-TURN MANIPULATION

by

Corey Johnson

A Dissertation

Submitted to the Faculty of Purdue University

In Partial Fulfillment of the Requirements for the degree of

Doctor of Philosophy

Department of Chemistry

West Lafayette, Indiana

May 2023

THE PURDUE UNIVERSITY GRADUATE SCHOOL
STATEMENT OF COMMITTEE APPROVAL

Dr. Jean Chmielewski, Chair

Department of Chemistry

Dr. Christine Hyrcyna

Department of Chemistry

Dr. Abram, Axelrod

Department of Chemistry

Dr. Chengde Mao

Department of Chemistry

Approved by:

Dr. Christine Hyrcyna

Dedicated to Family and Friends

ACKNOWLEDGMENTS

I am also thankful to my undergraduate advisor for pushing me to go to grad school and not settling for a masters. While I questioned that decision the whole time in graduate school I am glad that it was a choice I ultimately took. I would also like to thank all of my professors from undergrad for giving me opportunities to express myself and figure out who I am now as a person.

I would like to thank my girlfriend Brianne Nunez for always being a supportive voice in my life and always looking out for my best interest. Your bubbly personality and your soft-heartedness make going through tough situations a lot easier. Thank you for always being available for all my problems no matter how small. I look forward to our life together post graduate school. I would also like to give a huge thanks to my cats Malachi and Wednesday. I am very fortunate to come home to two troublesome but loving pets that always want to greet me when I come back and lay with me when I'm tired or down. These two have been one of the biggest reasons I've made it this far in grad school. Finally, I would like to give massive thanks to Jay at Fiesta for always providing good food at an affordable price and being so welcoming and thoughtful to even remember my order. You will be truly missed when I leave, and I wish you nothing but the best.

TABLE OF CONTENTS

LIST OF TABLES

LIST OF FIGURES

ABSTRACT

The concept of manipulating secondary structure has been a powerful method to alter chemical processes and interactions. One of the most recent avenues used in achieving this goal is the field of photopharmacology. The use of light to activate and control chemical processes has been extensively studied for this purpose. It was proposed in Chmielewski group that a cyclic peptide containing a azobenzene-like amino acid could be used to modulate a peptide conformation, into a β-turn. This first-generation macrocycle, FLAp, consisting of four alanine residues split by the azobenzene amino acid and a test β-turn sequence (Asn-Pro-Gly-Gly) showed type II β-turn conformation in the cis form, but no turn in the trans. This result, although promising, showed only a two-fold difference in inhibition of somatostatin receptor when using the somatostatin β-turn sequence (Phe-Trp-Lys-Thr). This small difference in activity was attributed to the flexibility of the macrocycle in the two conformations.

Efforts have been made to create a better, more rigid scaffold than that used with FLAp to allow for improved differences between the two conformations of the azobenzene. The FLAp cyclic peptide was altered by only having one alanine residue on either side of the azobenzene to create TAp, for increased rigidity. A second peptide, TApβ, was synthesized using β-alanine residues in place of alanine, for added flexibility within the peptide. The TAp and TApβ peptides were shown to possess type II and type II' β-turn properties respectively, supported by 2D NOESY NMR and restrained molecular dynamics. The trans isomer of TAp, however showed a kink in the peptide backbone, while the TApβ peptide showed a linear backbone with no kink.

With the scaffold of TApβ shown to be optimum for structural distinction between the cis and trans conformations. This sequence was carried forward for biological testing. As a proof of concept, the β-turn of tendamistat (Ser-Trp-Arg-Tyr) was chosen, for its hydrophilicity and its target α-amylase. The resulting peptide tendamistat β (TSβ) was synthesized and compared against its linear form (L-TSβ), as well as a literature control (Bartlett control). The cis conformation of the cyclic peptide TSβ showed lesser activity than its trans counterpart, as well as its linear cis and trans counterpart, against α-amylase. Due to unexpected results it was deemed that tendamistat was not suitable for use within the TApβ scaffold because of conformational restriction of the tendamistat sequence. This may be due to the type I β-turn of tendamistat where Tapβ induces type II' β-turn formation.

CHAPTER 1.   INTRODUCTION

1.1   Azobenzenes and their significance

Since their initial synthesis in the late 1800's and the discovery of their isomerization capabilities in 1937 by Hartley, the azobenzene moiety has been a staple in photopharmocolgy.[1–3] Azobenzenes exist as the trans isomer which can be photolyzed using ultraviolet (UV) light (~365 nm) to the less stable cis isomer. The cis isomer can be transitioned back to the more stable trans isomer using visible wavelength light (~420 nm) or heat (Figure 1.1).[2] Azobenzenes have been shown to be robust, highly tunable compounds that are tolerable to a wide variety of functional groups.[4–8] These properties allow azobenzene moieties to impact a wide array of subject areas, including materials science,[9–13] medicinal chemistry, chemical biology and biochemistry.[14–22]

$$h\nu_1$$
$$h\nu_2 \text{ or } \Delta$$

Trans isomer
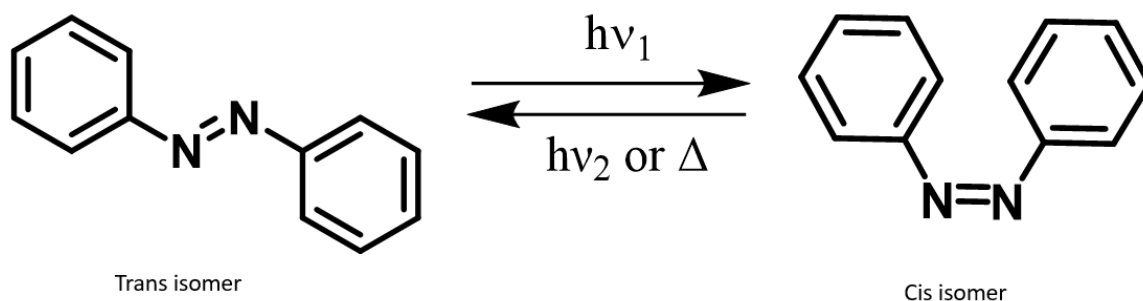
Cis isomer

Figure 1.1 Cis-trans isomerization of azobenzene

One of the most relevant uses for azobenzene functionalities is their on-off switching capabilities.[3,14] Using the azobenzene conformation change has allowed for the creation, innovation and progression of response-based systems.[3] This ability is highlighted in its use in biologically relevant pathways and signaling processes, allowing azobenzenes to be at the forefront of photo-pharmacological advances.[3] One of the most influential areas of azobenzene use is secondary structure manipulation of appended peptides.[23–26] Outlined below are examples of azobenzene incorporation into peptide containing α-helices, β-sheets, β-turns, and other secondary structure elements.

1.2 Azobenzene and their involvement with α-helices

Alpha helices are one of the most prevalent secondary structures found within proteins.[27,28] These prominent secondary structures are characterized by 3.6 amino acid residues per helical turn with hydrogen bonding between the *i* and i+4 residues within the helix.[27,28] Azobenzenes have been used with alpha helices to modulate their stability and helical chirality, as well as controlling inhibition of protein-protein interactions.

1.2.1 Azobenzene as stabilizers of α-helical backbones

A significant contribution to the use of azobenzene moieties with α-helical peptides has been reported by Andrew Woolley and coworkers in the early 2000's. This group developed linkers to act as backbone staples for α-helices. These staples used bis-diacetamide azobenzenes that would staple the *i* and *i+7* residues via cysteine residues using a model peptide, JRK [Ac-EACARVAibAACEAAARQ-NH$_2$], developed by Merutka *et al.* (Table 1.1).[29–32] When photolyzed with UV light, the azobenzene in the cis conformation stabilized the α-helical structure, whereas when the azobenzene was in the more stable trans conformation, the α-helical structure was lost. From this initial discovery Woolley found new ways to affect the stability of α-helical peptides using his photo-switchable staple. It was also observed that the position of the azobenzene within the sequence had an effect on helix stability.[33] The α-helix was most stable when the azobenzene staple was at a more central location on the peptide backbone. Peptides with the staple at the ends experienced a drop in α-helicity.

Woolley also demonstrated, that the distance between the residues modified with the photo-switchable staple could alter α-helix stability, using a new α-helical peptide Ac-[EAAAR]$_3$-NH$_2$.[34,35] They investigated, *i* to *i+4* (FK-4) and an *i* to *i+11* (FK-11) linkages (Figure 1.2) to manipulate α-helix stability (Table 1.1).[36] The *i* to *i+4* linkage show similar conformational preferences as compared to the JRK *i* to *i+7* linkage, with stabilization of the α-helical backbone with the cis version of the staple, and destabilization of the helix in the trans form. The *i* to *i+11* linkage inversely showed a greater stability of the α-helix with the trans conformation of the azobenzene staple while in the cis form the peptide adopted a random coil conformation.[37,38] This variability in conformation showed further demonstrates the utility of azobenzene in relation to α-helices.
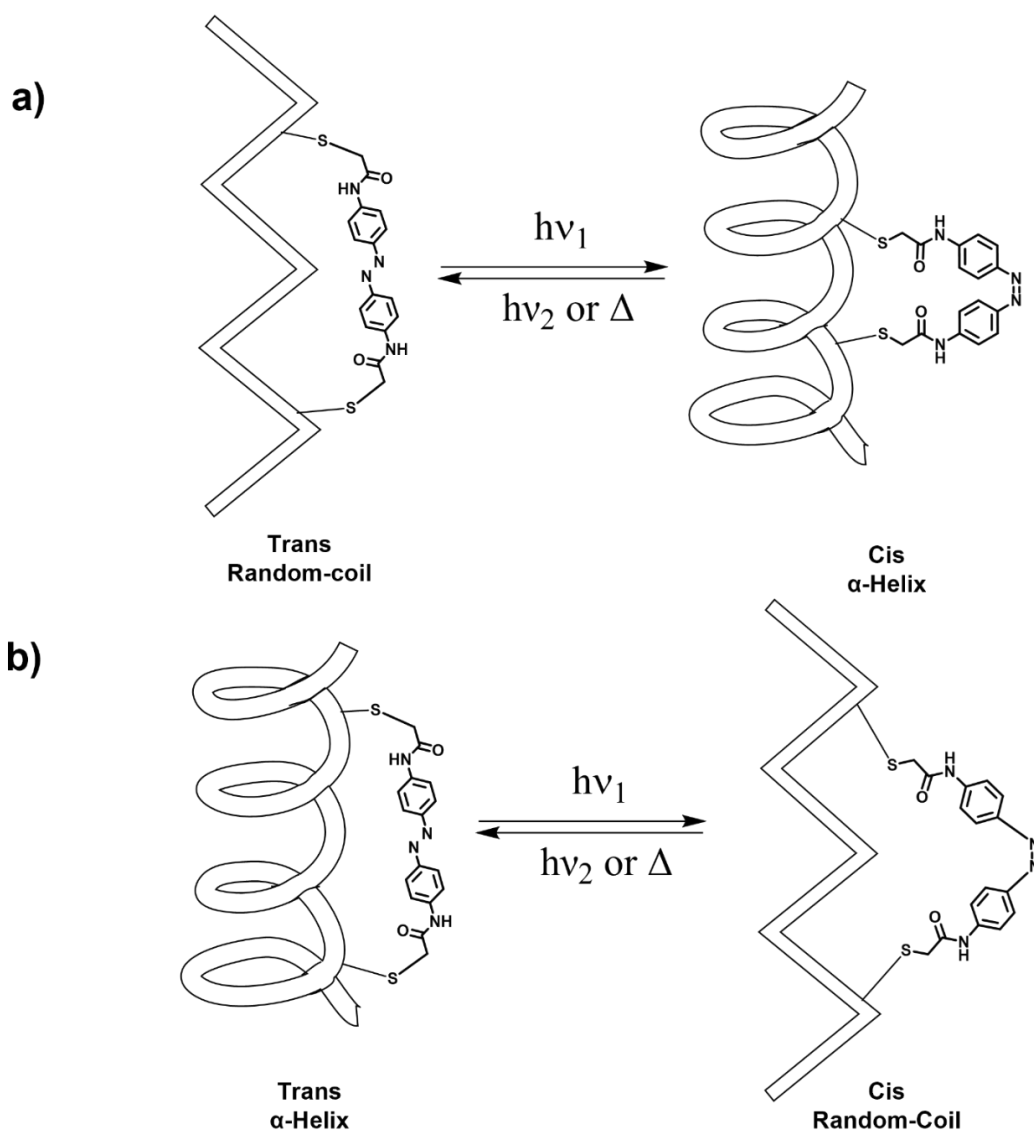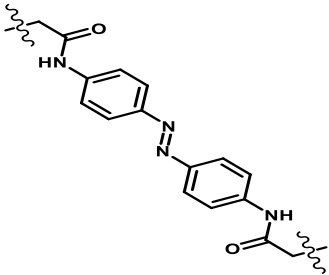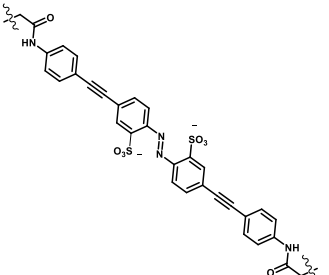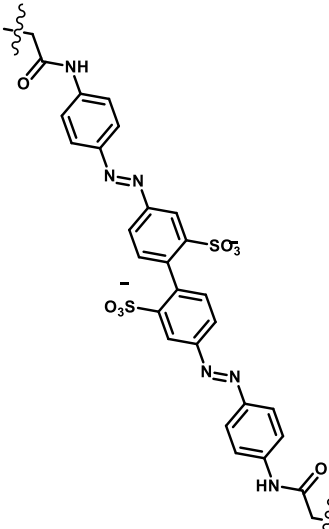
Figure 1.2 The backbone dynamics of the stapled JRK-7 and FK-4 peptides when the conformation of the azobenzene is changed from cis to trans and vice versa (Top). The backbone dynamics of the stapled FK-11 peptide when the conformation of the azobenzene is changed from cis to trans and vice versa (Bottom).[38]

Further derivatization of the azobenzene staple was made by the addition of a sulfonate group at the meta positions of the azobenzene, thereby increasing the water solubility of the staple without compromising performance.[39]The concept of staple length was investigated by Woolley, creating a longer azobenzene staple with alkynes on both sides. This allowed for an extended *i* to *i+14* (XFZ14) and *i* to *i+21* linkage (XFZ21) to an α-helix (Table 1.1).[40] The extended *i* to *i+14* provided similar results to the extended *c* that was shown previously, with a stabilizing effect in the cis isomer, while the *i* to *i+21* linkage showed comparable results to the *i* to *i+11* linkage. A bridged Azobenzene implanted as the staple linker was shown to affect the stability of helical backbones using the *i* to *i+11* linkage, with opposite conformational effect due to the photophysical properties of the bridged azobenzene.[41]A bis-azobenzene was also synthesized, but the peptide exhibited fairly inconclusive results due to the presence of two separate azobenzene within the staple.[42] The irradiated form of SS-11, whether it contained the cis,cis or trans,cis azobenzene showed greater α-helical stability than with the trans,trans linker.

The azobenzene staple was used further by introducing more modifications to the linker to increase performance. The ortho position of the azobenzene moiety, when modified with electron donating groups (EDG) allows for an increase in the azo-bond excitation wavelength. This increase in the λ_{max} allows for deeper penetration of the light within biological tissue. Woolley and coworkers synthesized azobenzene linkers that contained a wide range of EDG (-OEt, -OMe, -NRR', -SEt) which raise the λ_{max} into the visible light range and even to the near infrared (NIR) range (430 nm to 660 nm), while still manipulating helical stability.[4,6,7,43,44]Woolley also developed a reversible azobenzene staple using methanethiosulfonyl groups at the cysteine reaction site.[45]

Table 1.1 List of α-helical peptides stapled with an azobenzene linker.

Peptide	Linkage	
Ac-EACARVAibAACEAAARQ-NH$_2$ JRK-7[29]	*i- i+7*	
Ac-EAAAREACARECAARQ-NH$_2$ FK-4[36]	*i- i+4*	
Ac-EACAREAAAREAACRQ-NH$_2$ FK-11[36]	*i- i+11*	
Ac-WGA**C**EAAAREAAAREAA**C**RQ-NH$_2$ XFZ14[40]	*i- i+14*	
Ac-WGA**C**EAAAREAAAREAAAREAAAR**C**AQ-NH$_2$ XFZ21[40]	*i- i+21*	
Ac-WGA**C**EAAAREAAAREAAAREAAAR**C**AQ-NH$_2$ SS-11[42]	*i- i+11*	
Ac-WGA**C**EAAAREAAAREAAAREAAAR**C**AQ-NH$_2$ SS-14[42]	*i- i+14*	
Ac-WGA**C**EAAAREAAAREAAAREAAAR**C**AQ-NH$_2$ SS-19[42]	*i - i+19*	
Ac-WGA**C**EAAAREAAAREAAAREAAAR**C**AQ-NH$_2$ FZ-21[42]	*i-i+21*	

16

1.2.1.1 α-Helical stability and biological activity

Many have taken the concept of azobenzenes and α-helical stability, that have been studied extensively by Woolley, and have applied them to different targets in chemical biology and biochemistry. The azobenzene staple has been used to activate a DNA binding peptide, MyoD, using the *i* to *i+7* linkage to create an on/off photo-switch.[46] Peptides based on the BAK/BCL protein-protein interaction, that mediate apoptosis have been combined with an azobenzene photo-switchable staple to create another photo-controlled agent.[47,48] The same strategy was implemented using peptides that resembled β-arrestin to inhibit the interactions of β-Adaptin II.[49] The azobenzene crosslinker has also been used in processes the involve endocytosis, cytochrome c release and cell penetration.[25,50,51]

1.2.2   Azobenzene as components in α-helical biopolymers

When Linus Pauling discovered α-helices, his initial 1951 publication defined α-helices as right-handed.[52] However, sidechain incorporation of azobenzene residues into poly(aspartate) α-helical peptides have been shown to alter the helicity of peptides (Figure 1.3). A poly(aspartate) sequence, with azobenzene dispersed throughout the sidechain, initially exist as a left-handed helix with 59% loading of azobenzene within the biopolymer. Upon photolysis of the sidechain azobenzene the left-handed α-helix converted into a right-handed α-helix.[53] Poly(aspartate) modified with a long aliphatic chain with azobenzene esters, were right-handed helices with <50% loading of azobenzene and left-handed helices with >50% loading of azobenzene at room temperature.[54,55] When polymers containing 68% and 89% loading of azobenzene were irradiated with UV light, they changed from left-handed helices to right-handed helices.[56] Fissi and coworkers worked with poly(glutamate) esters and poly(lysine) amides containing azobenzenes that had similar effects to the poly(aspartate) sequences.[57–60]
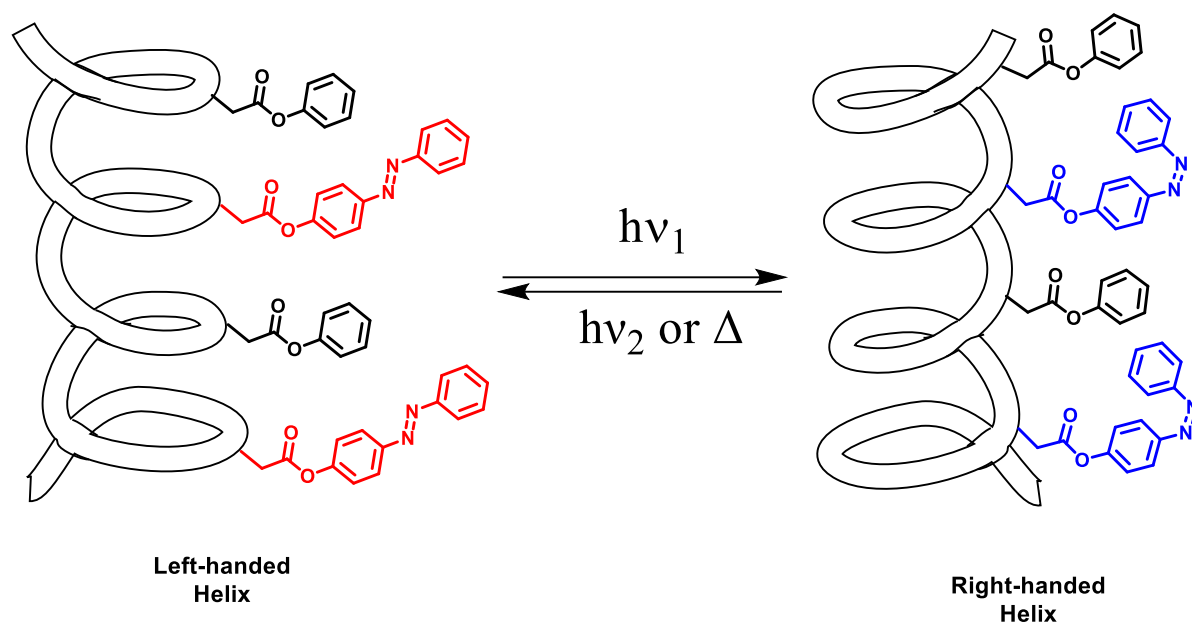
Figure 1.3 The photolysis of azo-esters sidechains in poly(aspartate) α-helices promotes a change in helix chirality.

1.2.3   Azobenzene as part of α-helical backbones

Azobenzene moieties have been inserted into the middle of α-helical peptides to modulate their conformation and activity. An azobenzene was conjugated to two bZIP α-helices via double nucleophilic attack by two terminal cysteines.[61] The peptide, when photolyzed to the cis conformation, was shown to bind DNA in the major groove as ordered α-helices. Azobenzene have also been inserted centrally into an incretin-like peptide, liraglutide, to induce insulin production.[62] The cis isomer of LirAzo generated two orders of magnitude more cAMP than its trans counterpart, and cis LirAzo induced three times more insulin secretion than trans LirAzo. Azobenzene was further substituted into melittin, a common membrane lytic peptide.[63] The substitution of proline within the melittin sequence allowed for an on/off membrane lytic peptide, with the cis form showing greater lytic potential than its trans counterpart.

1.2.4   Azobenzene as part of α-helical sidechains

Azobenzene has also been used as an amino acid sidechain. In the α-helical ribonuclease S. This peptide forms a complex with ribonuclease S protein.[64] The ribonuclease S was modified with phenylazophenylalanine (PAP) at various positions. When the PAP residue was at position 4, the cis form of the α-helical peptide showed high levels of reconstitution to form the native protein.

18

The trans form of this peptide showed less interaction with the S protein and, therefore, less overall activity. This concept was expanded to Gramicidin A where the α-helical peptide was substituted with the PAP residue.[65] The cis form of the PAP residue allowed for ion channel activation by the peptide, while the trans form did not invoke such a response.

1.3 Azobenzene as turn elements to initiate β-sheet formation

The β-sheet morphology was initially discovered by Astbury in 1933 before Pauling and Corey correctly discovered their proper orientation in 1951. β-sheets are one of the major structural motifs in the formation of proteins.[27,28,66] These β-sheet structures exist as parallel or anti-parallel polypeptide strands that are propagated together via a turn, consisting usually of four amino acids. Azobenzene moieties have been used to induce β-sheet by replacing the turn residues within the sequence (Figure 1.4).[24,67] This has been shown in a couple of examples, most notably with the tryptophan zipper (TrpZip) sequence.[67–75] The azobenzene making up the turn region of this β-sheet peptide demonstrates rapid loss of the β-sheet when photolyzed to the trans conformation, on the order of nanoseconds. The reverse trend to form the β-sheet is almost two orders of magnitude slower at around 30 µs. This trend allows for the rapid change between the two conformations, and the selective induction of β-sheets. Similar to the TrpZip peptides, a model β-sheet peptide, Chignolin, showed similar properties of folding and unfolding using an azobenzene moiety as a turn feature.[76,77]
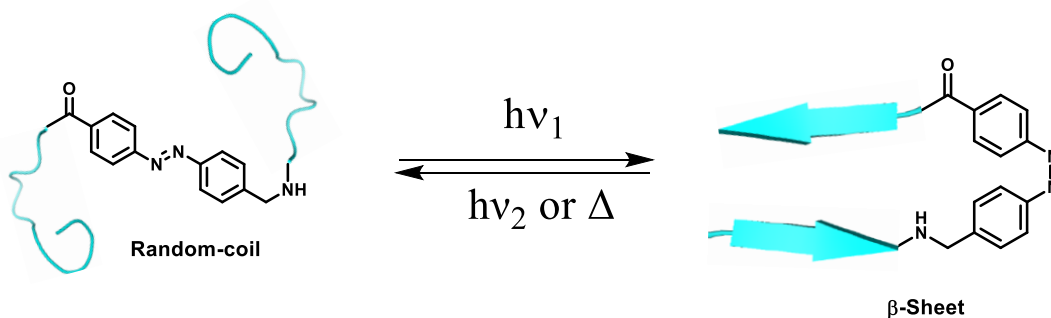
Figure 1.4 The isomerization of a trans azobenzene to a cis azobenzene induces the formation of β-sheets. Reversal of the isomerization results in random-coil formation.

The use of azobenzene's as a tool to enhance β-sheet formation is relevant for a few biologically relevant systems. One area using this modality is β-amyloid fiber formation.[78,79] Upon photolysis to the cis conformation the β-sheets of β-amyloid begin to form and cause toxicity to SH-SY5Y neuroblastoma cells. It was further shown by Doran *et al.* that amyloid-like fibrils can be generated that form self-assembled hydrogels.[80] Photo-switchable β-sheets have also been introduced into peptide sequences that activate neuronal synthase when the azobenzene is photolyzed into the cis conformation.[81–83]

1.4   Photo-inducing β-turn confirmations with azobenzene moieties

The β-turn motif is a common motif in proteins that is characterized by four amino acids that form a bend within a peptide structure.[28,84,85] Azobenzene's were first introduced into the β-turn motif by Ulysses and Chmielewski. They introduced an azobenzene unit, with four alanine residues within a cyclic peptide containing a β-turn sequence (Asn-Pro-Gly-Gly).[86] The residues were chosen for their propensity to exist within those positions of the β-turn. The cyclic peptide did not display a β-turn when the azobenzene was in the trans conformation of the macrocycle, while displaying a type II β-turn in the cis conformation of the azobenzene (Figure 1.5). The concept was further expanded when the biological β-turn of somatostatin was introduced into this macrocyclic scaffold, to provide a photo-switchable, biologically active construct against the somatostatin receptor.[87] Although the difference in activity between the two conformations was two-fold, it showed that the β-turn of somatostatin could be manipulated and controlled. The concept of photo-switchable cyclic peptides was also explored by Yeoh and co-workers using a similar strategy to Ulysses and Chmielewski. They took the structure of Gramicidin S and implemented an azobenzene within to induce β-turn formation.[26] This allowed for the optical control of antimicrobial clearance of *S. aureus* with four-fold better activity in the cis conformation (32 µM) than the trans (128 µM).

β-Turn Sequence

+

Azobenzene

hν₁ / hν₂ or Δ

Trans cyclic-photo peptide
No β-turn

β-Turn

Cis cyclic-photo peptide
β-turn formed
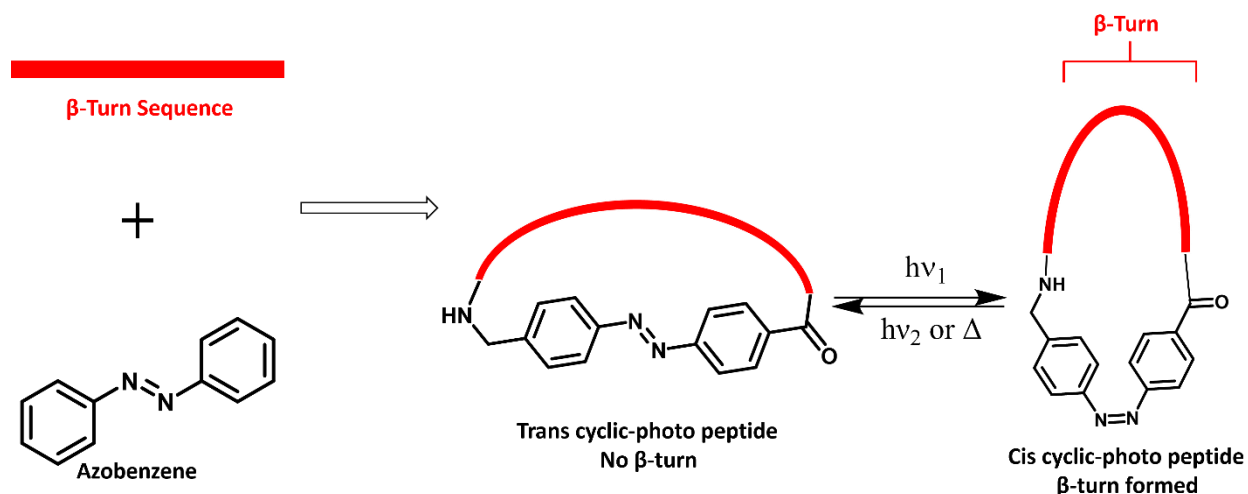
Figure 1.5 Schematic of photo-switchable cyclic peptides that induce β-turn formation.

1.5   Other applications of azobenzene within secondary structures

Other secondary structures that have been enriched by azobenzenes and their photo-switching capabilities include polyproline helices, and coiled coils. Polyproline helices exist in two forms as type I and a type II polyproline helices. The most common polyproline helix is found in collagen, an important structural protein.[88,89] Azobenzene moieties have been stapled into the center of the polyproline helix using cysteine residues, much like Woolley has done with α-helices.[90] The trans isomer of the azobenzene staple allowed for triple helix formation from the collagen peptide. The cis isomer distorted the polyproline helix of the collagen peptide to prevent triple helix formation. Similar results were seen when a thioproline residue was used to staple the azobenzene within the collagen sequence.[91]

Coiled-coils are super-secondary structures that consist of two or more α-helices.[92,93] These helices contain a heptad repeat that help to dictate their oligomeric states and structural properties.[94] The inclusion of azobenzenes into coiled-coils has involved placing two alpha helical sequences, that correspond to tropomyosin on either end of an azobenzene.[95] The trans conformation of the azobenzene allows for the two alpha helices to come together to form a coiled-coil. The cis conformation of the azobenzene caused the two helices to become too close and interfered with the hydrophobic interactions of the coiled coil, causing fraying. Other azobenzene involvement with coiled-coils involved the helical stability of DNA binding coiled-coils, like

21

GCN4 and the Jun/Fos coiled coils.[96,97] These coiled-coils combined with the azobenzene peptide staple via an *i to i+7* linkage showed coiled-coil disassembly in the trans conformation. The cis conformation of the staple allowed for proper helical formation, thus initiating coiled coil formation and DNA binding. Woolley and coworkers also showed that varying the position of the azobenzene staple on one of the alpha helices of the coiled-coil induced drastic differences to the stability of the alpha helix and thus the coiled coil.[98]

1.6   Conclusions

Azobenzenes and their photophysical properties have provided significant contributions in the field of peptide secondary structure manipulation. The constructs have been shown to affect the stability of α-helices, coiled-coils, β-sheets, and β-turns and modulate their activity within many biologically relevant pathways. There is currently a gap within the field of azobenzene manipulation of β-turn sequences. These motifs are very essential as they are involved in receptor stimulating peptides, such as enkephalins, oxytocin and somatostatin, that activate important cellular responses within the body.[85]The work described within this thesis aims to expand on the field of azobenzene mediated β-turn formation, and its ability to affect the responsiveness of chemical processes.

1.7   References

(1)   Griffiths, J. II. Photochemistry of Azobenzene and Its Derivatives. *Chem. Soc. Rev.* **1972**, *1* (4), 481–493. https://doi.org/10.1039/CS9720100481.

(2)   Hartley, G. S. The Cis-Form of Azobenzene [11]. *Nature* **1937**, *140* (3537), 281–281. https://doi.org/10.1038/140281a0.

(3)   Fuchter, M. J. On the Promise of Photopharmacology Using Photoswitches: A Medicinal Chemist's Perspective. *J. Med. Chem.* **2020**, *63* (20), 11436–11447. https://doi.org/10.1021/acs.jmedchem.0c00629.

(4)   Dong, M.; Babalhavaeji, A.; Collins, C. V.; Jarrah, K.; Sadovski, O.; Dai, Q.; Woolley, G. A. Near-Infrared Photoswitching of Azobenzenes under Physiological Conditions. *J. Am. Chem. Soc.* **2017**, *139* (38), 13483–13486. https://doi.org/10.1021/jacs.7b06471.

(5)   Dong, M.; Babalhavaeji, A.; Samanta, S.; Beharry, A. A.; Woolley, G. A. Red-Shifting Azobenzene Photoswitches for in Vivo Use. *Acc. Chem. Res.* **2015**, *48* (10), 2662–2670. https://doi.org/10.1021/acs.accounts.5b00270.

(6)   Samanta, S.; McCormick, T. M.; Schmidt, S. K.; Seferos, D. S.; Woolley, G. A. Robust Visible Light Photoswitching with Ortho-Thiol Substituted Azobenzenes. *Chem. Commun.* **2013**, *49* (87), 10314–10316. https://doi.org/10.1039/c3cc46045b.

(7)   Samanta, S.; Beharry, A. A.; Sadovski, O.; McCormick, T. M.; Babalhavaeji, A.; Tropepe, V.; Woolley, G. A. Photoswitching Azo Compounds in Vivo with Red Light. *J. Am. Chem. Soc.* **2013**, *135* (26), 9777–9784. https://doi.org/10.1021/ja402220t.

(8)   Beharry, A. A.; Woolley, G. A. Azobenzene Photoswitches for Biomolecules. *Chem. Soc. Rev.* **2011**, *40* (8), 4422–4437. https://doi.org/10.1039/c1cs15023e.

(9)   Yager, K. G.; Barrett, C. J. Novel Photo-Switching Using Azobenzene Functional Materials. *J. Photochem. Photobiol. A Chem.* **2006**, *182* (3), 250–261. https://doi.org/10.1016/j.jphotochem.2006.04.021.

(10)   Han, G. G. D.; Li, H.; Grossman, J. C. Optically-Controlled Long-Term Storage and Release of Thermal Energy in Phase-Change Materials. *Nat. Commun.* **2017**, *8* (1), 1446. https://doi.org/10.1038/s41467-017-01608-y.

(11)   Goulet-Hanssens, A.; Barrett, C. J. Photo-Control of Biological Systems with Azobenzene Polymers. *J. Polym. Sci. Part A Polym. Chem.* **2013**, *51* (14), 3058–3070. https://doi.org/10.1002/pola.26735.

(12)   Xu, G.; Li, S.; Liu, C.; Wu, S. Photoswitchable Adhesives Using Azobenzene-Containing Materials. *Chem. - An Asian J.* **2020**, *15* (5), 547–554. https://doi.org/10.1002/asia.201901655.

(13)   Gomy, C.; Schmitzer, A. R. Synthesis and Photoresponsive Properties of a Molecularly Imprinted Polymer. *Org. Lett.* **2007**, *9* (20), 3865–3868. https://doi.org/10.1021/ol701618n.

(14)   Wegener, M.; Hansen, M. J.; Driessen, A. J. M.; Szymanski, W.; Feringa, B. L. Photocontrol of Antibacterial Activity: Shifting from UV to Red Light Activation. *J. Am. Chem. Soc.* **2017**, *139* (49), 17979–17986. https://doi.org/10.1021/jacs.7b09281.

(15)   Borowiak, M.; Nahaboo, W.; Reynders, M.; Nekolla, K.; Jalinot, P.; Hasserodt, J.; Rehberg, M.; Delattre, M.; Zahler, S.; Vollmar, A.; et al. Photoswitchable Inhibitors of Microtubule Dynamics Optically Control Mitosis and Cell Death. *Cell* **2015**, *162* (2), 403–411. https://doi.org/10.1016/j.cell.2015.06.049.

(16)   Szymanski, W.; Ourailidou, M. E.; Velema, W. A.; Dekker, F. J.; Feringa, B. L. Light-Controlled Histone Deacetylase (HDAC) Inhibitors: Towards Photopharmacological Chemotherapy. *Chem. - A Eur. J.* **2015**, *21* (46), 16517–16524. https://doi.org/10.1002/chem.201502809.

(17)   Reis, S. A.; Ghosh, B.; Hendricks, J. A.; Szantai-Kis, D. M.; Törk, L.; Ross, K. N.; Lamb, J.; Read-Button, W.; Zheng, B.; Wang, H.; et al. Light-Controlled Modulation of Gene Expression by Chemical Optoepigenetic Probes. *Nat. Chem. Biol.* **2016**, *12* (5), 317–323. https://doi.org/10.1038/nchembio.2042.

(18) Broichhagen, J.; Johnston, N. R.; Von Ohlen, Y.; Meyer-Berg, H.; Jones, B. J.; Bloom, S. R.; Rutter, G. A.; Trauner, D.; Hodson, D. J. Allosteric Optical Control of a Class B G-Protein-Coupled Receptor. *Angew. Chemie - Int. Ed.* **2016**, *55* (19), 5865–5868. https://doi.org/10.1002/anie.201600957.

(19) Sawada, S.; Takao, T.; Kato, N.; Kaihatsu, K. Design of Tail-Clamp Peptide Nucleic Acid Tethered with Azobenzene Linker for Sequence-Specific Detection of Homopurine DNA. *Molecules* **2017**, *22* (11), 1840. https://doi.org/10.3390/molecules22111840.

(20) Bonardi, F.; London, G.; Nouwen, N.; Feringa, B. L.; Driessen, A. J. M. Light-Induced Control of Protein Translocation by the SecYEG Complex. *Angew. Chemie - Int. Ed.* **2010**, *49* (40), 7234–7238. https://doi.org/10.1002/anie.201002243.

(21) Shishido, H.; Yamada, M. D.; Kondo, K.; Maruta, S. Photocontrol of Calmodulin Interaction with Target Peptides Using Azobenzene Derivative. *J. Biochem.* **2009**, *146* (4), 581–590. https://doi.org/10.1093/jb/mvp107.

(22) Camarero, N.; Trapero, A.; Pérez-Jiménez, A.; Macia, E.; Gomila-Juaneda, A.; Martín-Quirós, A.; Nevola, L.; Llobet, A.; Llebaria, A.; Hernando, J.; et al. Photoswitchable Dynasore Analogs to Control Endocytosis with Light. *Chem. Sci.* **2020**, *11* (33), 8981–8988. https://doi.org/10.1039/d0sc03820b.

(23) Willner, I.; Rubin, S. Control of the Structure and Functions of Biomaterials by Light. *Angew. Chemie (International Ed. English)* **1996**, *35* (4), 367–385. https://doi.org/10.1002/anie.199603671.

(24) Nuti, F.; Gellini, C.; Larregola, M.; Squillantini, L.; Chelli, R.; Salvi, P. R.; Lequin, O.; Pietraperzia, G.; Papini, A. M. A Photochromic Azobenzene Peptidomimetic of a β-Turn Model Peptide Structure as a Conformational Switch. *Front. Chem.* **2019**, *7* (MAR), 180. https://doi.org/10.3389/fchem.2019.00180.

(25) Kim, G. C.; Ahn, J. H.; Oh, J. H.; Nam, S.; Hyun, S.; Yu, J.; Lee, Y. Photoswitching of Cell Penetration of Amphipathic Peptides by Control of α-Helical Conformation. *Biomacromolecules* **2018**, *19* (7), 2863–2869. https://doi.org/10.1021/acs.biomac.8b00428.

(26) Yeoh, Y. Q.; Yu, J.; Polyak, S. W.; Horsley, J. R.; Abell, A. D. Photopharmacological Control of Cyclic Antimicrobial Peptides. *ChemBioChem* **2018**, *19* (24), 2591–2597. https://doi.org/10.1002/cbic.201800618.

(27) PAULING, L.; COREY, R. B.; BRANSON, H. R. The Structure of Proteins; Two Hydrogen-Bonded Helical Configurations of the Polypeptide Chain. *Proc. Natl. Acad. Sci. U. S. A.* **1951**, *37* (4), 205–211. https://doi.org/10.1073/pnas.37.4.205.

(28) Richardson, J. S. The Anatomy and Taxonomy of Protein Structure. *Adv. Protein Chem.* **1981**, *34*, 167–339. https://doi.org/10.1016/S0065-3233(08)60520-3.

(29)   Kumita, J. R.; Smart, O. S.; Woolley, G. A. Photo-Control of Helix Content in a Short Peptide. *Proc. Natl. Acad. Sci. U. S. A.* **2000**, *97* (8), 3803–3808. https://doi.org/10.1073/pnas.97.8.3803.

(30)   Merutka, G.; Shalongo, W.; Stellwagen, E. A Model Peptide with Enhanced Helicity. *Biochemistry* **1991**, *30* (17), 4245–4248. https://doi.org/10.1021/bi00231a020.

(31)   Kumita, J. R.; Flint, D. G.; Smart, O. S.; Woolley, G. A. Photo-Control of Peptide Helix Content by an Azobenzene Cross-Linker: Steric Interactions with Underlying Residues Are Not Critical. *Protein Eng.* **2002**, *15* (7), 561–569. https://doi.org/10.1093/protein/15.7.561.

(32)   Burns, D. C.; Flint, D. G.; Kumita, J. R.; Feldman, H. J.; Serrano, L.; Zhang, Z.; Smart, O. S.; Woolley, G. A. Origins of Helix - Coil Switching in a Light-Sensitive Peptide. *Biochemistry* **2004**, *43* (49), 15329–15338. https://doi.org/10.1021/bi048152k.

(33)   Ali, A. M.; Woolley, G. A. The Effect of Azobenzene Cross-Linker Position on the Degree of Helical Peptide Photo-Control. *Org. Biomol. Chem.* **2013**, *11* (32), 5325–5331. https://doi.org/10.1039/c3ob40684a.

(34)   Marqusee, S.; Robbins, V. H.; Baldwin, R. L. Unusually Stable Helix Formation in Short Alanine-Based Peptides. *Proc. Natl. Acad. Sci. U. S. A.* **1989**, *86* (14), 5286–5290. https://doi.org/10.1073/pnas.86.14.5286.

(35)   Merutka, G.; Stellwagen, E. Positional Independence and Additivity of Amino Acid Replacements on Helix Stability in Monomeric Peptides. *Biochemistry* **1990**, *29* (4), 894–898. https://doi.org/10.1021/bi00456a007.

(36)   Flint, D. G.; Kumita, J. R.; Smart, O. S.; Woolley, G. A. Using an Azobenzene Cross-Linker to Either Increase or Decrease Peptide Helix Content upon Trans-to-Cis Photoisomerization. *Chem. Biol.* **2002**, *9* (3), 391–397. https://doi.org/10.1016/S1074-5521(02)00109-6.

(37)   Bredenbeck, J.; Helbing, J.; Kumita, J. R.; Woolley, G. A.; Hamm, P. α-Helix Formation in a Photoswitchable Peptide Tracked from Picoseconds to Microseconds by Time-Resolved IR Spectroscopy. *Proc. Natl. Acad. Sci. U. S. A.* **2005**, *102* (7), 2379–2384. https://doi.org/10.1073/pnas.0406948102.

(38)   Chen, E.; Kumita, J. R.; Woolley, G. A.; Kliger, D. S. The Kinetics of Helix Unfolding of an Azobenzen Cross-Linked Peptide Probed by Nanosecond Time-Resolved Optical Rotatory Dispersion. *J. Am. Chem. Soc.* **2003**, *125* (41), 12443–12449. https://doi.org/10.1021/ja030277+.

(39)   Zhang, Z.; Burns, D. C.; Kumita, J. R.; Smart, O. S.; Woolley, G. A. A Water-Soluble Azobenzene Cross-Linker for Photocontrol of Peptide Conformation. *Bioconjug. Chem.* **2003**, *14* (4), 824–829. https://doi.org/10.1021/bc0340161.

(40)   Zhang, F.; Sadovski, O.; Woolley, G. A. Synthesis and Characterization of a Long, Rigid Photoswitchable Cross-Linker for Promoting Peptide and Protein Conformational Change. *ChemBioChem* **2008**, *9* (13), 2147–2154. https://doi.org/10.1002/cbic.200800196.

(41)   Samanta, S.; Qin, C.; Lough, A. J.; Woolley, G. A. Bidirectional Photocontrol of Peptide Conformation with a Bridged Azobenzene Derivative. *Angew. Chemie - Int. Ed.* **2012**, *51* (26), 6452–6455. https://doi.org/10.1002/anie.201202383.

(42)   Samanta, S.; Woolley, G. A. Bis-Azobenzene Crosslinkers for Photocontrol of Peptide Structure. *ChemBioChem* **2011**, *12* (11), 1712–1723. https://doi.org/10.1002/cbic.201100204.

(43)   Sadovski, O.; Beharry, A. A.; Zhang, F.; Woolley, G. A. Spectral Tuning of Azobenzene Photoswitches for Biological Applications. *Angew. Chemie - Int. Ed.* **2009**, *48* (8), 1484–1486. https://doi.org/10.1002/anie.200805013.

(44)   Samanta, S.; Babalhavaeji, A.; Dong, M. X.; Woolley, G. A. Photoswitching of Ortho-Substituted Azonium Ions by Red Light in Whole Blood. *Angew. Chemie - Int. Ed.* **2013**, *52* (52), 14127–14130. https://doi.org/10.1002/anie.201306352.

(45)   Pozhidaeva, N.; Cormier, M. E.; Chaudhari, A.; Woolley, G. A. Reversible Photocontrol of Peptide Helix Content: Adjusting Thermal Stability of the Cis State. *Bioconjug. Chem.* **2004**, *15* (6), 1297–1303. https://doi.org/10.1021/bc049855h.

(46)   Guerrero, L.; Smart, O. S.; Weston, C. J.; Burns, D. C.; Woolley, G. A.; Allemann, R. K. Photochemical Regulation of DNA-Binding Specificity of MyoD. *Angew. Chemie - Int. Ed.* **2005**, *44* (47), 7956–7960. https://doi.org/10.1002/anie.200502666.

(47)   Kneissl, S.; Loveridge, E. J.; Williams, C.; Crump, M. P.; Allemann, R. K. Photocontrollable Peptide-Based Switches Target the Anti-Apoptotic Protein Bcl-XL. *Chembiochem* **2008**, *9* (18), 3046–3054. https://doi.org/10.1002/cbic.200800502.

(48)   Nevola, L.; Varese, M.; Martín-Quirós, A.; Mari, G.; Eckelt, K.; Gorostiza, P.; Giralt, E. Targeted Nanoswitchable Inhibitors of Protein–Protein Interactions Involved in Apoptosis. *ChemMedChem* **2019**, *14* (1), 100–106. https://doi.org/10.1002/cmdc.201800647.

(49)   Martín-Quirós, A.; Nevola, L.; Eckelt, K.; Madurga, S.; Gorostiza, P.; Giralt, E. Absence of a Stable Secondary Structure Is Not a Limitation for Photoswitchable Inhibitors of β-Arrestin/β-Adaptin 2 Protein-Protein Interaction. *Chem. Biol.* **2015**, *22* (1), 31–37. https://doi.org/10.1016/j.chembiol.2014.10.022.

(50)   Nevola, L.; Martín-Quirõs, A.; Eckelt, K.; Camarero, N.; Tosi, S.; Llobet, A.; Giralt, E.; Gorostiza, P. Light-Regulated Stapled Peptides to Inhibit Protein-Protein Interactions Involved in Clathrin-Mediated Endocytosis. *Angew. Chemie - Int. Ed.* **2013**, *52* (30), 7704–7708. https://doi.org/10.1002/anie.201303324.

(51)   Mart, R. J.; Errington, R. J.; Watkins, C. L.; Chappell, S. C.; Wiltshire, M.; Jones, A. T.; Smith, P. J.; Allemann, R. K. BH3 Helix-Derived Biophotonic Nanoswitches Regulate Cytochrome c Release in Permeabilised Cells. *Mol. Biosyst.* **2013**, *9* (11), 2597–2603. https://doi.org/10.1039/c3mb70246d.

(52)   Dunitz, J. D. Pauling's Left-Handed α-Helix. *Angew. Chemie - Int. Ed.* **2001**, *40* (22), 4167–4173. https://doi.org/10.1002/1521-3773(20011119)40:22<4167::AID-ANIE4167>3.0.CO;2-Q.

(53)   Ciardelli, F.; Pieroni, O.; Fissi, A.; Houben, J. L. Azobenzene-Containing Polypeptides: Photoregulation of Conformation in Solution. *Biopolymers* **1984**, *23* (7), 1423–1437. https://doi.org/10.1002/bip.360230723.

(54)   Ueno, A.; Anzai, J.; Osa, T.; Kadoma, Y. Light-Induced Conformational Changes of Polypeptides. Photoisomerization of Azoaromatic Polypeptides. *Bull. Chem. Soc. Jpn.* **1979**, *52* (2), 549–554. https://doi.org/10.1246/bcsj.52.549.

(55)   Ueno, A.; Takahashi, K.; Anzai, J. ichi; Osa, T. Photocontrol of Polypeptide Helix Sense by Cis-Trans Isomerism of Side-Chain Azobenzene Moieties. *J. Am. Chem. Soc.* **1981**, *103* (21), 6410–6415. https://doi.org/10.1021/ja00411a025.

(56)   Ueno, A.; Adachi, K.; Nakamura, J.; Osa, T. Photoinduced Conformational Changes of Azoaromatic Polyaspartates Containing Octadecyl Side Chains. *J. Polym. Sci. Part A Polym. Chem.* **1990**, *28* (5), 1161–1170. https://doi.org/10.1002/pola.1990.080280516.

(57)   Houben, J. L.; Fissi, A.; Bacciola, D.; Rosato, N.; Pieroni, O.; Ciardelli, F. Azobenzene-Containing Poly(l-Glutamates). Photochromism and Conformation in Solution. *Int. J. Biol. Macromol.* **1983**, *5* (2), 94–100. https://doi.org/10.1016/0141-8130(83)90018-1.

(58)   Pieroni, O.; Fissi, A.; Houben, J. L.; Ciardelli, F. Photoinduced Aggregation Changes in Photochromic Polypeptides. *J. Am. Chem. Soc.* **1985**, *107* (10), 2990–2991. https://doi.org/10.1021/ja00296a036.

(59)   Fissi, A.; Pieroni, O.; Ciardelli, F. Photoresponsive Polymers: Azobenzene-containing Poly(L-lysine). *Biopolymers* **1987**, *26* (12), 1993–2007. https://doi.org/10.1002/bip.360261203.

(60)   Fissi, A.; Pieroni, O.; Balestreri, E.; Amato, C. Photoresponsive Polypeptides. Photomodulation of the Macromolecular Structure in Poly(N∈((Phenylazophenyl)Sulfonyl)-L-Lysine). *Macromolecules* **1996**, *29* (13), 4680–4685. https://doi.org/10.1021/ma960280w.

(61)   Caamaño, A. M.; Vázquez, M. E.; Martínez-Costas, J.; Castedo, L.; Mascareñas, J. L. A Light-Modulated Sequence-Specific DNA-Binding Peptide. *Angew. Chemie - Int. Ed.* **2000**, *39* (17), 3234–3237. https://doi.org/10.1002/1521-3773(20000901)39:17<3104::AID-ANIE3104>3.0.CO;2-0.

(62)   Broichhagen, J.; Podewin, T.; Meyer-Berg, H.; Von Ohlen, Y.; Johnston, N. R.; Jones, B. J.; Bloom, S. R.; Rutter, G. A.; Hoffmann-Röder, A.; Hodson, D. J.; et al. Optical Control of Insulin Secretion Using an Incretin Switch. *Angew. Chemie - Int. Ed.* **2015**, *54* (51), 15565–15569. https://doi.org/10.1002/anie.201506384.

(63)   Ventura, C. R.; Wiedman, G. R. Substituting Azobenzene for Proline in Melittin to Create Photomelittin: A Light-Controlled Membrane Active Peptide. *Biochim. Biophys. Acta - Biomembr.* **2021**, *1863* (12), 183759. https://doi.org/10.1016/j.bbamem.2021.183759.

(64)   Liu, D.; Karanicolas, J.; Yu, C.; Zhang, Z.; Woolley, G. A. Site-Specific Incorporation of Photoisomerizable Azobenzene Groups into Ribonuclease S. *Bioorganic Med. Chem. Lett.* **1997**, *7* (20), 2677–2680. https://doi.org/10.1016/S0960-894X(97)10044-0.

(65)   Borisenko, V.; Burns, D. C.; Zhang, Z.; Woolley, G. A. Optical Switching of Ion-Dipole Interactions in a Gramicidin Channel Analogue. *J. Am. Chem. Soc.* **2000**, *122* (27), 6364–6370. https://doi.org/10.1021/ja000736w.

(66)   Astbury, W. T. Some Problems in the X-Ray Analysis of the Structure of Animal Hairs and Other Protein Fibres. *Trans. Faraday Soc.* **1933**, *29* (140), 193–205. https://doi.org/10.1039/tf9332900193.

(67)   Aemissegger, A.; Kräutler, V.; Van Gunsteren, W. F.; Hilvert, D. A Photoinducible β-Hairpin. *J. Am. Chem. Soc.* **2005**, *127* (9), 2929–2936. https://doi.org/10.1021/ja0442567.

(68)   Schrader, T. E.; Schreier, W. J.; Cordes, T.; Koller, F. O.; Babitzki, G.; Denschlag, R.; Renner, C.; Löweneck, M.; Dong, S. L.; Moroder, L.; et al. Light-Triggered β-Hairpin Folding and Unfolding. *Proc. Natl. Acad. Sci. U. S. A.* **2007**, *104* (40), 15729–15734. https://doi.org/10.1073/pnas.0707322104.

(69)   Schrader, T. E.; Cordes, T.; Schreier, W. J.; Koller, F. O.; Dong, S. L.; Moroder, L.; Zinth, W. Folding and Unfolding of Light-Triggered β-Hairpin Model Peptides. *J. Phys. Chem. B* **2011**, *115* (18), 5219–5226. https://doi.org/10.1021/jp107683d.

(70)   Zinth, W.; Schrader, T. E.; Schreier, W. J.; Koller, F. O.; Cordes, T.; Babizki, G.; Denschlag, R.; Tavan, P.; Löweneck, M.; Dong, S. L.; et al. Ultrafast Unzipping of a Beta-Hairpin Peptide. In *Optics InfoBase Conference Papers*; 2006. https://doi.org/10.1364/up.2006.we8.

(71)   Rampp, M. S.; Hofmann, S. M.; Podewin, T.; Hoffmann-Röder, A.; Moroder, L.; Zinth, W. Time-Resolved Infrared Studies of the Unfolding of a Light Triggered β-Hairpin Peptide. *Chem. Phys.* **2018**, *512*, 116–121. https://doi.org/10.1016/j.chemphys.2018.02.003.

(72)   Dong, S. L.; Löweneck, M.; Schrader, T. E.; Schreier, W. J.; Zinth, W.; Moroder, L.; Renner, C. A Photocontrolled β-Hairpin Peptide. *Chem. - A Eur. J.* **2006**, *12* (4), 1114–1120. https://doi.org/10.1002/chem.200500986.

(73)   Spekowius, J.; Pfister, R.; Helbing, J. Folding and Unfolding of the Tryptophan Zipper in the Presence of Two Thioamide Substitutions. *J. Phys. Chem. B* **2021**, *125* (28), 7662–7670. https://doi.org/10.1021/acs.jpcb.1c03327.

(74)   Deeg, A. A.; Schrader, T. E.; Kempter, S.; Pfizer, J.; Moroder, L.; Zinth, W. Light-Triggered Aggregation and Disassembly of Amyloid-like Structures. *ChemPhysChem* **2011**, *12* (3), 559–562. https://doi.org/10.1002/cphc.201001012.

(75) Deeg, A. A.; Rampp, M. S.; Popp, A.; Pilles, B. M.; Schrader, T. E.; Moroder, L.; Hauser, K.; Zinth, W. Isomerization- and Temperature-Jump-Induced Dynamics of a Photoswitchable β-Hairpin. *Chem. - A Eur. J.* **2014**, *20* (3), 694–703. https://doi.org/10.1002/chem.201303189.

(76) Podewin, T.; Rampp, M. S.; Turkanovic, I.; Karaghiosoff, K. L.; Zinth, W.; Hoffmann-Röder, A. Photocontrolled Chignolin-Derived β-Hairpin Peptidomimetics. *Chem. Commun.* **2015**, *51* (19), 4001–4004. https://doi.org/10.1039/c4cc10304a.

(77) Hofmann, S. M.; Frost, C. V.; Podewin, T.; Gailer, M.; Weber, E.; Zacharias, M.; Zinth, W.; Hoffmann-Röder, A. Folding and Unfolding of the Short Light-Triggered β-Hairpin Peptide AzoChignolin Occurs within 100 Ns. *J. Phys. Chem. B* **2020**, *124* (25), 5113–5121. https://doi.org/10.1021/acs.jpcb.0c02021.

(78) Hoppmann, C.; Barucker, C.; Lorenz, D.; Multhaup, G.; Beyermann, M. Light-Controlled Toxicity of Engineered Amyloid β-Peptides. *ChemBioChem* **2012**, *13* (18), 2657–2660. https://doi.org/10.1002/cbic.201200605.

(79) Doran, T. M.; Anderson, E. A.; Latchney, S. E.; Opanashuk, L. A.; Nilsson, B. L. An Azobenzene Photoswitch Sheds Light on Turn Nucleation in Amyloid-β Self-Assembly. *ACS Chem. Neurosci.* **2012**, *3* (3), 211–220. https://doi.org/10.1021/cn2001188.

(80) Doran, T. M.; Ryan, D. M.; Nilsson, B. L. Reversible Photocontrol of Self-Assembled Peptide Hydrogel Viscoelasticity. *Polym. Chem.* **2014**, *5* (1), 241–248. https://doi.org/10.1039/c3py00903c.

(81) Hoppmann, C.; Seedorff, S.; Richter, A.; Fabian, H.; Schmieder, P.; Rück-Braun, K.; Beyermann, M. Light-Directed Protein Binding of a Biologically Relevant β-Sheet. *Angew. Chemie - Int. Ed.* **2009**, *48* (36), 6636–6639. https://doi.org/10.1002/anie.200901933.

(82) Hoppmann, C.; Schmieder, P.; Domaing, P.; Vogelreiter, G.; Eichhorst, J.; Wiesner, B.; Morano, I.; Rück-Braun, K.; Beyermann, M. Photocontrol of Contracting Muscle Fibers. *Angew. Chemie - Int. Ed.* **2011**, *50* (33), 7699–7702. https://doi.org/10.1002/anie.201101398.

(83) Horsley, J. R.; Yu, J.; Wegener, K. L.; Hoppmann, C.; Rück-Braun, K.; Abell, A. D. Photoswitchable Peptide-Based 'on-off' Biosensor for Electrochemical Detection and Control of Protein-Protein Interactions. *Biosens. Bioelectron.* **2018**, *118*, 188–194. https://doi.org/10.1016/j.bios.2018.07.057.

(84) Venkatachalam, C. M. Stereochemical Criteria for Polypeptides and Proteins. V. Conformation of a System of Three Linked Peptide Units. *Biopolymers* **1968**, *6* (10), 1425–1436. https://doi.org/10.1002/bip.1968.360061006.

(85) Ruiz-Gómez, G.; Tyndall, J. D. A.; Pfeiffer, B.; Abbenante, G.; Fairlie, D. P. Update 1 of: Over One Hundred Peptide-Activated g Protein-Coupled Receptors Recognize Ligands with Turn Structure. *Chem. Rev.* **2010**, *110* (4), 793–826. https://doi.org/10.1021/cr900344w.

(86)   Ulysse, L.; Cubillos, J.; Chmielewski, J. Photoregulation of Cyclic Peptide Conformation. *J. Am. Chem. Soc.* **1995**, *117* (32), 8466–8467. https://doi.org/10.1021/ja00137a023.

(87)   Ulysse, L. G.; Chmielewski, J. A Light-Activated β-Turn Scaffold within a Somatostatin Analog: NMR Structure and Biological Activity. *Chem. Biol. Drug Des.* **2006**, *67* (2), 127–136. https://doi.org/10.1111/j.1747-0285.2005.00337.x.

(88)   Shoulders, M. D.; Raines, R. T. Collagen Structure and Stability. *Annu. Rev. Biochem.* **2009**, *78*, 929–958. https://doi.org/10.1146/annurev.biochem.77.032207.120833.

(89)   Adzhubei, A. A.; Sternberg, M. J. E.; Makarov, A. A. Polyproline-II Helix in Proteins: Structure   and   Function.   *J.   Mol.   Biol.*   **2013**,   *425*   (12),   2100–2132. https://doi.org/10.1016/j.jmb.2013.03.018.

(90)   Kusebauch, U.; Cadamuro, S. A.; Musiol, H. J.; Moroder, L.; Renner, C. Photocontrol of the Collagen Triple Helix: Synthesis and Conformational Characterization of Bis-Cysteinyl Collagenous Peptides with an Azobenzene Clamp. *Chem. - A Eur. J.* **2007**, *13* (10), 2966–2973. https://doi.org/10.1002/chem.200601162.

(91)   Kusebauch, U.; Cadamuro, S. A.; Musiol, H. J.; Lenz, M. O.; Wachtveitl, J.; Moroder, L.; Renner, C. Photocontrolled Folding and Unfolding of a Collagen Triple Helix. *Angew. Chemie - Int. Ed.* **2006**, *45* (42), 7015–7018. https://doi.org/10.1002/anie.200601432.

(92)   Liu, J.; Zheng, Q.; Deng, Y.; Cheng, C. S.; Kallenbach, N. R.; Lu, M. A Seven-Helix Coiled Coil.   *Proc.   Natl.   Acad.   Sci.   U.   S.   A.*   **2006**,   *103*   (42),   15457–15462. https://doi.org/10.1073/pnas.0604871103.

(93)   Grigoryan, G.; Keating, A. E. Structural Specificity in Coiled-Coil Interactions. *Curr. Opin. Struct. Biol.* **2008**, *18* (4), 477–483. https://doi.org/10.1016/j.sbi.2008.04.008.

(94)   Jorgensen, M. D.; Chmielewski, J. Recent Advances in Coiled-Coil Peptide Materials and Their   Biomedical   Applications.   *Chem.   Commun.*   **2022**,   11625–11636. https://doi.org/10.1039/d2cc04434j.

(95)   Torner, J. M.; Arora, P. S. Conformational Control in a Photoswitchable Coiled Coil. *Chem. Commun.* **2021**, *57* (12), 1442–1445. https://doi.org/10.1039/d0cc08318f.

(96)   Kumita, J. R.; Flint, D. G.; Woolley, G. A.; Smart, O. S. Achieving Photo-Control of Protein Conformation and Activity: Producing a Photo-Controlled Leucine Zipper. In *Faraday Discussions*; 2002; Vol. 122, pp 89–103. https://doi.org/10.1039/b200897a.

(97)   Zhang, F.; Timm, K. A.; Arndt, K. M.; Woolley, G. A. Photocontrol of Coiled-Coil Proteins in   Living   Cells.   *Angew.   Chemie   -   Int.   Ed.*   **2010**,   *49*   (23),   4035–4038. https://doi.org/10.1002/anie.201000909.

(98)   Ali, A. M.; Forbes, M. W.; Woolley, G. A. Optimizing the Photocontrol of BZIP Coiled Coils with Azobenzene Crosslinkers: Role of the Crosslinking Site. *ChemBioChem* **2015**, *16* (12), 1757–1763. https://doi.org/10.1002/cbic.201500191.

CHAPTER 2.   A REFINED PHOTO-SWITCHABLE CYCLIC PEPTIDE SCAFFOLD FOR USE IN BETA-TURN ACTIVATION.

2.1   Introduction

Photo-controlled compounds represent an important class of molecules that have been shown to be useful in drug discovery.[1–6] The azobenzene group represents an important portion of these photo-controlled compounds that are highly tuneable, and can be multipurposed for various applications.[7–10] These molecules undergo cis-trans isomerization of the azobenzene in a controlled fashion via ultraviolet (UV) light. The azobenzene moiety has been used for α-helix stabilization,[11–15]β-turn formation,[16–18] β-sheet formation,[19–21] protein binding and activation,[22–24] cell-mediated binding,[25–27] and within DNA.[28–32] More specifically, an azobenzene-containing amino acid, (4-aminomethyl)phenylazobenzoic acid (Azo), and its derivatives can be used to promote light mediated conformational switching that can selectively initiate a range of chemical responses.[16,17,33–38]

The β-turn motif is an important component in biological signalling, and mediates a number of peptide- and protein-protein interactions.[39] This motif consists of four amino acid residues that form a hydrogen bond between the i and $i+3$ residues in the sequence. β-turn mimetics have been used for a variety of applications,[39,40,49,41–48] including targeting β-turn-mediated G-protein coupled receptors.[39,45] While these mimetics are active against their specified targets, controlled activation is difficult to achieve. There is great interest, therefore, in developing tools to modulate the binding of therapeutics. In this regard, cyclic azobenzene-containing peptides have demonstrated photo-control in receptor binding,[17] cell surface signaling,[27] antimicrobial clearance,[18] nanotube formation,[50] and affinity labeling.[51]

Previously, cyclic peptides incorporating Azo were investigated for controlled β-turn formation.[16,17] In one example, a peptide sequence with a propensity to form a β-turn, Asn-Pro-Gly-Gly, was used with two di-alanine spacers flanking the azobenzene moiety (Figure 1a, FLAp).[16] In another instance, a β-turn sequence known to bind the somatotropin release-inhibiting factor (SRIF) receptor, Thr-Lys-Phe-Trp, was used within a cyclic peptide containing the Ala-Ala-Azo-Ala-Ala scaffold.[17] In this latter case, the photo-induced trans to cis switch of the azobenzene achieved a β-turn within the macrocycle. However, the trans-Azo form of the cyclic peptide also maintained some turn character. This residual turn structure may account for the similarities in

SRIF binding with the cis and trans isomers of the cyclic peptide.[17] From these data, it was hypothesized that increasing the rigidity of the peptide scaffold may provide more effective control of the β-turn conformation (Figure 2.1a).
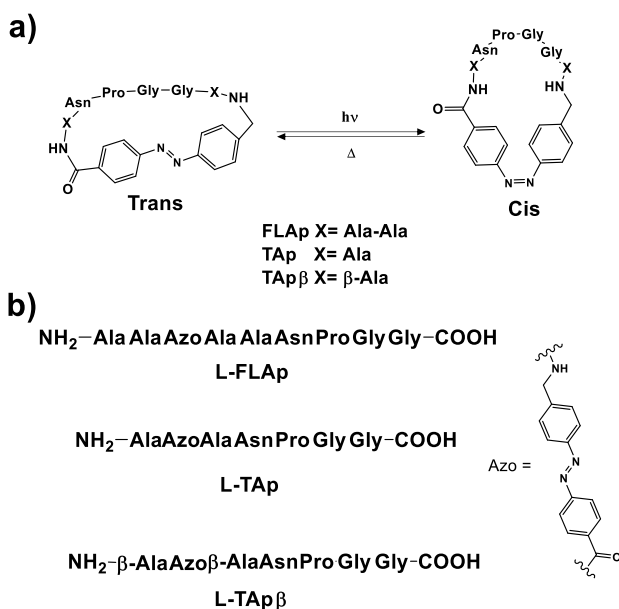
Figure 2.1 a) The tetrapeptide, Asn-Pro-Gly-Gly, is a part of a cyclic peptide containing an azobenzene moiety flanked by either Ala-Ala, Ala, or β-Ala to investigate the rigidity of the scaffold. The cyclic peptides can be isomerized to the cis and trans versions using either UV light or elevated temperature, respectively. b) The pre-cyclized linear peptide sequences containing the azobenzene amino acid (Azo).

2.2 Results & Discussion

2.2.1 Design of Cyclic Peptide Scaffolds

The design of more rigid cyclic azobenzene-containing peptides was based on a previously described photo-switchable peptide, FLAp (Figure 2.1a).[16] It was hypothesized that a more constrained cyclic peptide would show greater differentiation in forming the β-turn when in the cis versus the trans azobenzene conformations. To rigidify the original scaffold, second generation peptides were envisaged in which the two di-alanine spacers of FLAp were replaced with either two alanine (TAp) or two of the somewhat longer β-alanine residues (TApβ). This reduction in the number of atoms between the Azo residue and the β-turn tetrapeptide should allow for investigation of the role that rigidity of the scaffold plays on the photo-control of the β-turn (Figure 2.1a).

2.2.2   Synthesis of Cyclic Azo-containing Peptides using Cyclonic Photoreactor

To accomplish these above goals, therefore, two peptides were synthesized, one with an alanine residue on each side of the Azo residue (TAp) and another with flanking β-alanines (TApβ). Synthesis of the linear versions of the known FLAp and the newly designed TAp and Tapβ (L-FLAp, L-TAp, L-Tapβ) (Figure 2.1b) was performed on a glycine p-alkoxybenzyl alcohol resin using standard Fmoc-based solid phase peptide synthesis with HATU. Once the linear sequences were complete, the resin was treated with a trifluoroacetic acid cocktail to concomitantly remove the protecting groups and cleave the peptides from the resin. The linear peptides were purified to homogeneity on reverse phase HPLC to afford the three peptides in 40-50% yield.
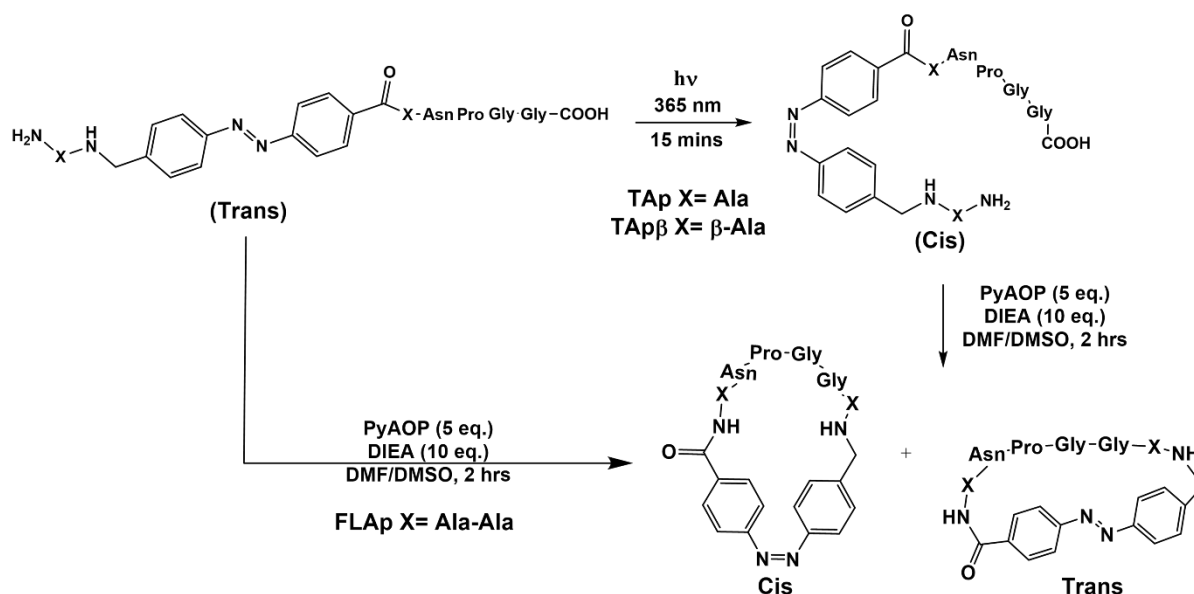
Figure 2.2 Scheme of synthesis of cyclic peptides with (TAp and Tapβ) and without (FLAp) initial photo-isomerization of the azobenzene

Once the linear peptides were obtained, these peptides were subjected to cyclization at a concentration of 1 mM using PyAOP and DIEA in DMSO (Figure 2.2).[52] The L-FLAp peptide was successfully cyclized with the azobenzene in its trans conformation, to provide FLAp in 15% yield. In contrast, cyclization of L-TApβ with the trans azobenzene provided a low 5% yield of the cyclic peptide, whereas L-TAp produced only its corresponding cyclic dimer in 10% yield (Table 2.1). To improve the cyclization yields, we investigated using the cis form of the azobenzene in the linear peptides to bring the C-and N-termini into closer proximity for the reaction. With this in

mind, the peptides were isomerized to the cis conformation using a cyclonic ultraviolet photochemical reactor (Mini-CUPR) before cyclization using above conditions.[53] The cyclic peptides were purified to homogeneity by RP-HPLC and characterized by MALDI-TOF mass spectrometry. In this way the TAp and TApβ peptides were obtained in 35% and 60% yields, respectively (Table 2.1).

Table 2.1   Yields of cyclic azobenzene-containing peptides with and without photoexcitation at 365 nm for isomerization.

Peptide	No Isomerization Yield	Isomerization Yield
FLAp	15%	N/A
TAp	10% (Dimer)	35%
TApβ	5%	60%

2.2.3   Isomerization of Cyclic Azobenzene-containing Peptides

After purification of TAp and Tapβ, the macrocycles were found to have a 60:40 and 70:30 ratio of trans:cis azobenzene, respectively, presumably due to some heating of the sample during solvent removal. These mixtures of the cyclic peptides (1 mM) were irradiated from 15 mins to 2 hours in the Mini-CUPR to photo-isomerize the trans to the cis isomer. Both TAp and TApβ reached their optimal conversion after 15 mins, providing 90% and 86% of the cis form, respectively (Figures S7 and S9). TAp and Tapβ were subjected to thermal isomerization to determine the rate at which the cis conformation of the Azo residue reverts to the trans isomer at 37°C. The cis to trans ratio was quantified by RP-UPLC over the course of seven days (Figure 2.3). These data demonstrate that both cyclic peptides have similar rates of thermal isomerization, and the peptides were converted to their maximum trans form (97% and 98%, respectively) after seven days at 37°C. Together, these data indicate that both peptides can be photo-isomerized to mostly the cis form, and the cis form persists as the major isomer for about one day, with almost complete conversion to the trans isomer in a week. Thereby demonstrating the potential to control the cyclic peptide conformation with both light and heat.

34
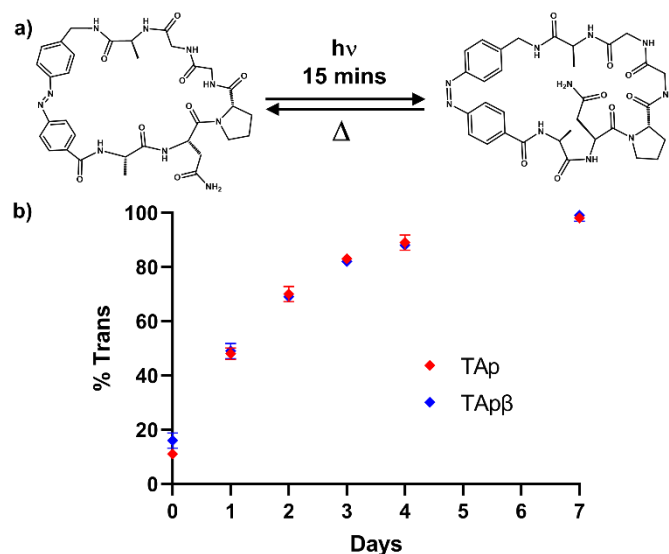
Figure 2.3 a) The use of heat and light to interconvert the cis and trans isomers of TAP. b) Thermal relaxation of cis-TAp and cis-TApβ to their trans isomer at 37°C. Cis and trans percentages were determined by RP-UPLC measurements.

2.2.4   Structural Elucidation of the cis and trans Isomers of the Cyclic Azobenzene-containing Peptides.

We hypothesized that having a cis-Azo residue within the macrocycles would effectively promote a β-turn conformation within the attached tetrapeptide. Also, the design sought to limit turn structures within the macrocycle when the Azo residue was in the trans conformation. We turned to two-dimensional NMR and molecular dynamics to probe if those features were obtained. NOESY spectroscopy was performed on both the cis and trans TAp and TApβ peptides to determine if a β-turn was present. Samples of the cis versions of each peptide were obtained by photo-isomerization for 15 mins in the Mini-CUPR as described above, and then shielded from ambient light. For samples of the trans isomers of TAp and TApβ, mixtures were used that contained 70% and 95% of the trans, respectively. NMR samples of the cyclic peptides were prepared at a 10 mM concentration in deuterated dimethylsulfoxide (DMSO-d_6).

The data from the resulting 2D spectra (NOESY, TOCSY, HMBC, HMQC) were used to model the cis and trans conformations of the cyclic peptides using restrained molecular dynamics as implemented in the Macromodel molecular modelling suite (Schrodinger).[54] According to our design, it was anticipated that the cis conformation of TAp and TApβ would exhibit a β-turn motif within the central tetrapeptide, while the trans isomer should have these residues in a more extended conformation. Distances were measured from the backbone carbonyl of the asparagine

residue (C=O) to the amide proton of the i+3 glycine (H-N) to probe for a β-turn. For TAp, the cis version was found to contain a type II β-turn with an average C=O--H-N distance of 2.2 Å (Figure 2.4a). These same atoms in the trans isomer had a distance of 6.8 Å, indicating that no β-turn was present. The Asn-Pro-Gly-Gly tetrapeptide with *trans*-TAp, however, displayed a kinked structure instead of an extended conformation (Figure 2.4a). Additionally, the azobenzene showed distortion from planarity when in the trans form. Within the cis version of TApβ the average C=O--H-N distance was found to be 3.2 Å, which is within an acceptable distance for the hydrogen bond in a β-turn, and the dihedral angles are consistent with a type II' β-turn. In this case, the tetrapeptide within the trans form of TApβ was found to exist in an extended conformation. This extended conformation lacks intramolecular hydrogen bonding, whereas the kinked structure of *trans*-TAp has one transannular hydrogen bond and a g-turn at the expense of a planar azobenzene. In comparison, the known *trans*-FLAp (Figure 2.4a) has a turn within the tetrapeptide and maintains the planarity of the azobenzene, while cis-FLAp forms a type II β-turn within the tetrapeptide.[16] Overall, when comparing these three macrocyclic designs, TApβ may be optimum as there is a clear structural distinction in the central tetrapeptide when the macrocycle contains a trans versus cis azobenzene isomer.
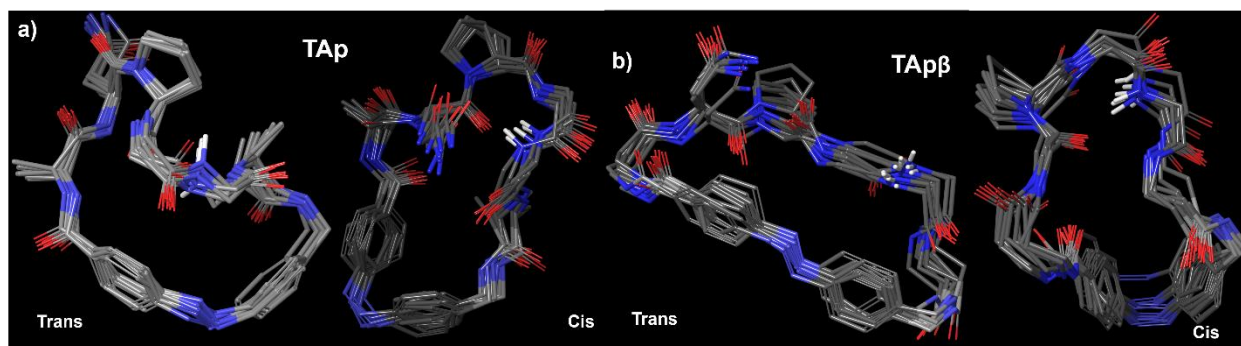
Figure 2.4   a) Overlay of ten time-sampled structures of the *trans*-TAp and *cis*-TAp macrocycles as obtained from restrained molecular dynamics simulations using NOESY data (Left). b) Ten overlaid time-sampled structures of *trans*-TApβ and *cis*-TApβ macrocycles (Right) using the same methodology as in a) (Asn sidechain is hidden in *cis*-TApβ to facilitate visualization).

2.3   Conclusion

Herein we describe the design and synthesis of two cyclic peptides, TAp and Tapβ, that incorporate a photo-isomerizable azobenzene moiety flanked by either alanine or β-alanine residues with a central tetrapeptide (AsnProGlyGly). Interestingly, the cyclization of the linear forms of these peptides was not successful when the azobenzene was in the trans form, with formation of a cyclic dimer or low yield of the macrocycle, respectively. These data suggest that the trans form of the Azo residue imparts some amount of ring strain to the macrocycle. This is in contrast to the previously described FLAp peptide that provided a modest yield for the cyclization even in the trans form. However, isomerization of the azobenzene to the cis conformation allowed for facile cyclization of both linear peptides in good to very good yields. The trans conformation of the Azo residue within these peptides was efficiently isomerized with light to the cis conformation. These cyclic peptides also showed steady thermal relaxation from the cis to trans form at 37°C over the course of a week. Importantly, the cis and trans conformations of the peptides show clear structural differences by 2D NMR spectroscopy in conjunction with restrained molecular dynamics. The cis isomers of both TAp and TApβ demonstrated β-turn conformations. Conversely, the trans isomers do not exhibit a β-turn structure; the tetrapeptide within TAp adopts a kinked structure, whereas this sequence within TApβ exists in a more extended conformation. The higher cyclization yield and greater structural distinction between the cis and trans forms for TApβ suggest that the βAla-Azo-βAla scaffold appears to be more promising for future use with biologically active β-turn sequences where control of receptor binding is desired.

2.4   Materials and Methods

2.4.1   Materials

All Fmoc-protected amino acids, the glycine p-alkoxybenzyl alcohol resin, HATU and PyOAP were purchased from Chem-Impex International. All solvents were purchased from Fisher Scientific. HPLC columns were the Luna C18 (250 x 21.20mm, 100 Å pore size, particle size 10 µm, Phenomenex) for Semi-preparative purification and Luna 5u C18 (250 x 4.60mm, 100 Å pore size, particle size 5 µm, Phenomenex). Traces for Semi-prep were run for 60 min at 12 ml/min flowrate and analytical traces were run for 30 min at 1.2 ml/min flowrate. The UPLC column was

a C18, Waters Acquity, (50.0 x 2.1 mm, particle size 1.7 µm). Traces on the UPLC were run for 10 min at 0.5 ml/min flowrate. All spectra were monitored at 214 nm.

2.4.2   General procedure for synthesis of FLAp, TAp and TApβ peptides

2.4.2.1 Linear Peptides

Synthesis of the L-FLAp, L-TAp, L-TApβ peptides was performed on glycine p-alkoxybenzyl alcohol resin (500 mg) in a 10 ml synthesis flask using solid phase peptide synthesis. The resin-bound Fmoc was deprotected using a 20% piperidine in DMF solution (5 ml) for 25 min. The resin was then washed with DMF, DCM, MEOH, DCM (3 x 5 ml) and treated with the desired Fmoc-protected amino acid (4 eq), HATU (4 eq) and DIEA (8 eq) in DMF for 2 hrs. The solution was drained, and the resin-bound sequence was washed with DMF, DCM, MEOH, DCM (3 x 5 ml). The subsequent resin-bound Fmoc was deprotected using a 20% piperidine in DMF solution (5 ml) for 25 min. After washing with DMF, DCM, MEOH, DCM (3 x 5 ml), the peptide was elongated with the next desired Fmoc-protected amino acid (4 eq), (HATU) (4 eq) and diisopropylethylamine (DIEA) (8 eq) in DMF for 2 hrs. Once the peptide sequence was complete the resin was washed with DMF, DCM, MEOH, DCM (3 x 5 ml), dried on vacuum and treated with a trifluoroacetic acid cocktail (5 ml) of trifluoroacetic acid, triisopropylsilane, water (95:2.5:2.5). The cleavage solution was drained into a tared 50 ml falcon tube and the remaining resin washed with trifluoroacetic acid (5 ml) and DCM (10 ml). The cleavage solution was evaporated under reduced pressure, and the peptide was precipitated using cold diethyl ether and centrifuged to a pellet. The ether was discarded, and the pellet was dried under vacuum, and the crude mass was determined. The crude peptides were purified on reverse phase HPLC using a Luna C18 semi-prep column with an eluent of solvent A (CH_3CN/0.1% TFA) and solvent B (Water/0.1% TFA). Crude L-FLAp was purified to homogeneity using a gradient of 10-30% Solvent A over 60 minutes with 214 nm and 254 nm detection and a 12 ml/min flowrate, while crude L-TAp and L-TApβ were purified at 10-25% Solvent A over 60 minutes with 214 nm and 254 nm detection and a 12 ml/min flowrate. The purified peptides were characterized by matrix assisted laser desorption ionization- time of flight (MALDI-TOF) mass spectrometry: L-FLAp (Expected mass - 865.4 m/z, Observed mass 866.1 m/z.) L-TAp (Expected mass - 723.2 m/z Observed mass 723.4 m/z). L-TApβ (Expected mass - 723.2 m/z Observed mass 723.4 m/z).

2.4.2.2 Cyclization

2.4.2.2.1   No isomerization prior to cyclization

The L-FLAp peptide (1 mM) was dissolved in DMSO (5 ml) stirred with (7-Azabenzotriazol-1-yloxy) tripyrrolidinophosphonium hexafluorophosphate (PyAOP) (35 µmol, 18 mg) and DIEA (70 µmol, 12 µl) in a 50 ml Falcon tube for 2 hours at room temperature. The resulting reaction solution was filtered through a 0.2 µm filter and purified directly by RP-HPLC using a Luna C18 semi-prep column with an eluent of solvent A (CH_3CN/0.1% TFA) and solvent B (Water/0.1% TFA), with a gradient of 5-50% Solvent A over 60 minutes with 214 nm and 254 nm detection and a 12 ml/min flowrate. The purified peptide was characterized by MALDI-TOF mass spectrometry: FLAp (Expected mass – 847.5 m/z, Observed mass 847.8 m/z.).

2.4.2.2.2   Isomerization prior to cyclization

L-TAp, and L-TApβ peptides (5 mg, 1 mM) were isomerized in DMSO for 15 mins in the Miniature Cyclonic Ultraviolet Photochemical Reactor (Mini-CUPR™) in a Quartz glass screw cap vial (5 ml). The resulting solution of predominantly cis azobenzene-containing peptide (80-90%) was stirred with (7-Azabenzotriazol-1-yloxy) tripyrrolidinophosphonium hexafluorophosphate (PyAOP) (35 µmol, 18 mg) and DIEA (70 µmol, 12 µl) in a 50 ml Falcon tube for 2 hours at room temperature.[52] The resulting reaction solution was filtered through a 0.2 µm filter and purified directly by RP-HPLC using a Luna C18 semi-prep column with an eluent of solvent A (CH_3CN/0.1% TFA) and solvent B (Water/0.1% TFA), with a gradient of 5-50% Solvent A over 60 minutes with 214 nm and 254 nm detection and a 12 ml/min flowrate.The purified peptides were characterized by MALDI-TOF mass spectrometry: TAp (Expected mass - 705.3 m/z Observed mass 705.7 m/z). TApβ (Expected mass – 705.3m/z Observed mass 705.7 m/z).

2.4.3   Thermal Isomerization of TAp and TApβ peptides

Cyclic peptides were solubilized (1 mM) in DMSO, then isomerized in the Mini-CUPR™ for two hours in a Quartz glass screw cap vial (5 ml). The predominantly cis solutions were analyzed by reverse phase UPLC using a Luna C18 analytical column with an eluent of solvent A (CH_3CN/0.1% TFA) and solvent B (Water/0.1% TFA) to determine the starting percentage of cis

and trans isomers in solution with a gradient of 10-25% Solvent A over 10 minutes with 214 nm and 254 nm detection and a 0.5 ml/min flowrate. The two peptides were incubated in a 37°C water bath with reverse phase UPLC measurements taken once a day, over the course of a week. The ratio of cis to trans isomers was quantified using reverse phase UPLC as described above.

2.4.4 NMR characterization of Cyclic TAp and TApβ Peptides

The cis and trans forms of TAp and TApβ were characterized on a Bruker Avance-III-800 MHz NMR. [1]H characterization was carried out in DMSO-d6 at 1 mM concentration with a H_2O cryoprobe, and shielded from the light. Two-dimensional NMR techniques were performed directly after the initial ^{1}H and ^{13}C experiments described below.

NMR spectra were obtained using a Bruker AV-III-800 spectrometer operating at 800 MHz for ^{1}H and 201 MHz for ^{13}C and equipped with a 5mm QCI Z-gradient cryoprobe. Bruker TopSpin 3.2 software was used for both data acquisition and processing. Samples were made up in conventional 5mm NMR tubes and were run at ca. 300K. Spectra were referenced to the chemical shift of the residual DMSO-d6 solvent peak (2.49 ppm for 1H, 39.5 ppm for 13C) (Table S1-4).

1D ^{1}H spectra were obtained using the following parameters: pulse program, zg30; sweep width, ca. 15 ppm; acquisition time, ca. 2.7 seconds; relaxation delay, 2 seconds; digital resolution of final spectrum, ca. 0.4 Hz.; number of scans, 8.

1D ^{13}C and ^{13}C DEPT-135 spectra were obtained using the following parameters: pulse program, zgpg30 and dept (respectively); sweep width, ca. 250 ppm; acquisition time, ca. 0.7 seconds; relaxation delay, 2 seconds; digital resolution of final spectrum, ca. 1.5 Hz.; number of scans, 4k – 12k, (depending on experiment and sample concentration), 1J(C-H) optimization (DEPT), 135 – 140 Hz.

2D ^{1}H COSY: pulse program, cosygpqf; number of scans per increment, 2; number of increments, 128; data acquisition mode, QF (magnitude mode).

2D ^{1}H TOCSY: pulse program, mlevph; mixing time, 80 milliseconds; number of scans per increment, 4; number of increments, 256; data acquisition mode, States-TPPI.

2D ^{1}H NOESY: pulse program, noesygpphpr; mixing time, 200 milliseconds; number of scans per increment, 8; number of increments, 256; data acquisition mode, States-TPPI.

2D ^{1}H-13C HSQC: pulse program, hsqcetgpsi2; 1J(C-H) optimization, 135 Hz.; number of scans per increment, 4 or 8; number of increments, 256; data acquisition mode, echo-antiecho.

2D ^{1}H-^{13}C HMBC: pulse program, clhmbcetgpl3nd; 1J(C-H) optimization, 135 Hz.; nJ(LR) optimization, 6 Hz.; number of scans per increment, 8; number of increments, 256; data acquisition mode, echo-antiecho.

For all 2D experiments the observation windows were optimized according to the locations of the relevant peaks as observed in the corresponding 1D spectra

2.4.5 Restrained Molecular Dynamics Simulations of cis and trans forms of TAp and TApβ

Restrained Molecular Dynamics simulations were performed using the Macromodel software package (Schrodinger, inc). NOE interactions obtained from NOESY spectra were implemented as distance constraints using flat-bottomed harmonic pseudopotentials. H-H distances were constrained to 3Å (±1Å) for those. NOE's observed to methylenes in which the diastereotopic protons could not be resolved, employed an H-C restraint of 4Å (±1.5Å). Stochastic dynamic simulations were performed using a modified AMBER forcefield at 300 K with an equilibration time of 50 ps and an evolution time of 200 ps, with sampling every 10 ps. The 20 conformers thus obtained formed a single cluster for each of the four structures studied, 10 overlays are shown in Figure 3.[54–57]

2.5 References

(1)   Jia, S.; Fong, W. K.; Graham, B.; Boyd, B. J. Photoswitchable Molecules in Long-Wavelength Light-Responsive Drug Delivery: From Molecular Design to Applications. *Chem. Mater.* **2018**, *30* (9), 2873–2887. https://doi.org/10.1021/acs.chemmater.8b00357.

(2)   Liu, R.; Yang, Y.; Cui, Q.; Xu, W.; Peng, R.; Li, L. A Diarylethene-Based Photoswitch and Its Photomodulation of the Fluorescence of Conjugated Polymers. *Chem. - A Eur. J.* **2018**, *24* (67), 17756–17766. https://doi.org/10.1002/chem.201803473.

(3)   Helmy, S.; Leibfarth, F. A.; Oh, S.; Poelma, J. E.; Hawker, C. J.; De Alaniz, J. R. Photoswitching Using Visible Light: A New Class of Organic Photochromic Molecules. *J. Am. Chem. Soc.* **2014**, *136* (23), 8169–8172. https://doi.org/10.1021/ja503016b.

(4)   Maly, K. E.; Wand, M. D.; Lemieux, R. P. Bistable Ferroelectric Liquid Crystal Photoswitch Triggered by a Dithienylethene Dopant. *J. Am. Chem. Soc.* **2002**, *124* (27), 7898–7899. https://doi.org/10.1021/ja025954z.

(5)   Blanco-Lomas, M.; Samanta, S.; Campos, P. J.; Woolley, G. A.; Sampedro, D. Reversible Photocontrol of Peptide Conformation with a Rhodopsin-like Photoswitch. *J. Am. Chem. Soc.* **2012**, *134* (16), 6960–6963. https://doi.org/10.1021/ja301868p.

(6)   Wiedbrauk, S.; Dube, H. Hemithioindigo-An Emerging Photoswitch. *Tetrahedron Lett.* **2015**, *56* (29), 4266–4274. https://doi.org/10.1016/j.tetlet.2015.05.022.

(7)   Dong, M.; Babalhavaeji, A.; Collins, C. V.; Jarrah, K.; Sadovski, O.; Dai, Q.; Woolley, G. A. Near-Infrared Photoswitching of Azobenzenes under Physiological Conditions. *J. Am. Chem. Soc.* **2017**, *139* (38), 13483–13486. https://doi.org/10.1021/jacs.7b06471.

(8)   Dong, M.; Babalhavaeji, A.; Samanta, S.; Beharry, A. A.; Woolley, G. A. Red-Shifting Azobenzene Photoswitches for in Vivo Use. *Acc. Chem. Res.* **2015**, *48* (10), 2662–2670. https://doi.org/10.1021/acs.accounts.5b00270.

(9)   Samanta, S.; Beharry, A. A.; Sadovski, O.; McCormick, T. M.; Babalhavaeji, A.; Tropepe, V.; Woolley, G. A. Photoswitching Azo Compounds in Vivo with Red Light. *J. Am. Chem. Soc.* **2013**, *135* (26), 9777–9784. https://doi.org/10.1021/ja402220t.

(10)   Beharry, A. A.; Woolley, G. A. Azobenzene Photoswitches for Biomolecules. *Chem. Soc. Rev.* **2011**, *40* (8), 4422–4437. https://doi.org/10.1039/c1cs15023e.

(11)   Kumita, J. R.; Smart, O. S.; Woolley, G. A. Photo-Control of Helix Content in a Short Peptide. *Proc. Natl. Acad. Sci. U. S. A.* **2000**, *97* (8), 3803–3808. https://doi.org/10.1073/pnas.97.8.3803.

(12)   Kumita, J. R.; Flint, D. G.; Woolley, G. A.; Smart, O. S. Achieving Photo-Control of Protein Conformation and Activity: Producing a Photo-Controlled Leucine Zipper. In *Faraday Discussions*; 2002; Vol. 122, pp 89–103. https://doi.org/10.1039/b200897a.

(13)   Kumita, J. R.; Flint, D. G.; Smart, O. S.; Woolley, G. A. Photo-Control of Peptide Helix Content by an Azobenzene Cross-Linker: Steric Interactions with Underlying Residues Are Not Critical. *Protein Eng.* **2002**, *15* (7), 561–569. https://doi.org/10.1093/protein/15.7.561.

(14)   Flint, D. G.; Kumita, J. R.; Smart, O. S.; Woolley, G. A. Using an Azobenzene Cross-Linker to Either Increase or Decrease Peptide Helix Content upon Trans-to-Cis Photoisomerization. *Chem. Biol.* **2002**, *9* (3), 391–397. https://doi.org/10.1016/S1074-5521(02)00109-6.

(15)   Chen, E.; Kumita, J. R.; Woolley, G. A.; Kliger, D. S. The Kinetics of Helix Unfolding of an Azobenzen Cross-Linked Peptide Probed by Nanosecond Time-Resolved Optical Rotatory Dispersion. *J. Am. Chem. Soc.* **2003**, *125* (41), 12443–12449. https://doi.org/10.1021/ja030277+.

(16)   Ulysse, L.; Cubillos, J.; Chmielewski, J. Photoregulation of Cyclic Peptide Conformation. *J. Am. Chem. Soc.* **1995**, *117* (32), 8466–8467. https://doi.org/10.1021/ja00137a023.

(17)   Ulysse, L. G.; Chmielewski, J. A Light-Activated β-Turn Scaffold within a Somatostatin Analog: NMR Structure and Biological Activity. *Chem. Biol. Drug Des.* **2006**, *67* (2), 127–136. https://doi.org/10.1111/j.1747-0285.2005.00337.x.

(18)   Yeoh, Y. Q.; Yu, J.; Polyak, S. W.; Horsley, J. R.; Abell, A. D. Photopharmacological Control of Cyclic Antimicrobial Peptides. *ChemBioChem* **2018**, *19* (24), 2591–2597. https://doi.org/10.1002/cbic.201800618.

(19)   Hoppmann, C.; Seedorff, S.; Richter, A.; Fabian, H.; Schmieder, P.; Rück-Braun, K.; Beyermann, M. Light-Directed Protein Binding of a Biologically Relevant β-Sheet. *Angew. Chemie - Int. Ed.* **2009**, *48* (36), 6636–6639. https://doi.org/10.1002/anie.200901933.

(20)   Doran, T. M.; Nilsson, B. L. Incorporation of an Azobenzene β-Turn Peptidomimetic into Amyloid-β to Probe Potential Structural Motifs Leading to β-Sheet Self-Assembly. In *Methods in Molecular Biology*; 2018; Vol. 1777, pp 387–406. https://doi.org/10.1007/978-1-4939-7811-3_25.

(21)   Nuti, F.; Gellini, C.; Larregola, M.; Squillantini, L.; Chelli, R.; Salvi, P. R.; Lequin, O.; Pietraperzia, G.; Papini, A. M. A Photochromic Azobenzene Peptidomimetic of a β-Turn Model Peptide Structure as a Conformational Switch. *Front. Chem.* **2019**, *7* (MAR), 180. https://doi.org/10.3389/fchem.2019.00180.

(22)   Gascón-Moya, M.; Pejoan, A.; Izquierdo-Serra, M.; Pittolo, S.; Cabré, G.; Hernando, J.; Alibés, R.; Gorostiza, P.; Busqué, F. An Optimized Glutamate Receptor Photoswitch with Sensitized Azobenzene Isomerization. *J. Org. Chem.* **2015**, *80* (20), 9915–9925. https://doi.org/10.1021/acs.joc.5b01402.

(23)   Kuil, J.; van Wandelen, L. T. M.; de Mol, N. J.; Liskamp, R. M. J. A Photoswitchable ITAM Peptidomimetic: Synthesis and Real Time Surface Plasmon Resonance (SPR) Analysis of the Effects of Cis-Trans Isomerization on Binding. *Bioorganic Med. Chem.* **2008**, *16* (3), 1393–1399. https://doi.org/10.1016/j.bmc.2007.10.049.

(24)   Kuil, J.; Van Wandelen, L. T. M.; De Mol, N. J.; Liskamp, R. M. J. Switching between Low and High Affinity for the Syk Tandem SH2 Domain by Irradiation of Azobenzene Containing ITAM Peptidomimetics. *J. Pept. Sci.* **2009**, *15* (10), 685–691. https://doi.org/10.1002/psc.1173.

(25) Schütt, M.; Krupka, S. S.; Milbradt, A. G.; Deindl, S.; Sinner, E. K.; Oesterhelt, D.; Renner, C.; Moroder, L. Photocontrol of Cell Adhesion Processes: Model Studies with Cyclic Azobenzene-RGD Peptides. *Chem. Biol.* **2003**, *10* (6), 487–490. https://doi.org/10.1016/S1074-5521(03)00128-5.

(26) Auernheimer, J.; Dahmen, C.; Hersel, U.; Bausch, A.; Kessler, H. Photoswitched Cell Adhesion on Surfaces with RGD Peptides. *J. Am. Chem. Soc.* **2005**, *127* (46), 16107–16110. https://doi.org/10.1021/ja053648q.

(27) Milbradt, A. G.; Löweneck, M.; Krupka, S. S.; Reif, M.; Sinner, E. K.; Moroder, L.; Renner, C. Photomodulation of Conformational States. IV. Integrin-Binding RGD-Peptides with (4-Aminomethyl)Phenylazobenzoic Acid as Backbone Constituent. *Biopolymers* **2005**, *77* (5), 304–313. https://doi.org/10.1002/bip.20226.

(28) Yamana, K.; Yoshikawa, A.; Noda, R.; Nakano, H. Synthesis and Binding Properties of Oligonucleotides Containing an Azobenzene Linker. *Nucleosides and Nucleotides* **1998**, *17* (1–3), 233–242. https://doi.org/10.1080/07328319808005172.

(29) Yamana, K.; Kan, K.; Nakano, H. Synthesis of Oligonucleotides Containing a New Azobenzene Fragment with Efficient Photoisomerizability. *Bioorganic Med. Chem.* **1999**, *7* (12), 2977–2983. https://doi.org/10.1016/S0968-0896(99)00244-8.

(30) Erdélyi, M.; Karlén, A.; Gogoll, A. A New Tool in Peptide Engineering: A Photoswitchable Stilbene-Type β-Hairpin Mimetic. *Chem. - A Eur. J.* **2005**, *12* (2), 403–412. https://doi.org/10.1002/chem.200500648.

(31) Zhang, Y.; Zhang, Y.; Song, G.; He, Y.; Zhang, X.; Liu, Y.; Ju, H. A DNA–Azobenzene Nanopump Fueled by Upconversion Luminescence for Controllable Intracellular Drug Release. *Angew. Chemie - Int. Ed.* **2019**, *58* (50), 18375–18379. https://doi.org/10.1002/anie.201909870.

(32) Murawska, G. M.; Poloni, C.; Simeth, N. A.; Szymanski, W.; Feringa, B. L. Comparative Study of Photoswitchable Zinc-Finger Domain and AT-Hook Motif for Light-Controlled Peptide–DNA Binding(1) Murawska, G. M.; Poloni, C.; Simeth, N. A.; Szymanski, W.; Feringa, B. L. Comparative Study of Photoswitchable Zinc-Finger Domain and AT-. *Chem. - A Eur. J.* **2019**, *25* (19), 4965–4973. https://doi.org/10.1002/chem.201900090.

(33) Ulysse, L.; Chmielewski, J. The Synthesis of a Light-Switchable Amino Acid for Inclusion into Conformationally Mobile Peptides. *Bioorganic Med. Chem. Lett.* **1994**, *4* (17), 2145–2146. https://doi.org/10.1016/S0960-894X(01)80118-9.

(34) Wachtveitl, J.; Spörlein, S.; Satzger, H.; Fonrobert, B.; Renner, C.; Behrendt, R.; Oesterhelt, D.; Moroder, L.; Zinth, W. Ultrafast Conformational Dynamics in Cyclic Azobenzene Peptides of Increased Flexibility. *Biophys. J.* **2004**, *86* (4), 2350–2362. https://doi.org/10.1016/S0006-3495(04)74292-7.

(35) Rudolph-Böhner, S.; Krüger, M.; Oesterhelt, D.; Moroder, L.; Nägele, T.; Wachtveitl, J. Photomodulation of Conformational States of P-Phenylazobenzyloxycarbonyl-L-Proline and Related Peptides. *J. Photochem. Photobiol. A Chem.* **1997**, *105* (2–3), 235–248. https://doi.org/10.1016/S1010-6030(96)04497-8.

(36) Behrendt, R.; Renner, C.; Schenk, M.; Wang, F.; Wachtveitl, J.; Oesterhelt, D.; Moroder, L. Photomodulation of the Conformation of Cyclic Peptides with Azobenzene Moieties in the Peptide Backbone. *Angew. Chemie - Int. Ed.* **1999**, *38* (18), 2771–2774. https://doi.org/10.1002/(SICI)1521-3773(19990917)38:18<2771::AID-ANIE2771>3.0.CO;2-W.

(37) Renner, C.; Behrendt, R.; Spörlein, S.; Wachtveitl, J.; Moroder, L. Photomodulation of Conformational States. I. Mono- and Bicyclic Peptides with (4-Amino)Phenylazobenzoic Acid as Backbone Constituent. *Biopolymers* **2000**, *54* (7), 489–500. https://doi.org/10.1002/1097-0282(200012)54:7<489::AID-BIP20>3.0.CO;2-F.

(38) Renner, C.; Behrendt, R.; Heim, N.; Moroder, L. Photomodulation of Conformational States. III. Water-Soluble Bis-Cysteinyl-Peptides with (4-Aminomethyl) Phenylazobenzoic Acid as Backbone Constituent. *Biopolymers* **2002**, *63* (6), 382–393. https://doi.org/10.1002/bip.10127.

(39) Ruiz-Gómez, G.; Tyndall, J. D. A.; Pfeiffer, B.; Abbenante, G.; Fairlie, D. P. Update 1 of: Over One Hundred Peptide-Activated g Protein-Coupled Receptors Recognize Ligands with Turn Structure. *Chem. Rev.* **2010**, *110* (4), 793–826. https://doi.org/10.1021/cr900344w.

(40) Whitby, L. R.; Boger, D. L. Comprehensive Peptidomimetic Libraries Targeting Protein-Protein Interactions. *Acc. Chem. Res.* **2012**, *45* (10), 1698–1709. https://doi.org/10.1021/ar300025n.

(41) Eckhardt, B.; Grosse, W.; Essen, L. O.; Geyer, A. Structural Characterization of a β-Turn Mimic within a Protein-Protein Interface. *Proc. Natl. Acad. Sci. U. S. A.* **2010**, *107* (43), 18336–18341. https://doi.org/10.1073/pnas.1004187107.

(42) Pelay-Gimeno, M.; Glas, A.; Koch, O.; Grossmann, T. N. Structure-Based Design of Inhibitors of Protein-Protein Interactions: Mimicking Peptide Binding Epitopes. *Angew. Chemie - Int. Ed.* **2015**, *54* (31), 8896–8927. https://doi.org/10.1002/anie.201412070.

(43) Glas, A.; Bier, D.; Hahne, G.; Rademacher, C.; Ottmann, C.; Grossmann, T. N. Constrained Peptides with Target-Adapted Cross-Links as Inhibitors of a Pathogenic Protein-Protein Interaction. *Angew. Chemie - Int. Ed.* **2014**, *53* (9), 2489–2493. https://doi.org/10.1002/anie.201310082.

(44) Suat, K.; Jois, S. Design of β-Turn Based Therapeutic Agents. *Curr. Pharm. Des.* **2003**, *9* (15), 1209–1224. https://doi.org/10.2174/1381612033454900.

(45) Zhang, J.; Xiong, C.; Ying, J.; Wang, W.; Hruby, V. J. Stereoselective Synthesis of Novel Dipeptide β-Turn Mimetics Targeting Melanocortin Peptide Receptors. *Org. Lett.* **2003**, *5* (17), 3115–3118. https://doi.org/10.1021/ol0351347.

(46) Deike, S.; Rothemund, S.; Voigt, B.; Samantray, S.; Strodel, B.; Binder, W. H. β-Turn Mimetic Synthetic Peptides as Amyloid-β Aggregation Inhibitors. *Bioorg. Chem.* **2020**, *101*, 104012. https://doi.org/10.1016/j.bioorg.2020.104012.

(47) Brahimi, F.; Malakhov, A.; Lee, H. B.; Pattarawarapan, M.; Ivanisevic, L.; Burgess, K.; Saragovi, H. U. A Peptidomimetic of NT-3 Acts as a TrkC Antagonist. *Peptides* **2009**, *30* (10), 1833–1839. https://doi.org/10.1016/j.peptides.2009.07.015.

(48) Brahimi, F.; Ko, E.; Malakhov, A.; Burgess, K.; Saragovi, H. U. Combinatorial Assembly of Small Molecules into Bivalent Antagonists of TrkC or TrkA Receptors. *PLoS One* **2014**, *9* (3), e89617. https://doi.org/10.1371/journal.pone.0089617.

(49) Zaccaro, M. C.; Hong, B. L.; Pattarawarapan, M.; Xia, Z.; Caron, A.; L'Heureux, P. J.; Bengio, Y.; Burgess, K.; Saragovi, H. U. Selective Small Molecule Peptidomimetic Ligands of TrkC and TrkA Receptors Afford Discrete or Complete Neurotrophic Activities. *Chem. Biol.* **2005**, *12* (9), 1015–1028. https://doi.org/10.1016/j.chembiol.2005.06.015.

(50) Shimizu, T. Self-Assembly of Discrete Organic Nanotubes. *Bull. Chem. Soc. Jpn.* **2018**, *91* (4), 623–668. https://doi.org/10.1246/bcsj.20170424.

(51) Day, K.; Schneible, J. D.; Young, A. T.; Pozdin, V. A.; Van Den Driessche, G.; Gaffney, L. A.; Prodromou, R.; Freytes, D. O.; Fourches, D.; Daniele, M.; et al. Photoinduced Reconfiguration to Control the Protein-Binding Affinity of Azobenzene-Cyclized Peptides. *J. Mater. Chem. B* **2020**, *8* (33), 7413–7427. https://doi.org/10.1039/d0tb01189d.

(52) Albericio, F.; Cases, M.; Alsina, J.; Triolo, S. A.; Carpino, L. A.; Kates, S. A. On the Use of PyAOP, a Phosphonium Salt Derived from HOAt, in Solid-Phase Peptide Synthesis. *Tetrahedron Lett.* **1997**, *38* (27), 4853–4856. https://doi.org/10.1016/S0040-4039(97)01011-3.

(53) Eakins, G.S.; Niedrauer, M.L.; Lipton, M. A. Innovation Infosheet Photochemical Reactor for Solid Phase Synthesis. U.S. Patent 63,029,491, 2020.

(54) Mohamadi, F.; Richards, N. G. J.; Guida, W. C.; Liskamp, R.; Lipton, M.; Caufield, C.; Chang, G.; Hendrickson, T.; Still, W. C. Macromodel—an Integrated Software System for Modeling Organic and Bioorganic Molecules Using Molecular Mechanics. *J. Comput. Chem.* **1990**, *11* (4), 440–467. https://doi.org/10.1002/jcc.540110405.

(55) Van Gunsteren, W. F.; Berendsen, H. J. C. A Leap-Frog Algorithm for Stochastic Dynamics. *Mol. Simul.* **1988**, *1* (3), 173–185. https://doi.org/10.1080/08927028808080941.

(56) Weiner, S. J.; Kollman, P. A.; Singh, U. C.; Case, D. A.; Ghio, C.; Alagona, G.; Profeta, S.; Weiner, P. A New Force Field for Molecular Mechanical Simulation of Nucleic Acids and Proteins. *J. Am. Chem. Soc.* **1984**, *106* (3), 765–784. https://doi.org/10.1021/ja00315a051.

(57)   Weiner, S. J.; Kollman, P. A.; Nguyen, D. T.; Case, D. A. An All Atom Force Field for Simulations of Proteins and Nucleic Acids. *J. Comput. Chem.* **1986**, *7* (2), 230–252. https://doi.org/10.1002/jcc.540070216.

CHAPTER 3.   PHOTO-ACTIVE CONTROL OF AN ALPHA-AMYLASE INHIBITION BASED ON TENDAMISTAT.

3.1   Introduction

The β-turn motif is an important secondary structure that affects protein folding and protein-protein interactions.[1,2] This motif activates a wide array of biological processes including hormone secretion, antimicrobial clearance, and neurological pathways within the body.[3,4] Some of the most notable peptide examples for this class of activation include somatostatin,[5–7] oxytocin,[8,9] daptomycin,[10] polymixin B/E,[11,12] and urotensin II.[13] One of the key characteristics of these peptides are the cyclic nature that help to facilitate β-turn formation and thus receptor activation.[14,15]

Tendamistat is a 74 residue protein that was isolated from the *Streptomyces tendae*.[16] The protein was shown to inhibit α-amylase from cleavage of the 1,4-linkages of polysaccharide chains in a competitive manner (Figure 3.1).[16,17] Inhibition is mediated by a β-turn ($S_{17}WRY_{20}$) of tendamistat.[18,19] This turn sequence blocks the active site of α-amylase with an K_i value as low as 14 µM.[20] Cyclic peptide inhibitors have been explored to mimic the active turn within tendamistat.[18–23] Previous work focused on creating a photo-active cyclic peptide scaffold that can selectively "turn on" β-turns.[24,25] In the work described herein, we sought to create a photo-switch to control the activity of α-amylase, using a β-turn inducing scaffold.
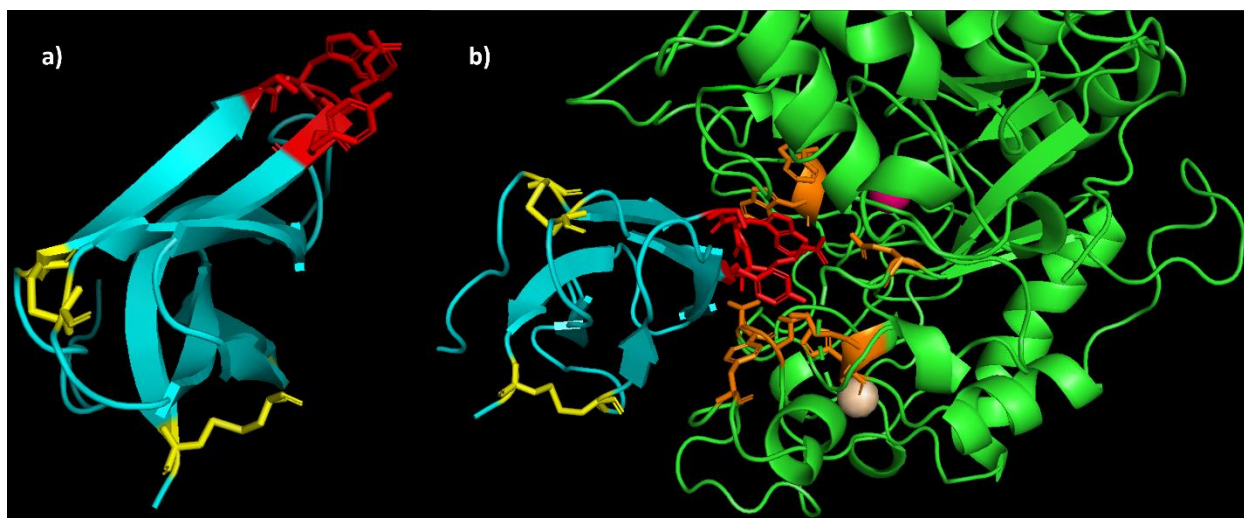
Figure 3.1a) Structural representation of tendamistat from *S. tendae,* with the disulfides (yellow) and the active turn residues (red) depicted. b) Interaction of tendamistat within the enzyme active site of α-amylase, with enzyme active site residues (orange) and tendamistat active residues (red) displayed, along with ions (purple and tan)

3.2   Results and Discussion

3.2.1   Design of Photo-switchable Tendamistat Mimic TSβ

The goal of this designed peptide mimic is to manipulate the β-turn sequence of tendamistat ($S_{17}WRY_{20}$) that corresponds to its inhibitory mode of action.[16] To achieve this the photo-switchable β-turn manipulating scaffold, TApβ, will be modified using the tendamistat active sequence to produce tendamistat β (TSβ) (Figure 3.2). The overall hypothesis of this design is that the cis conformation of the photo-switchable drug scaffold will promote a β-turn conformationin the tendamistat peptide, thereby inhibiting α-amylase. The trans conformation of the scaffold should promote a more elongated tendamistat peptide backbone, which should be a less active inhibitor. This manipulation of the β-turn conformation should therefore allow for selective control of α-amylase activity.
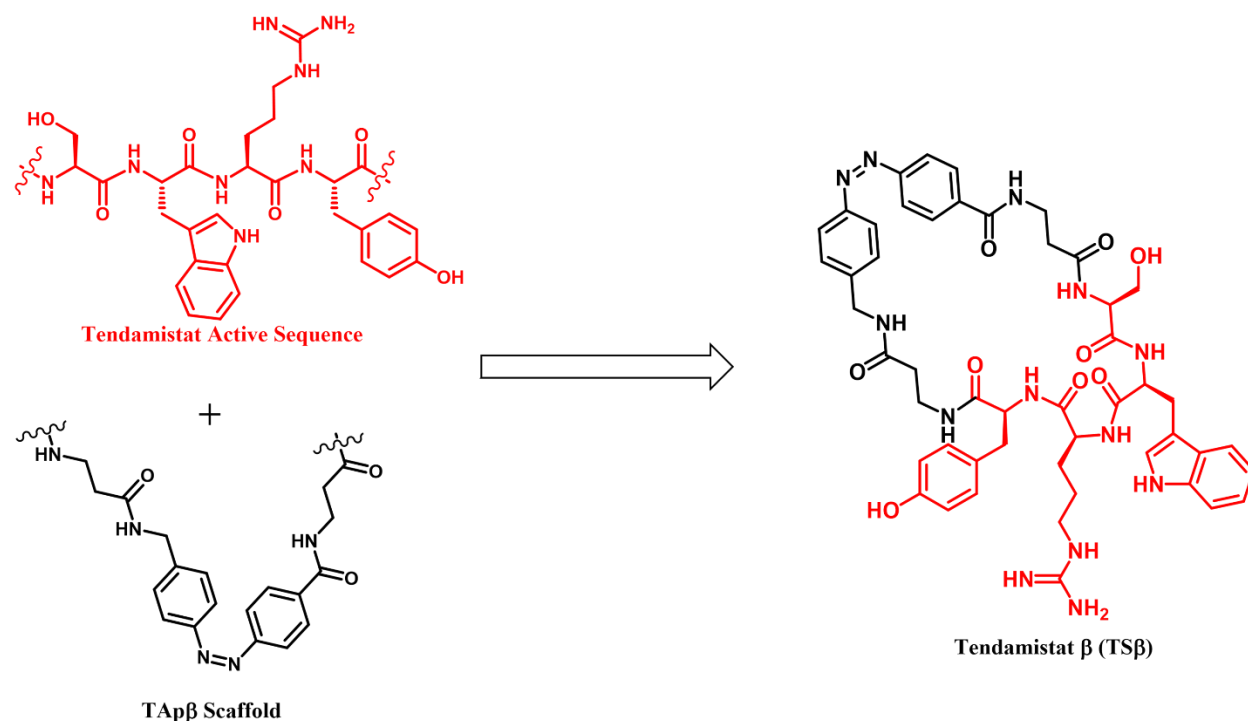
Figure 3.2. Combination of the photo-switchable peptide scaffold from TApβ with the tendamistat active β-turn sequence to form a new photo-switchable, biologically active peptide TSβ.

3.2.2 Synthesis of TSβ and Tendamistat Mimic Peptides

To determine the effectiveness of a photo-switchable cyclic tendamistat peptides, three different peptides were synthesized, a literature hexapeptide control (Bartlett control),[20] a linear photo-switchable tendamistat peptide (L-TSβ), and a cyclic photo-switchable tendamistat peptide (TSβ) (Figure 3.2). Synthesis of the Bartlett control peptide (Ac-Phe-Ser-Trp-Arg-Tyr-dPro-NH$_2$) was performed on Rink amide Chemmatrix resin, using standard solid phase peptide synthesis, and HATU as a coupling agent. The synthesis of L-TSβ and TSβ was carried out on 2-chlorotrityl resin, loaded with Fmoc-protected tyrosine, using standard solid phase peptide synthesis, and HATU as coupling agent. The Bartlett control and L-TSβ were treated with a trifluoroacetic acid cocktail upon completion of the sequence to concomitantly remove the protecting groups and cleave the peptides from the resin. The peptides were purified to homogeneity on reverse phase HPLC and characterized by MALDI-TOF mass spectrometry to afford the Bartlett control and L-TSβ peptides in 80% and 10% yield, respectively.

The TSβ peptide was cleaved from the resin using a 30% hexafluoroisopropanol in dichloromethane, to maintain the sidechain protecting groups and prevent cross-reactivity during cyclization. The peptide was used without further purification in the next steps. The TSβ peptide was isomerized to the cis conformation using a cyclonic ultraviolet photochemical reactor (Mini-CUPR), followed by cyclization using PyAOP and DIEA in DMSO (Figure 3.3).[25] The cyclic peptide was purified to homogeneity by RP-HPLC, followed by removal of the protecting groups using a cleavage cocktail described above. The now deprotected cyclic TSβ was purified to homogeneity by RP-HPLC, providing a 15 % yield and characterized by MALDI-TOF mass spectrometry.

Figure 3.3. Schematic of the TSβ synthesis from the protected linear precursor

3.2.3 Photoisomerization of Photo-switchable Tendamistat Mimics

The peptides (1 mM, MOPS buffer, pH 6.9) were photolyzed within the mini-CUPR to convert the photo-switchable peptides from their trans conformation to the cis and assess photostationary states.[25,26] The L-TSβ peptide was optimally converted to cis conformation after 3.5 hrs of UV stimulation at a level of 60% cis (Figure 3.4a). The TSβ peptide was optimally converted to cis conformation after 15 mins, but to a 66% conversion to cis (Figure 3.4b). Additional photolysis did not increase the percentage of the cis conformation. This lower level of conversion to cis was lower than that observed for the TApβ peptide (86% conversion). The

decrease in photo-conversion could be due to the increased steric effect from the bulkier sidechains, as well as potential aromatic interactions of the tryptophan and tyrosine residues, as compared to proline and glycine in TApβ. The L-TSβ-and the TSβ peptides exhibited full conversion to the trans conformation when incubated at 37°C for 48 hrs (Figure 3.4). These data demonstrate that the two sets of peptides can interconvert between the cis and trans conformations using light and heat, respectively.
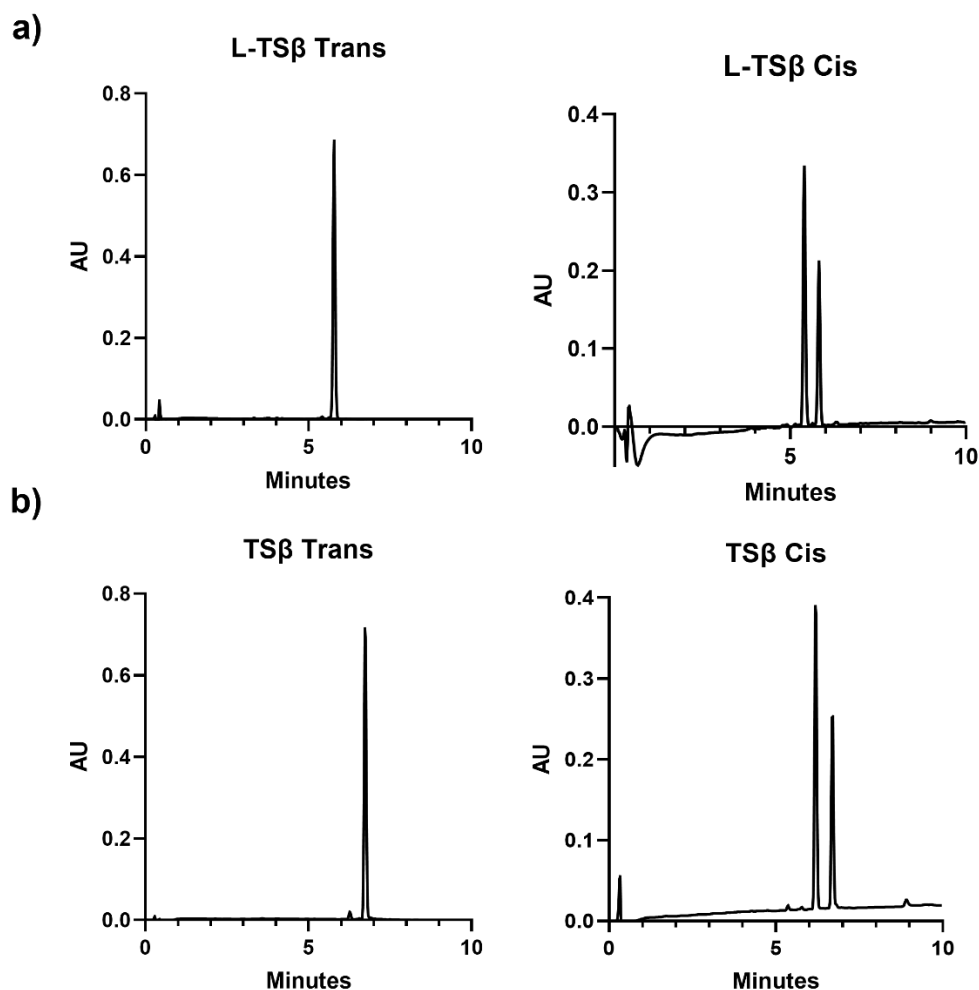

Figure 3.4 a) UPLC of L-TSβ trans (left) after 37°C incubation for 48 hrs and cis (right) after 3.5 hrs of UV photolysis. b) UPLC of TSβ trans (left) after 37°C incubation for 48 hrs and cis (right) after 15 mins of UV photolysis.

3.2.4 Inhibition of α-Amylase using Photo-switchable Tendamistat Mimics

The hypothesis of this work is that incorporating the active β-turn sequence of tendamistat, into the β-turn inducing scaffold of TApβ, should allow for photo-activatable α-amylase inhibition. The three sets of peptides were tested against α-amylase using the EnzChek ® Ultra Amylase Assay Kit from Thermo Fisher (Figure 3.5), the Bartlett control peptide, the linear L-TSβ peptide in its cis and trans form, and the cyclic TSβ peptide in its cis and trans form. All peptides demonstrated a concentration dependent increase in inhibition of α-amylase, with the L-TSβ cis and trans peptides demonstrating the best potency, followed by TSβ trans, TSβ cis, and the Bartlett control. The Bartlett control peptide exhibited an IC_{50} that was about 35-fold worse than the L-TSβ peptides (Table 3.1) with and IC_{50} of 867 µM. When comparing the L-TSβ peptides in their cis and trans conformations, both showed similar activity in inhibiting α-amylase with IC_{50} values around 25 µM. When comparing the cis and trans conformations of the cyclic tendamistat mimic TSβ there were some interesting results. The cis conformation of the cyclic peptide, which was hypothesized to be the more active form, was about 2.8-fold less active than the trans conformation of the cyclic mimic, at 113 µM and 40.2 µM, respectively. The cyclic peptides also showed lesser activity compared to the linear precursor of these peptides. Due to unknown peptide dynamics and receptor binding within the active sight of the TSβ peptide, it remains difficult to dissect the reasons for these results. The tendamistat β-turn peptide has a distorted type I β-turn, while the TApβ sequence showed a type II' β-turn character. Based on the α-amylase inhibition data of the tendamistat sequences, it appears that the cyclic peptide scaffold does not perform well with this system.
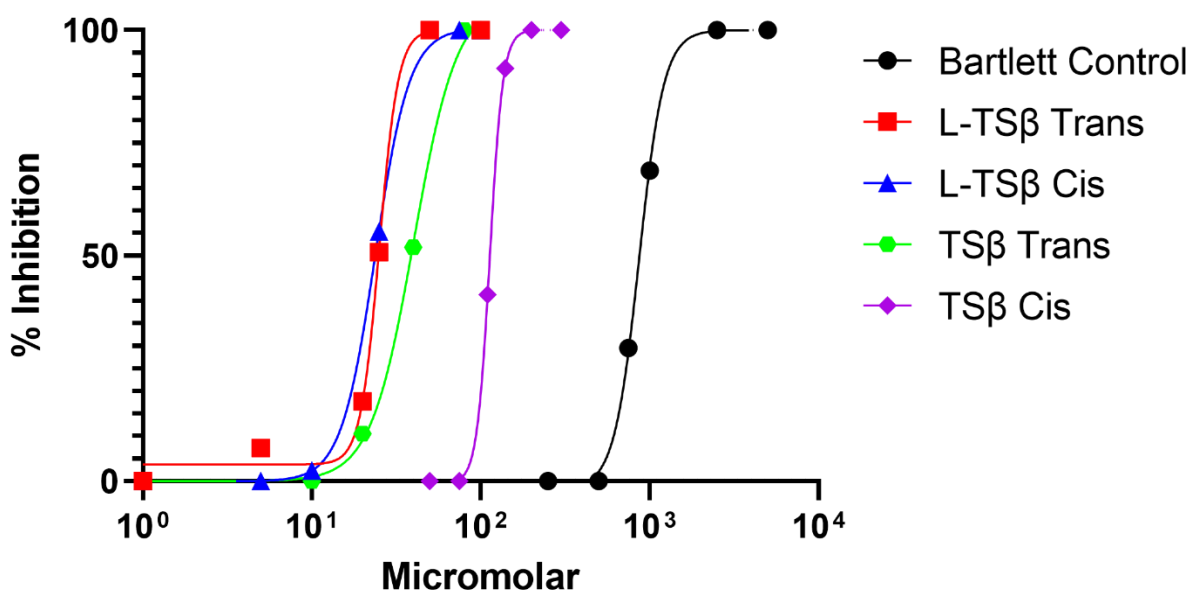
Figure 3.5   Inhibition of α-amylase (10 mU) with the three sets of peptides (Bartlett control, L-TSβ and TSβ)

Table 3.1   IC$_{50}$ values of the tendamistat mimics as inhibitors of α-amylase (10 mU)

	Bartlett Control	L-TSβ Trans	L-TSβ Cis	Trans	Cis
IC50 (µM)	867 ± 55	25.2 ± 3.6	23.8 ± 0.4	40.2 ± 13	113 ± 0.5

3.3   Conclusions

Herein, the design and synthesis of a biologically active, photo-switchable cyclic peptide containing an α-amylase inhibitory sequence, TSβ, using the scaffold from TApβ is described. The cyclic peptide was synthesized in low yields, despite mostly successful photoisomerization of the trans linear tendamistat peptide to the cis conformation prior to cyclization. The trans cyclic peptide showed slightly less efficient isomerization to the cis form, as compared to its TApβ counterpart, potentially due to the increased structural complexity of the sequence. The inhibitory data observed from TSβ against α-amylase contradicts the hypothesis that the cis confirmation of the cyclic peptide would be the more active form of the photo-switchable construct, being 2.8-fold less active than the trans conformation. The linear precursor of the TSβ peptide, L-TSβ, also

exhibited more activity than its cyclic counterpart. These data may be due to an enforced conformation for the β-turn within the cyclic peptide that is not optimal due to the rigid azobenzene scaffold. As such, we conclude that the tendamistat sequence isn't suitable for this cyclic peptide construct.

3.4   Materials and Methods

3.4.1   Materials

All Fmoc-protected amino acids, HATU and PyOAP were purchased from Chem-Impex International. H-Rink Chem Matrix Rink amide resin (0.45 mmol/g) was purchased from Pcas Biomatrix Inc and Fmoc-Tyr(OtBu) 2-chlorotrityl resin (0.8 mmol/g) was purchased from Advanced Chemtech. All solvents were purchased from Fisher Scientific. HPLC columns were the Luna C18 (250 x 21.20mm, 100 Å pore size, particle size 10 µm, Phenomenex) for Semi-preparative purification and Luna C18 (250 x 4.60mm, 100 Å pore size, particle size 5 µm, Phenomenex) for analytical quantification. Traces for Semi-prep were run for 60 min at 12 ml/min flowrate and analytical traces were run for 30 min at 1.2 ml/min flowrate. The UPLC column was a C18, Waters Acquity, (50.0 x 2.1 mm, particle size 1.7 µm). Traces on the UPLC were run for 10 min at 0.5 ml/min flowrate. All spectra were monitored at 214 nm.

3.4.2   Synthesis of the Bartlett control

Synthesis of the Bartlett control peptide (Ac-Phe-Ser-Trp-Arg-Tyr-dPro-NH$_2$) was performed on Chemmatrix Rink Amide resin (200 mg) in a 10 ml synthesis flask using solid phase peptide synthesis. The resin was treated with the desired Fmoc-protected amino acid (4 eq), 1-[bis(dimethylamino)methylene]-1H-1,2,3-triazolo[4,5-b]   pyridinium   3-oxide hexafluorophosphate (HATU) (4 eq) and DIEA (8 eq) in DMF for 2 hrs. The solution was drained, and the resin-bound sequence was washed with DMF, DCM, MEOH, DCM (3 x 5 ml). The resin-bound Fmoc was deprotected using a 20% piperidine in DMF solution (5 ml) for 25 min. After washing with DMF, DCM, MEOH, DCM (3 x 5 ml), the peptide was elongated with the next desired Fmoc-protected amino acid (4 eq), (HATU) (4 eq) and diisopropylethylamine (DIEA) (8 eq) in DMF for 2 hrs. After the final residue was coupled, the Fmoc was removed using 20% piperidine in DMF and the N-terminus peptide was protected with an acetyl cap by adding 5%

Ac$_2$O and 8.5% DIEA in DMF for 25 minutes. Once the peptide sequence was complete the resin was washed with DMF, DCM, MEOH, DCM (3 x 5 ml), dried on vacuum and treated with a trifluoroacetic acid cocktail (5 ml) of trifluoroacetic acid, triisopropylsilane, water (95:2.5:2.5). The cleavage solution was drained into a tared 50 ml falcon tube and the remaining resin washed with trifluoroacetic acid (5 ml) and DCM (10 ml). The cleavage solution was evaporated under reduced pressure, and the peptide was precipitated using cold diethyl ether and centrifuged to a pellet. The ether was discarded, and the pellet was dried under vacuum, and the crude mass was determined. The crude peptide was purified on reverse phase HPLC using a Luna C18 semi-prep column with an eluent of solvent A (CH$_3$CN/0.1% TFA) and solvent B (Water/0.1% TFA). The crude Bartlett control peptide was purified to homogeneity using a gradient of 10-60% Solvent A over 60 minutes with 214 nm and 254 nm detection and a 12 ml/min flowrate. The purified peptide was characterized by matrix assisted laser desorption ionization- time of flight (MALDI-TOF) mass spectrometry: Bartlett control (Expected mass – 897.0 m/z, Observed mass 897.1 m/z.)

3.4.3   Synthesis of linear tendamistat β (L-TSβ)

Synthesis of the L-TSβ peptide was performed on Fmoc-Tyr(OtBu) 2-chlorotrityl resin (100 mg) in a 10 ml synthesis flask using solid phase peptide synthesis. The resin-bound Fmoc was deprotected using a 20% piperidine in DMF solution (5 ml) for 25 min. The resin was then washed with DMF, DCM, MEOH, DCM (3 x 5 ml) and treated with the desired Fmoc-protected amino acid (4 eq), HATU (4 eq) and DIEA (8 eq) in DMF for 2 hrs. The solution was drained, and the resin-bound sequence was washed with DMF, DCM, MEOH, DCM (3 x 5 ml). The subsequent resin-bound Fmoc was deprotected using a 20% piperidine in DMF solution (5 ml) for 25 min. After washing with DMF, DCM, MEOH, DCM (3 x 5 ml), the peptide was elongated with the next desired Fmoc-protected amino acid (4 eq), (HATU) (4 eq) and diisopropylethylamine (DIEA) (8 eq) in DMF for 2 hrs. Once the peptide sequence was complete the resin was washed with DMF, DCM, MEOH, DCM (3 x 5 ml), dried on vacuum and treated with a trifluoroacetic acid cocktail (5 ml) of trifluoroacetic acid, triisopropylsilane, water (95:2.5:2.5). The cleavage solution was drained into a tared 50 ml falcon tube and the remaining resin washed with trifluoroacetic acid (5 ml) and DCM (10 ml). The cleavage solution was evaporated under reduced pressure, and the peptide was precipitated using cold diethyl ether and centrifuged to a pellet. The ether was discarded, and the pellet was dried under vacuum, and the crude mass was determined. The crude

peptide was purified on reverse phase HPLC using a Luna C18 semi-prep column with an eluent of solvent A (CH₃CN/0.1% TFA) and solvent B (Water/0.1% TFA). The L-TSβ peptide was purified to homogeneity using a gradient of 15-35% Solvent A over 60 minutes with 214 nm and 254 nm detection and a 12 ml/min flowrate. The purified peptide was characterized by matrix assisted laser desorption ionization- time of flight (MALDI-TOF) mass spectrometry: L-TSβ (Expected mass – 990.1 m/z, Observed mass 990.8 m/z.)

3.4.4 Synthesis of protected linear tendamistat β (L-TSβ protected)

Synthesis of the linear precursor TSβ peptide was performed on Fmoc-Tyr(OtBu) 2-chlorotrityl resin (100 mg) in a 10 ml synthesis flask using solid phase peptide synthesis. The resin-bound Fmoc was deprotected using a 20% piperidine in DMF solution (5 ml) for 25 min. The resin was then washed with DMF, DCM, MEOH, DCM (3 x 5 ml) and treated with the desired Fmoc-protected amino acid (4 eq), HATU (4 eq) and DIEA (8 eq) in DMF for 2 hrs. The solution was drained, and the resin-bound sequence was washed with DMF, DCM, MEOH, DCM (3 x 5 ml). The subsequent resin-bound Fmoc was deprotected using a 20% piperidine in DMF solution (5 ml) for 25 min. After washing with DMF, DCM, MEOH, DCM (3 x 5 ml), the peptide was elongated with the next desired Fmoc-protected amino acid (4 eq), (HATU) (4 eq) and diisopropylethylamine (DIEA) (8 eq) in DMF for 2 hrs. Once the peptide sequence was complete the resin was washed with DMF, DCM, MEOH, DCM (3 x 5 ml), dried on vacuum and treated with a 30% hexafluoroisopropanol in dichloromethane. The cleavage solution was drained into a tared 50 ml falcon tube and the remaining resin washed with DCM (10 ml). The cleavage solution was evaporated under reduced pressure and was used without further purification. The peptide was dissolved in DMSO (5 mM) to form a stock solution. The cleaved peptide was characterized by matrix assisted laser desorption ionization- time of flight (MALDI-TOF) mass spectrometry: Protected L-TSβ (Expected mass – 1454.7 m/z, Observed mass 1454.7 m/z.)

3.4.5 Synthesis of protected cyclized tendamistat β (TSβ protected)

The protected linear tendamistat β peptide (30 mg) was isomerized in DMSO for 15 mins in the Miniature Cyclonic Ultraviolet Photochemical Reactor (Mini-CUPR™) in a Quartz glass screw cap vial (5 ml). The resulting solution of predominantly cis azobenzene-containing peptide

(75%) was stirred with (7-azabenzotriazol-1-yloxy) tripyrrolidinophosphonium hexafluorophosphate (PyAOP) (103 µmol, 54 mg) and DIEA (206 µmol, 36 µl) in a 50 ml Falcon tube for 2 hours at room temperature.[27] The resulting reaction solution was filtered through a 0.2 µm filter and purified directly by RP-HPLC using a Luna C18 semi-prep column with an eluent of solvent A (CH$_3$CN/0.1% TFA) and solvent B (Water/0.1% TFA), with a gradient of 50-95% Solvent A over 60 minutes, 214 nm and 254 nm detection and a 12 ml/min flowrate. The purified peptide was characterized by MALDI-TOF mass spectrometry: Protected TSβ (Expected mass – 1436.7 m/z Observed mass 1437 m/z).

3.4.6 Synthesis of cyclized tendamistat β (TSβ)

The protected, cyclized tendamistat β from the previous reaction (10 mg) was incubated with a trifluoroacetic acid cocktail of trifluoroacetic acid, triisopropylsilane, water (95:2.5:2.5) (5 ml) before the peptide was precipitated with ice-cold diethyl ether (15 mL) at -79°C. The solution was centrifuged (4000 RPM, 10 min), and the pellet was dissolved in water The crude peptide was purified on reverse phase HPLC using a Luna C18 semi-prep column with an eluent of solvent A (CH$_3$CN/0.1% TFA) and solvent B (Water/0.1% TFA). The TSβ peptide was purified to homogeneity using a gradient of 10-40% Solvent A over 60 minutes with 214 nm and 254 nm detection and a 12 ml/min flowrate. The purified peptides were characterized by MALDI-TOF mass spectrometry: TSβ (Expected mass – 972.1 m/z, Observed mass 972.4 m/z.)

3.4.7 α-Amylase Inhibition Assay

The investigation of α-Amylase Inhibition was performed using the EnzChek ® Ultra Amylase Assay Kit from Thermo Fisher. First the trans form of the L-TSβ and TSβ were obtained by incubating the peptides in a 37°C water bath for 48 hrs. The amount of cis peptide present was determined by reverse phase UPLC using a Luna C18 analytical column with an eluent of solvent A (CH$_3$CN/0.1% TFA) and solvent B (Water/0.1% TFA). The peptide solutions were analyzed using a gradient of 10-40% Solvent A over 10 minutes with 214 nm and 254 nm detection and a 0.5 ml/min flowrate. The cis form of the L-TSβ and TSβ peptides were obtained by photolyzing L-TSβ and TSβ for 3.5 hrs and 15 mins, respectively in the Mini-CUPR™ in a Quartz glass screw cap vial (5 ml), before the assay. The amount of cis peptide present was determined by reverse

phase UPLC using a Luna C18 analytical column with an eluent of solvent A (CH_3CN/0.1% TFA) and solvent B (Water/0.1% TFA). The peptide solutions were analyzed using a gradient of 10-40% Solvent A over 10 minutes with 214 nm and 254 nm detection and a 0.5 ml/min flowrate. Working α-amylase solutions (4 mU, 8 mU, 10 mU, 12 mU, 16 mU, and 20 mU) (1 ml) were prepared from 1 U/ml and 1x reaction buffer (.05 M MOPS pH 6.9). The Bartlett control peptide and the photo-switchable tendamistat mimics were prepared into six working concentrations (200 µl) using 1x reaction buffer to perform IC_{50} analysis (1 µM-5mM). The fluorescently labeled starch solution was prepared just prior to 96-well plate addition by mixing 100 µl of substrate solvent (50 mM sodium acetate, pH4.0) with 4.9 ml of µl 1x reaction buffer and was added to the wells last. All inhibitor samples were run with 10 mU of α-amylase and all wells were made to a final well volume of 100 µl. This includes ten background wells (75 µl of 1x reaction buffer and 25 µl fluorescent starch solution) , which were made as a control, enzyme standard curve wells (25 µl enzyme, 25 µl fluorescent starch solution, 50 µl 1x reaction buffer) and sample wells (25 µl enzyme, 25 µl fluorescent starch solution, 50 µl peptide inhibitor) Once the fluorescent starch solution was added, the 96-well plate was gently agitated on a shaker for 30 mins, before being read on a Tecan plate reader using an excitation and emission wavelength of 485/20 and 535/35 nm, respectively. The wells were run in duplicate and the percent inhibition was calculated by first averaging out the background well values, then subtracting that value out from the enzyme standard values and sample values. The sample well values were divided by the enzyme standard (10 mU) value and then multiplied by 100 to determine percent inhibition.

3.5   References

(1)   Venkatachalam, C. M. Stereochemical Criteria for Polypeptides and Proteins. V. Conformation of a System of Three Linked Peptide Units. *Biopolymers* **1968**, *6* (10), 1425–1436. https://doi.org/10.1002/bip.1968.360061006.

(2)   Richardson, J. S. The Anatomy and Taxonomy of Protein Structure. *Adv. Protein Chem.* **1981**, *34*, 167–339. https://doi.org/10.1016/S0065-3233(08)60520-3.

(3)   Marcelino, A. M. C.; Gierasch, L. M. Roles of β-Turns in Protein Folding: From Peptide Models to Protein Engineering. *Biopolymers* **2008**, *89* (5), 380–391. https://doi.org/10.1002/bip.20960.

(4)   Ruiz-Gómez, G.; Tyndall, J. D. A.; Pfeiffer, B.; Abbenante, G.; Fairlie, D. P. Update 1 of: Over One Hundred Peptide-Activated g Protein-Coupled Receptors Recognize Ligands with Turn Structure. *Chem. Rev.* **2010**, *110* (4), 793–826. https://doi.org/10.1021/cr900344w.

(5)   Bo, Q.; Yang, F.; Li, Y.; Meng, X.; Zhang, H.; Zhou, Y.; Ling, S.; Sun, D.; Lv, P.; Liu, L.; et al. Structural Insights into the Activation of Somatostatin Receptor 2 by Cyclic SST Analogues. *Cell Discov.* **2022**, *8* (1), 47. https://doi.org/10.1038/s41421-022-00405-2.

(6)   Hruby, V. J. Conformational and Topographical Considerations in the Design of Biologically Active Peptides. *Biopolymers* **1993**, *33* (7), 1073–1082. https://doi.org/10.1002/bip.360330709.

(7)   Ulysse, L. G.; Chmielewski, J. A Light-Activated β-Turn Scaffold within a Somatostatin Analog: NMR Structure and Biological Activity. *Chem. Biol. Drug Des.* **2006**, *67* (2), 127–136. https://doi.org/10.1111/j.1747-0285.2005.00337.x.

(8)   Urry, D. W.; Walter, R. Proposed Conformation of Oxytocin in Solution. *Proc. Natl. Acad. Sci. U. S. A.* **1971**, *68* (5), 956–958. https://doi.org/10.1073/pnas.68.5.956.

(9)   Roy, U.; Gazis, D.; Schwartz, I. L.; Roy, J. Biofunctional Evaluation of Two Hydrogen Bonds Stabilizing the B-turn in the Acyclic Component of Oxytocin. *Int. J. Pept. Protein Res.* **1983**, *22* (4), 398–403. https://doi.org/10.1111/j.1399-3011.1983.tb02108.x.

(10)   Rotondi, K. S.; Gierasch, L. M. A Well-Defined Amphipathic Conformation for the Calcium-Free Cyclic Lipopeptide Antibiotic, Daptomycin, in Aqueous Solution. *Biopolym. - Pept. Sci. Sect.* **2005**, *80* (2–3), 374–385. https://doi.org/10.1002/bip.20238.

(11)   Velkov, T.; Thompson, P. E.; Nation, R. L.; Li, J. Structure-Activity Relationships of Polymyxin Antibiotics. *J. Med. Chem.* **2010**, *53* (5), 1898–1916. https://doi.org/10.1021/jm900999h.

(12)   Velkov, T.; Roberts, K. D.; Nation, R. L.; Thompson, P. E.; Li, J. Pharmacology of Polymyxins: New Insights into an 'old Class of Antibiotics. *Future Microbiol.* **2013**, *8* (6), 711–724. https://doi.org/10.2217/fmb.13.39.

(13)   Carotenuto, A.; Grieco, P.; Campiglia, P.; Novellino, E.; Rovero, P. Unraveling the Active Conformation of Urotensin II. *J. Med. Chem.* **2004**, *47* (7), 1652–1661. https://doi.org/10.1021/jm0309912.

(14)   Hill, T. A.; Shepherd, N. E.; Diness, F.; Fairlie, D. P. Constraining Cyclic Peptides to Mimic Protein Structure Motifs. *Angew. Chemie - Int. Ed.* **2014**, *53* (48), 13020–13041. https://doi.org/10.1002/anie.201401058.

(15)   Malde, A. K.; Hill, T. A.; Iyer, A.; Fairlie, D. P. Crystal Structures of Protein-Bound Cyclic Peptides. *Chem. Rev.* **2019**, *119* (17), 9861–9914. https://doi.org/10.1021/acs.chemrev.8b00807.

(16)   Vértesy, L.; Oeding, V.; Bender, R.; Zepf, K.; Nesemann, G. Tendamistat (HOE 467), a Tight-binding A-amylase Inhibitor from Streptomyces Tendae 4158: Isolation, Biochemical Properties. *Eur. J. Biochem.* **1984**, *141* (3), 505–512. https://doi.org/10.1111/j.1432-1033.1984.tb08221.x.

(17)   Machius, M.; Vértesy, L.; Huber, R.; Wiegand, G. Carbohydrate and Protein-Based Inhibitors of Porcine Pancreatic α-Amylase: Structure Analysis and Comparison of Their Binding Characteristics. *J. Mol. Biol.* **1996**, *260* (3), 409–421. https://doi.org/10.1006/jmbi.1996.0410.

(18)   Wiegand, G.; Epp, O.; Huber, R. The Crystal Structure of Porcine Pancreatic α-Amylase in Complex with the Microbial Inhibitor Tendamistat. *J. Mol. Biol.* **1995**, *247* (1), 99–110. https://doi.org/10.1006/jmbi.1994.0125.

(19)   BLANCO, F. J.; JIMÉNEZ, M. A.; RICO, M.; SANTORO, J.; HERRANZ, J.; NIETO, J. L. Tendamistat (12–26) Fragment: NMR Characterization of Isolated B-turn Folding Intermediates. *Eur. J. Biochem.* **1991**, *200* (2), 345–351. https://doi.org/10.1111/j.1432-1033.1991.tb16191.x.

(20)   Etzkorn, F. A.; Guo, T.; Lipton, M. A.; Goldberg, S. D.; Bartlett, P. A. Cyclic Hexapeptides and Chimeric Peptides as Mimics of Tendamistat. *J. Am. Chem. Soc.* **1994**, *116* (23), 10412–10425. https://doi.org/10.1021/ja00102a008.

(21)   Ono, S.; Umezaki, M.; Tojo, N.; Hashimoto, S.; Taniyama, H.; Kaneko, T.; Fujii, T.; Morita, H.; Shimasaki, C.; Yamazaki, I.; Yoshimura, T; Kato, T. Cyclic and Linear Peptides Derived from α-Amylase Inhibitory Protein Tendamistat. *J. Biochem.* **2001**, *129* (5), 783–790. https://doi.org/10.1093/oxfordjournals.jbchem.a002920.

(22)   Ono, S.; Hirano, T.; Yasutake, H.; Matsumoto, T.; Yamaura, I.; Kato, T.; Morita, H.; Fujii, T.; Yamazaki, I.; Shimasaki, C. Biological and Structural Properties of Cyclic Peptides Derived from the α-Amylase Inhibitor Tendamistat. *Biosci. Biotechnol. Biochem.* **1998**, *62* (8), 1621–1623. https://doi.org/10.1271/bbb.62.1621.

(23)   Sefler, A. M.; Kozlowski, M. C.; Guo, T.; Bartlett, P. A. Design, Synthesis, and Evaluation of a Depsipeptide Mimic of Tendamistat. *J. Org. Chem.* **1997**, *62* (1), 93–102. https://doi.org/10.1021/jo9616062.

(24)   Ulysse, L.; Cubillos, J.; Chmielewski, J. Photoregulation of Cyclic Peptide Conformation. *J. Am. Chem. Soc.* **1995**, *117* (32), 8466–8467. https://doi.org/10.1021/ja00137a023.

(25)   Johnson, C.; Harwood, J. S.; Lipton, M.; Chmielewski, J. A Refined Photo-Switchable Cyclic Peptide Scaffold for Use in β-Turn Activation. *Pept. Sci.* **2022**, *114* (5), e24265. https://doi.org/10.1002/pep2.24265.

(26)   Eakins, G.S.; Niedrauer, M.L.; Lipton, M. A. Innovation Infosheet Photochemical Reactor for Solid Phase Synthesis. U.S. Patent 63,029,491, 2020.

(27) Albericio, F.; Cases, M.; Alsina, J.; Triolo, S. A.; Carpino, L. A.; Kates, S. A. On the Use of PyAOP, a Phosphonium Salt Derived from HOAt, in Solid-Phase Peptide Synthesis. *Tetrahedron Lett.* **1997**, *38* (27), 4853–4856. https://doi.org/10.1016/S0040-4039(97)01011-3.
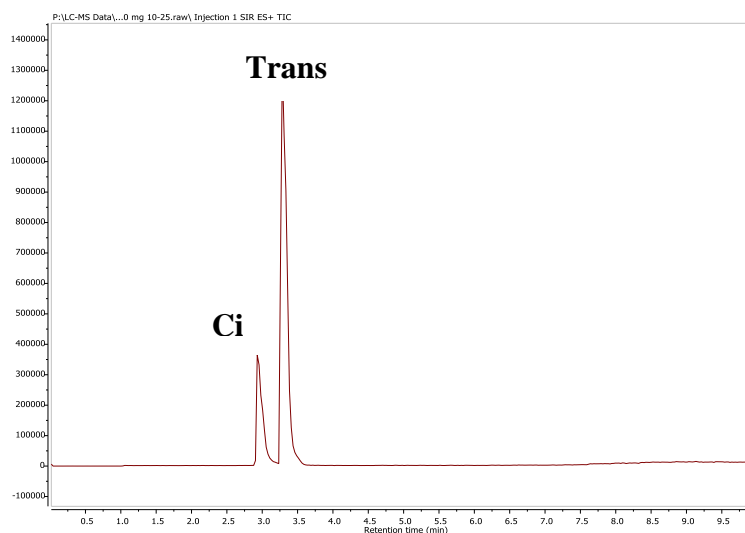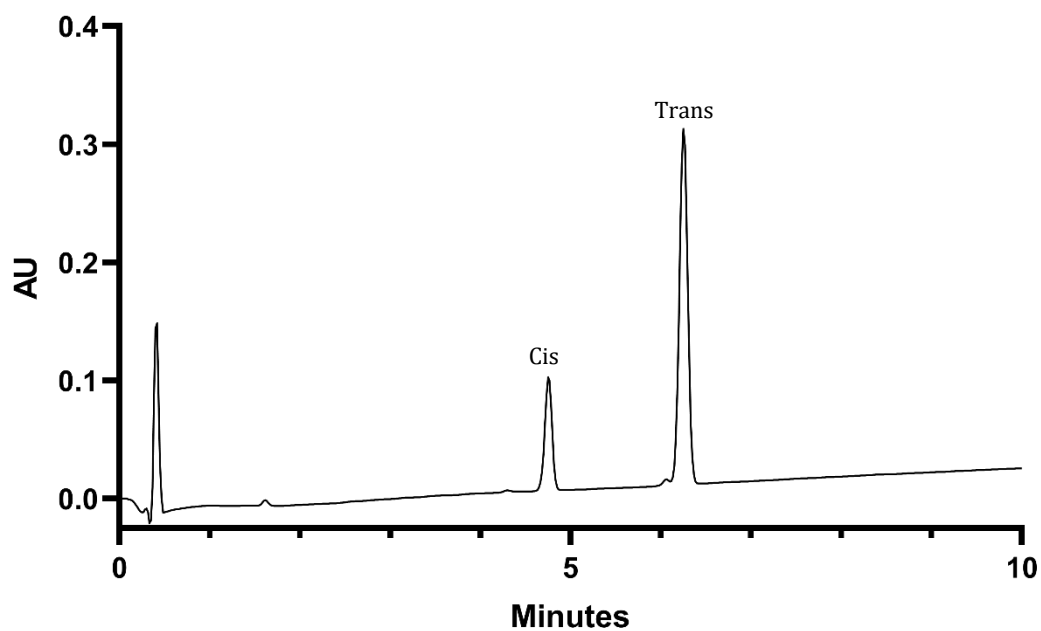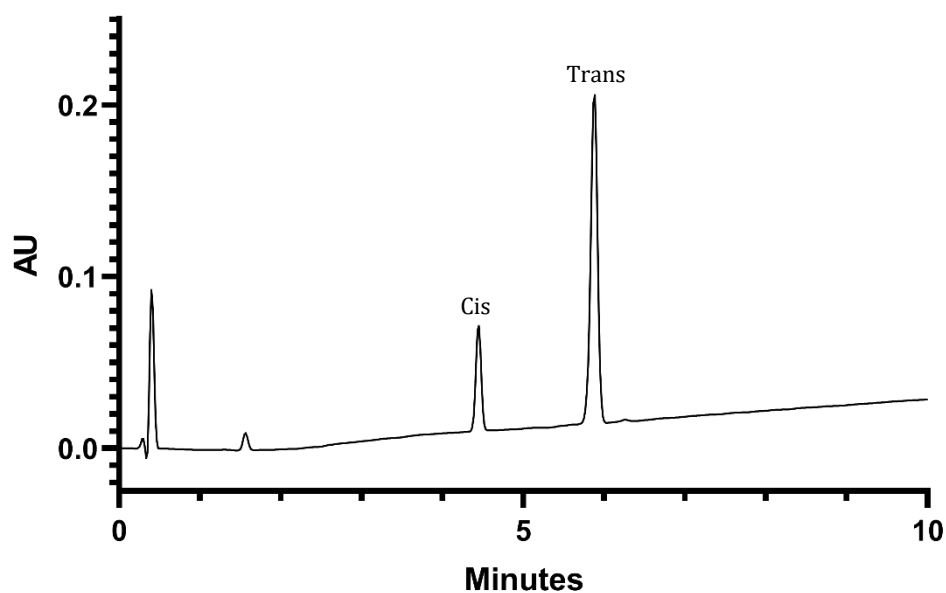
APPENDIX A. ADDITIONAL FIGURES AND TABLES

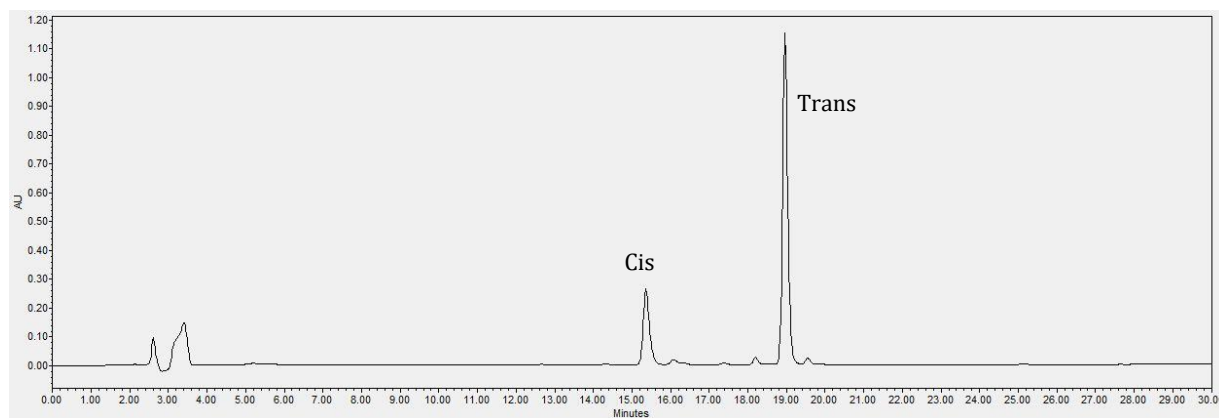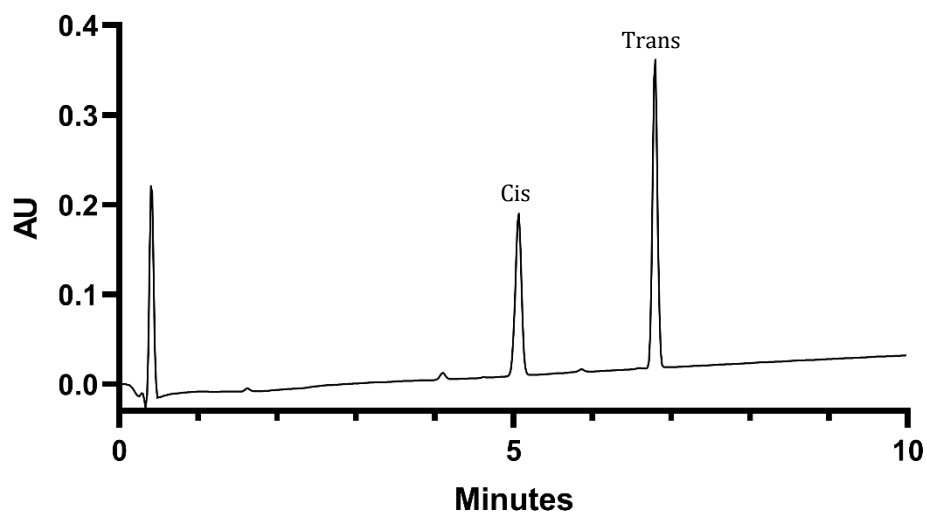Figure A1. Purity of L-FLAp by UPLC (C18 Waters Acquity column, 0.5 ml/min flowrate, 10-25% Solvent A (CH$_3$CN/0.1% TFA) in Solvent B (Water/0.1% TFA), 214 nm).
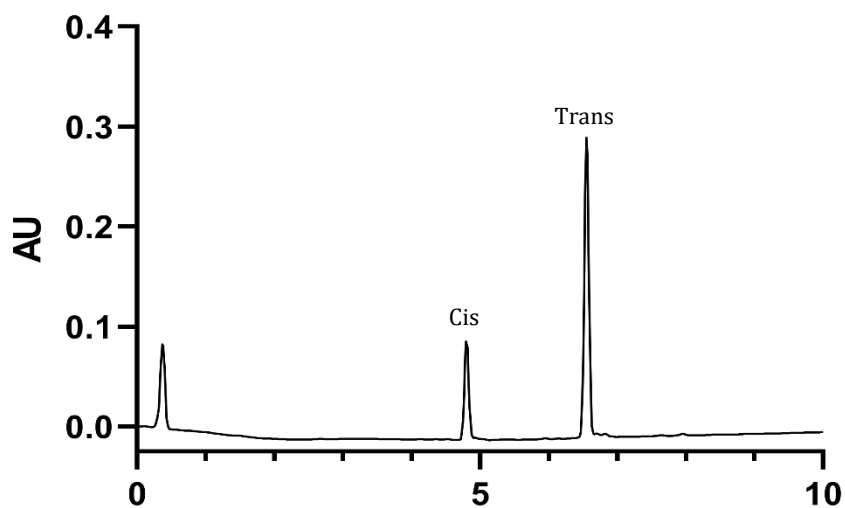

Figure A2. Purity of L-TAp by UPLC (C18 Waters Acquity column, 0.5 ml/min flowrate, 10-25% Solvent A (CH$_3$CN/0.1% TFA) in Solvent B (Water/0.1% TFA), 214 nm).

Figure A3. Purity of L-TApβ by UPLC (C18 Waters Acquity column, 0.5 ml/min flowrate, 10-25% Solvent A (CH₃CN/0.1% TFA) in Solvent B (Water/0.1% TFA), 214 nm).

Figure A4. Purity of FLAp by HPLC (C18 Phenomenex column, 0.5 ml/min flowrate, 10-25% Solvent A (CH₃CN/0.1% TFA) in Solvent B (Water/0.1% TFA), 214 nm).

Figure A5. Purity of TAp by UPLC (C18 Waters Acquity, 0.5 ml/min flowrate, 10-25% Solvent A (CH₃CN/0.1% TFA) in Solvent B (Water/0.1% TFA), 214 nm).

Figure A6. Purity of TApβ by UPLC (C18 Waters Acquity column, 0.5 ml/min flowrate, 10-25% Solvent A (CH₃CN/0.1% TFA) in Solvent B (Water/0.1% TFA), 214 nm).
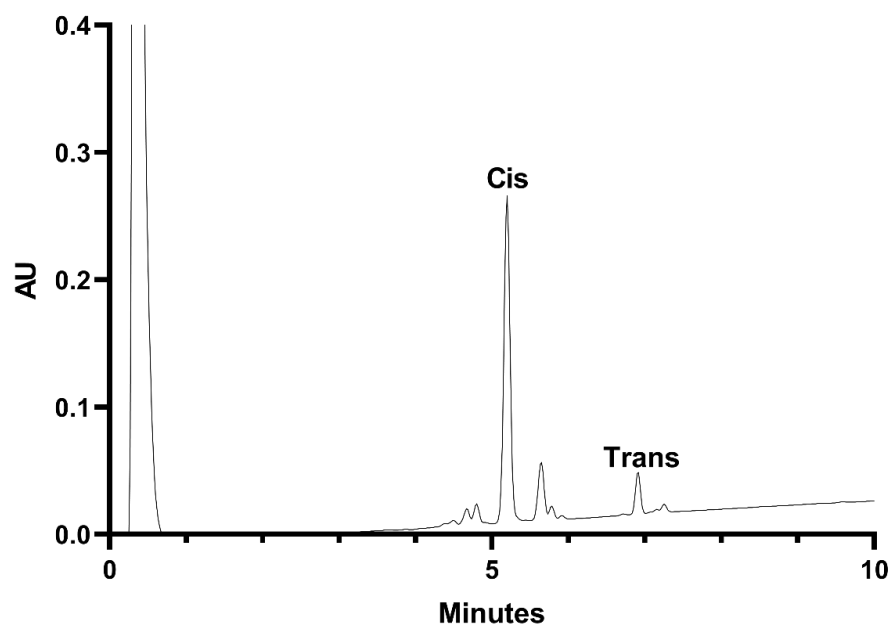
Figure A7. UPLC chromatogram of TAp isomers after photoexcitation at 365 nm, (C18 Waters Acquity column, 0.5 ml/min flowrate, 10-25% Solvent A (CH$_3$CN/0.1% TFA) in Solvent B (Water/0.1% TFA), 214 nm).
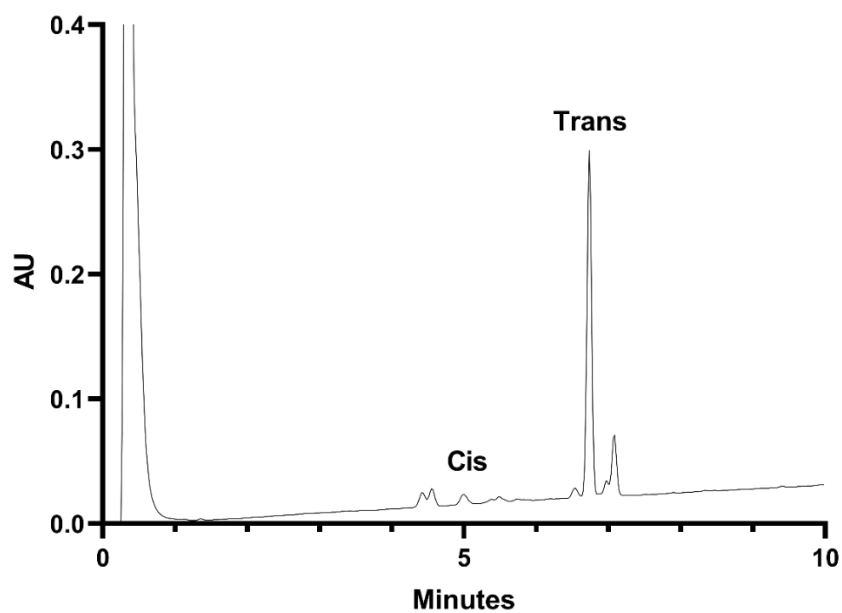

Figure A8. UPLC chromatogram of ratio of TAp after 1 week at 37°C (C18 Waters Acquity column, 0.5 ml/min flowrate, 10-25% Solvent A (CH$_3$CN/0.1% TFA) in Solvent B (Water/0.1% TFA), 214 nm).
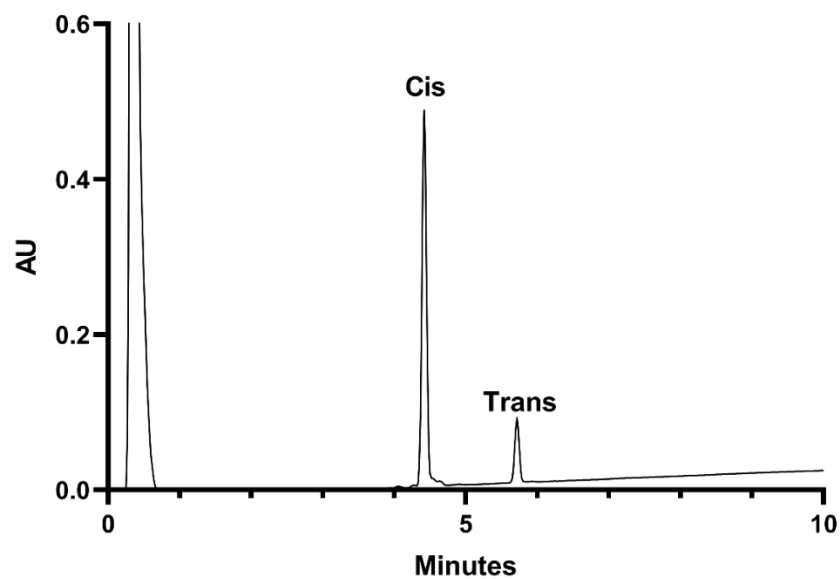
66

Figure A9. UPLC chromatogram of TApβ isomers after photoexcitation at 365 nm (C18 Waters Acquity column, 0.5 ml/min flowrate, 10-25% Solvent A (CH$_3$CN/0.1% TFA) in Solvent B (Water/0.1% TFA), 214 nm).
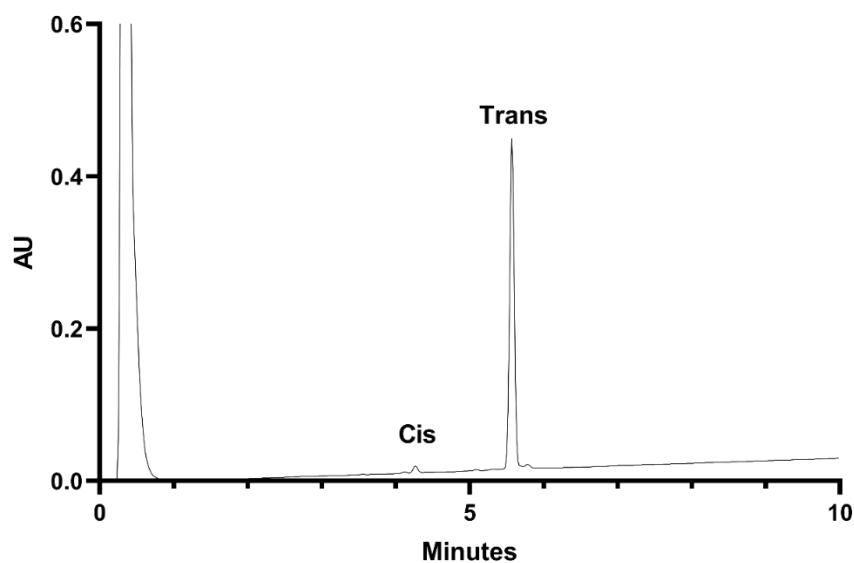

Figure A10. UPLC chromatogram of ratio of TApβ isomers after 1 week at 37°C (C18 Waters Acquity column, 0.5 ml/min flowrate, 10-25% Solvent A (CH$_3$CN/0.1% TFA) in Solvent B (Water/0.1% TFA), 214 nm).

Table A1. TAp (Trans) Chemical shift table

Amino Acid	NH proton in ppm	αH and αH' in ppm	Side chain H protons in ppm
Ala 1	8.09	4.24	1.20
Azo 2	8.58	4.03, 4.52	ArHa 7.47 ArHb 7.82 ArHc 7.91 ArHd 8.06
Ala 3	8.49	4.45	1.37
Asn 4	7.65	4.69	βH, βH'- 2.17, 2.50 Asn(NH$_2$)- Not found
Pro 5		3.98	βH 1.09 βH' 1.35 δH 1.31 δH' 1.66 γH 3.03 γH' 3.30
Gly 6	7.79	3.49, 3.77	
Gly 7	7.84	3.47, 3.92	

Table A2. TAp (Cis) Chemical shift table

Amino Acid	NH proton in ppm	αH and αH' in ppm	Side chain H protons in ppm
Ala 1	8.00	4.24	1.21
Azo 2	8.45	3.99,4.56	ArHa 6.90 ArHb 7.17 ArHc 6.96 ArHd 7.82
Ala 3	8.42	4.27	1.29
Asn 4	7.94	4.87	βH, βH'- 2.36, 2.61 Asn(NH$_2$)- Not found
Pro 5		4.13	βH 1.80 βH' 2.01 δH 1.79 δH' 1.87 γH 3.63 γH' 3.78
Gly 6	8.24	3.50, 3.77	
Gly 7	7.55	3.34, 3.95	

Table A3. TApβ (Trans) Chemical shift table

Amino Acid	NH proton in ppm	αH and αH' in ppm	Side chain H protons in ppm
β-Ala 1	7.97	3.21, 3.62	βH, βH' 2.48, 2.20
Azo 2	8.45	4.36	ArHa 7.39 ArHb 7.84 ArHc 7.89 ArHd 8.10
β-Ala 3	8.05	3.83, 3.29	βH, βH' 2.46, 2.34
Asn 4	8.18	4.81	βH, βH'- 2.36, 2.61 Asn(NH$_2$)- Not found
Pro 5		4.43	βH 1.88 βH' 1.71 δH 1.85 δH' 1.73 γH 3.53 γH' 3.48
Gly 6	8.01	4.04, 3.63	
Gly 7	8.03	3.79, 3.70	

Table A4. TApβ (Cis) Chemical shift table

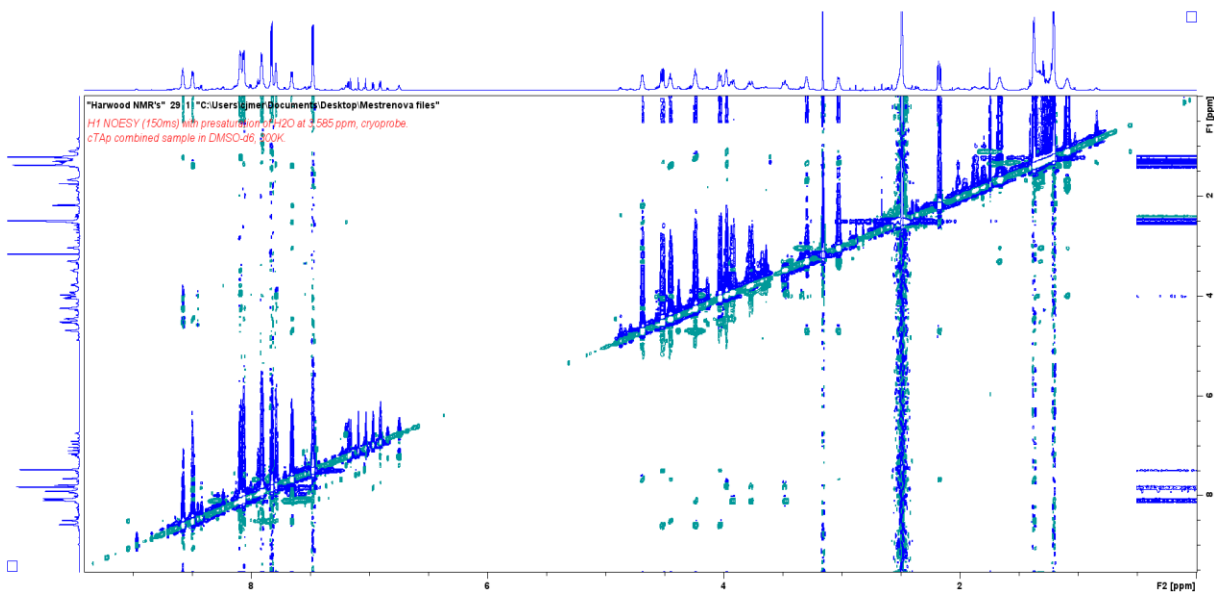| Amino Acid	NH proton in ppm	αH and αH' in ppm	Side chain H protons in ppm
β-Ala 1	7.59	3.18, 3.31	βH, βH' 2.29
Azo 2	8.23	4.2	ArHa 7.15 ArHb 6.83 ArHc 6.89 ArHd 7.75
β-Ala 3	8.39	3.43	βH, βH' 2.40, 2.29
Asn 4	8.27	4.82	βH, βH'- 2.33, 2.65 Asn(NH$_2$)- Not found
Pro 5		4.19	βH 1.89 βH' 1.77 δH 1.81 δH' 1.64 γH 3.60 γH' 3.60
Gly 6	8.16	3.61, 3.69	
Gly 7	7.58	3.60, 3.66	

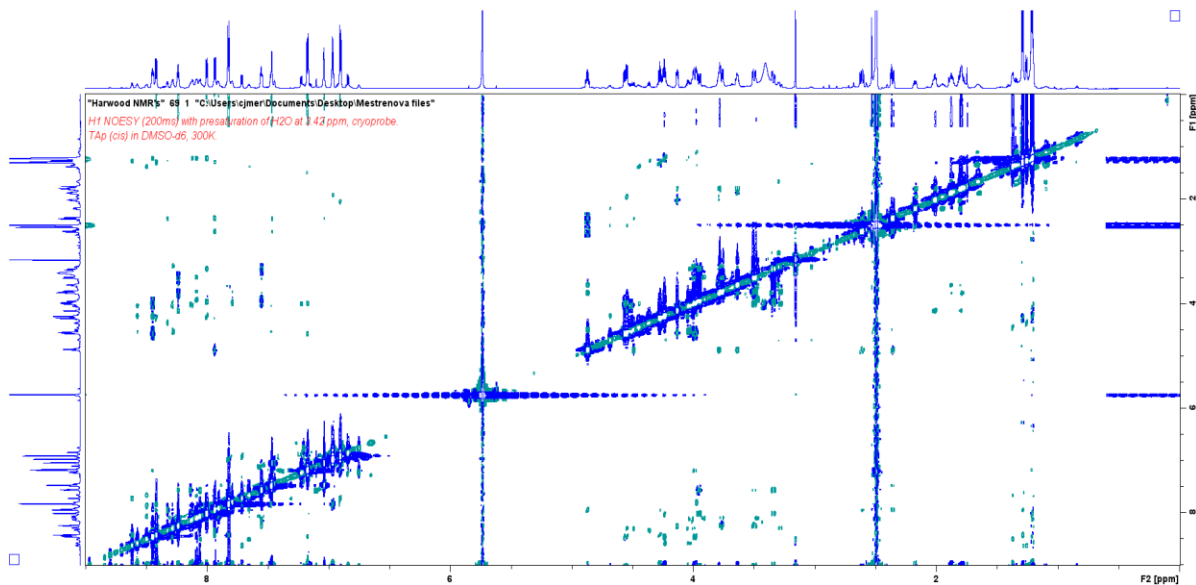Figure A11. NOESY spectra of TAp trans in DMSO-d_6 (800 MHz)

Figure A12. NOESY spectra of TAp cis in DMSO-d_6 (800 MHz)
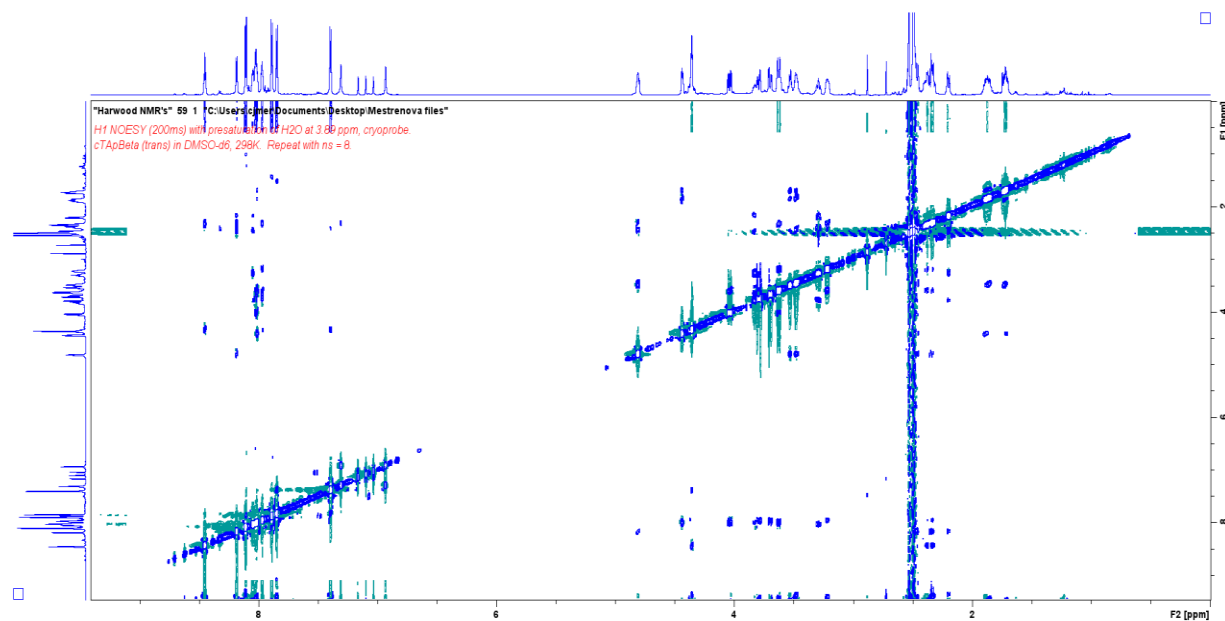
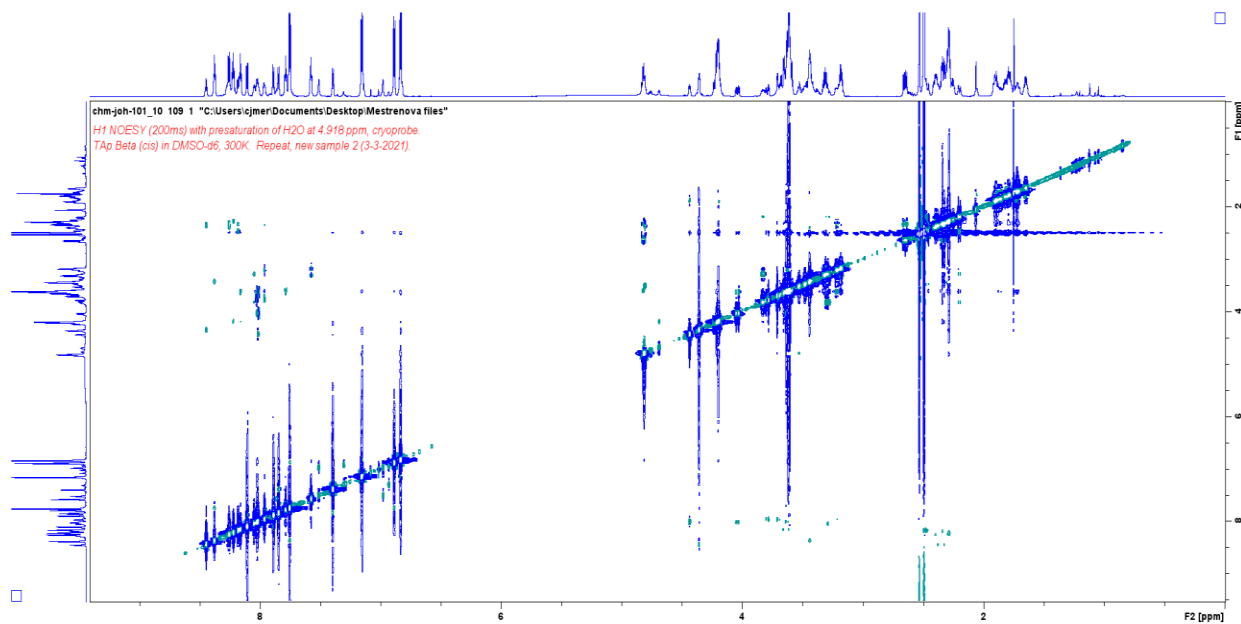Figure A13. NOESY spectra of TApβ trans in DMSO-$_{d6}$ (800 MHz)

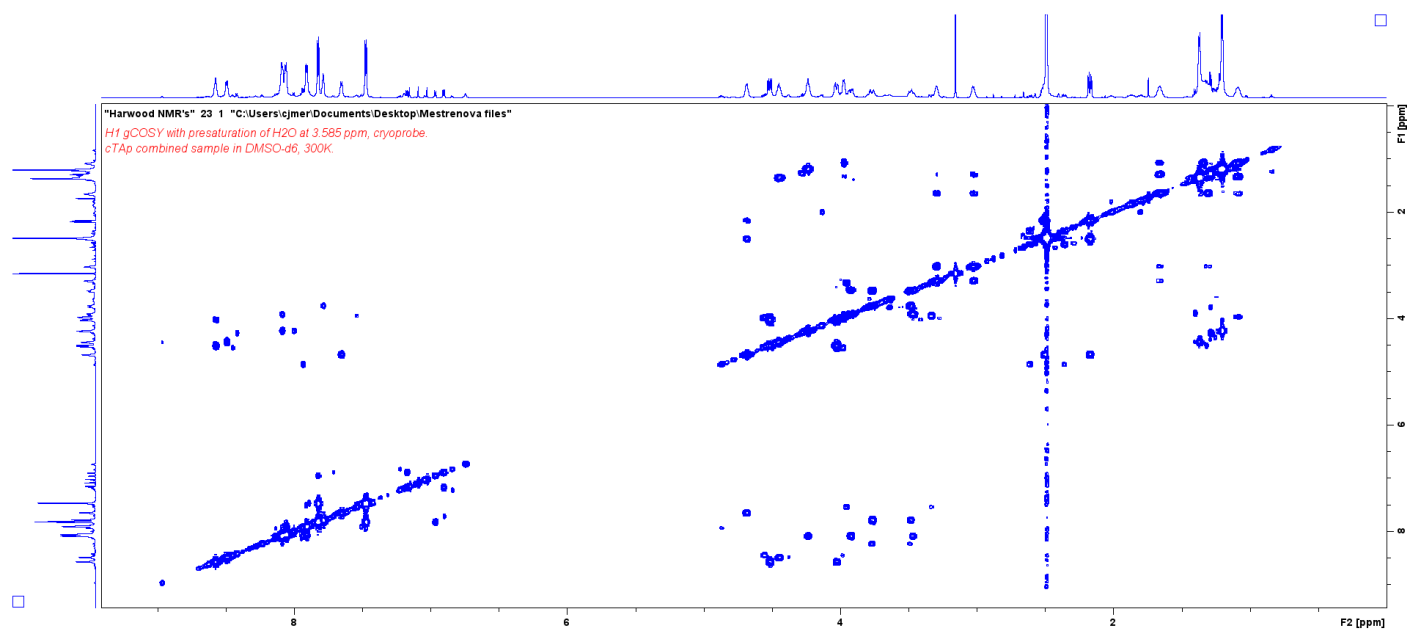Figure A14. NOESY spectra of TApβ cis in DMSO-$_{d6}$ (800 MHz)

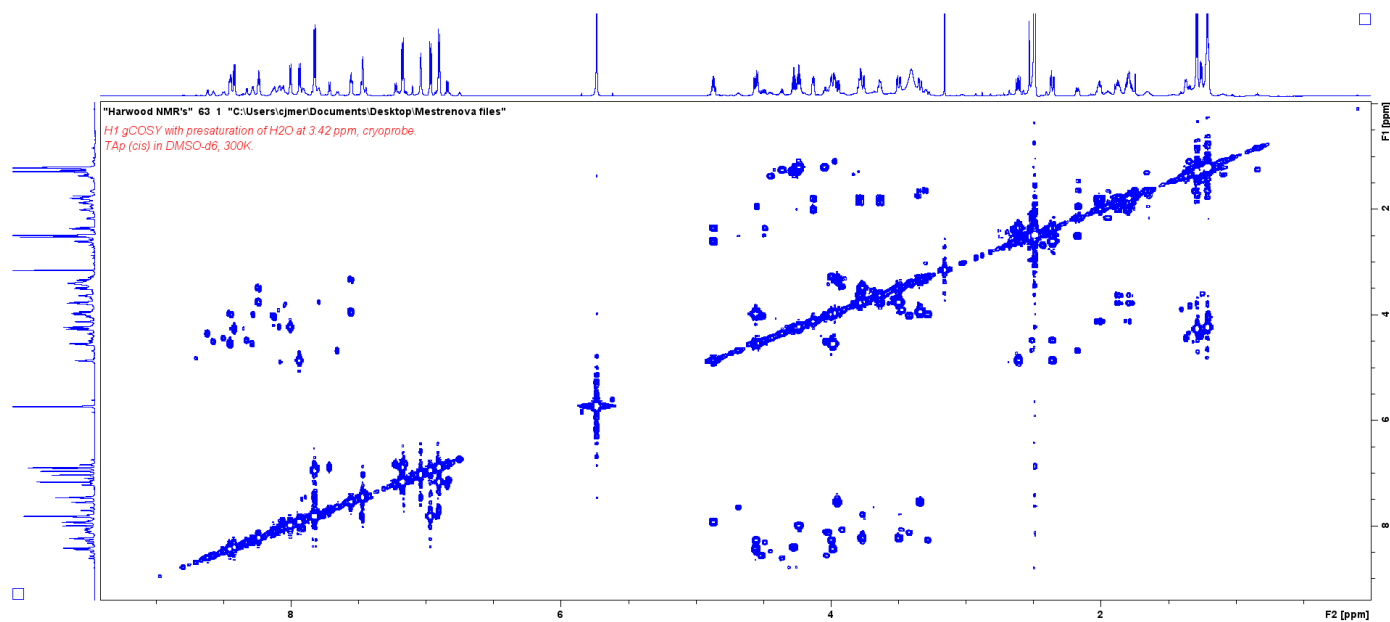Figure A15. ^{1}H-COSY spectra of TAp trans in DMSO-$_{d6}$ (800 MHz)

Figure A16. ^{1}H-COSY spectra of TAp cis in DMSO-$_{d6}$ (800 MHz)

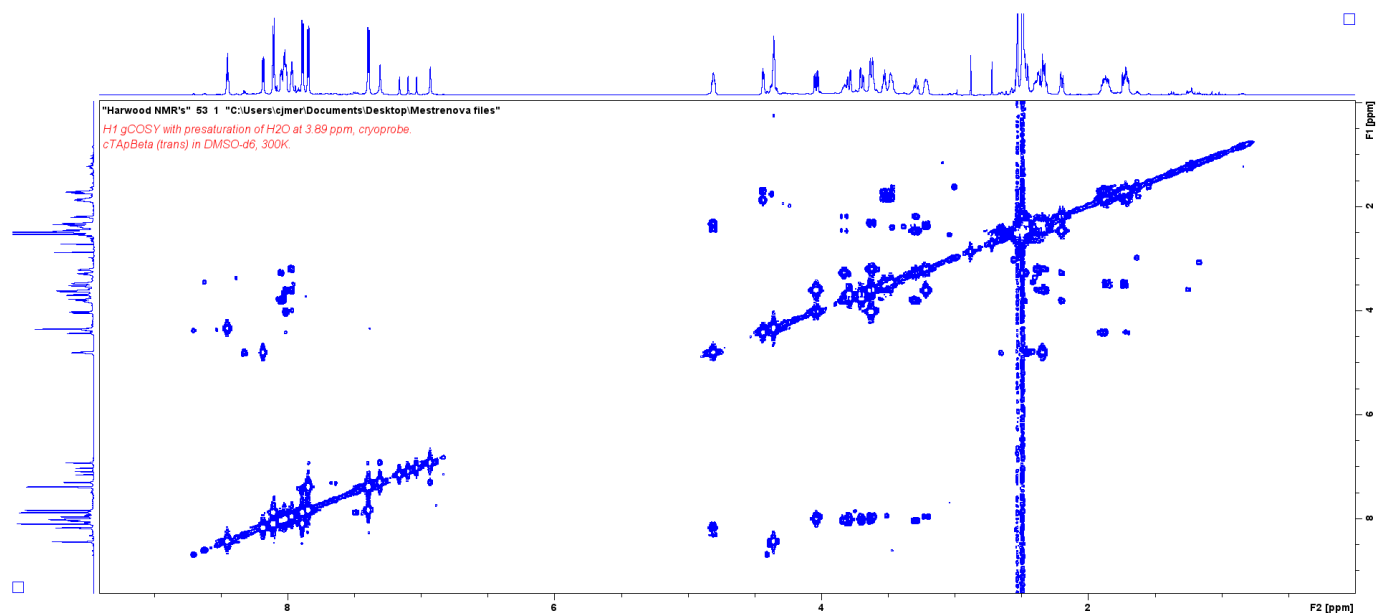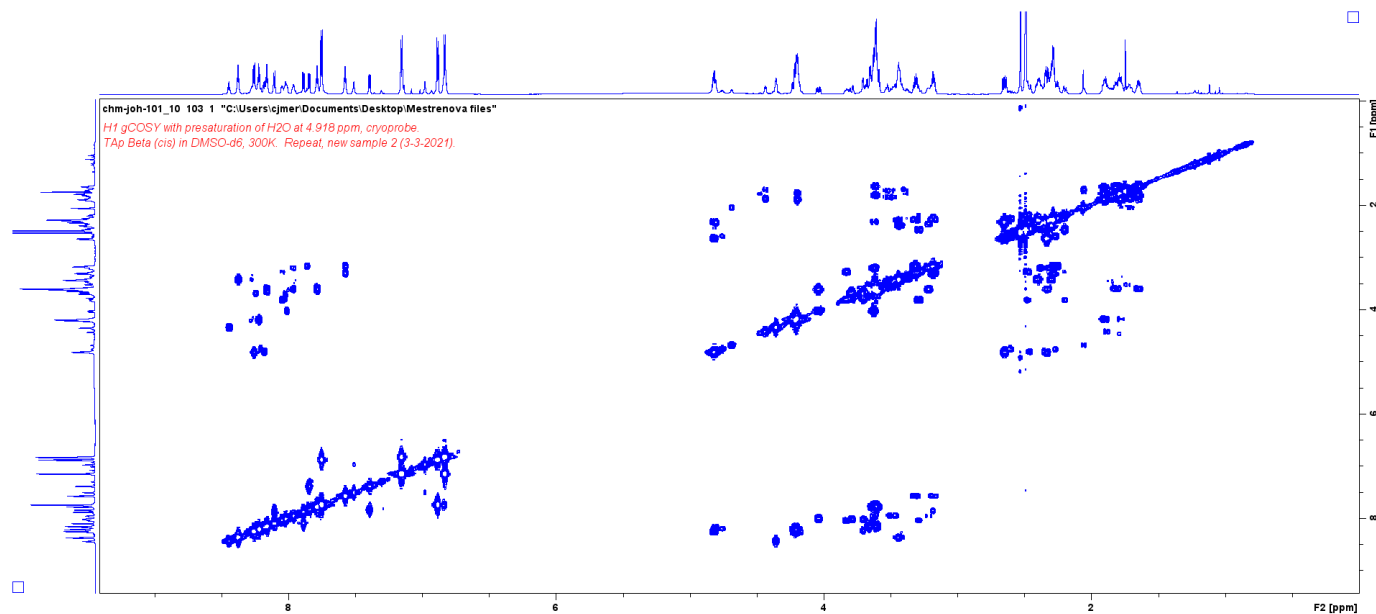Figure A17. ^{1}H-COSY spectra of TApβ trans in DMSO-$_{d6}$ (800 MHz)

Figure A18. ^{1}H-COSY spectra of TApβ cis in DMSO-$_{d6}$ (800 MHz)
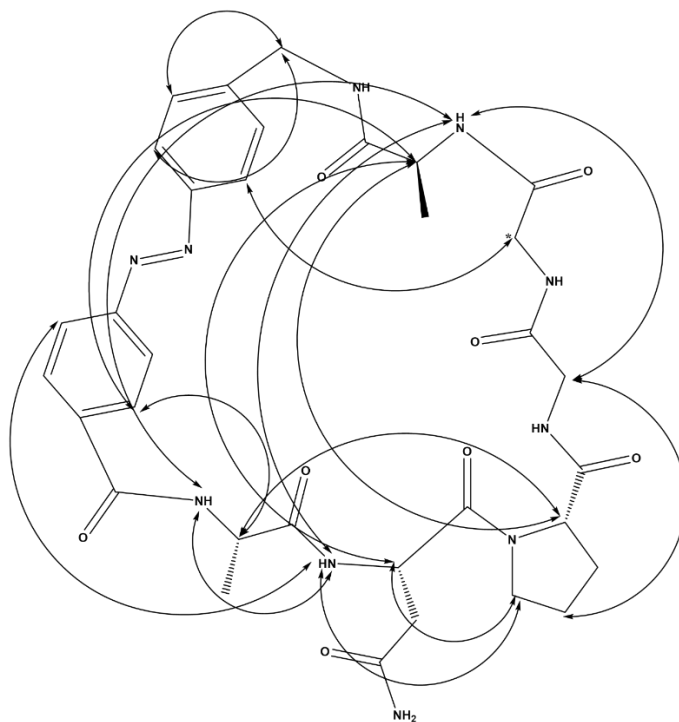
Figure A19. NOEs determined for TAp (trans).
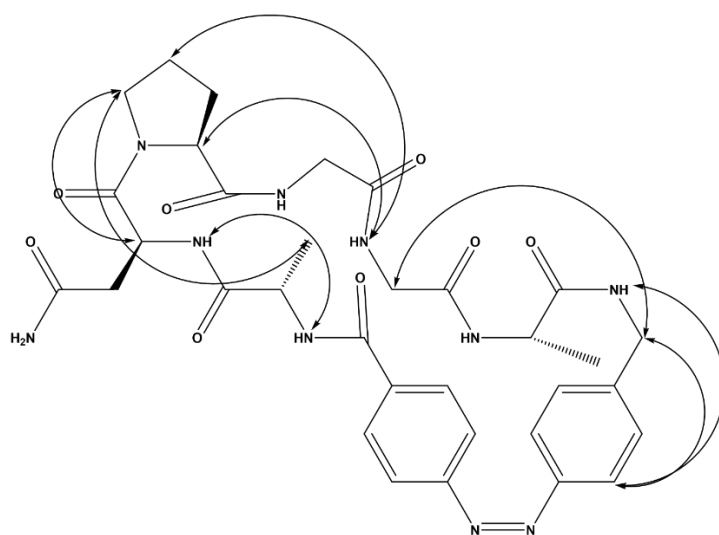
Figure A20. NOEs determined for TAp (cis).
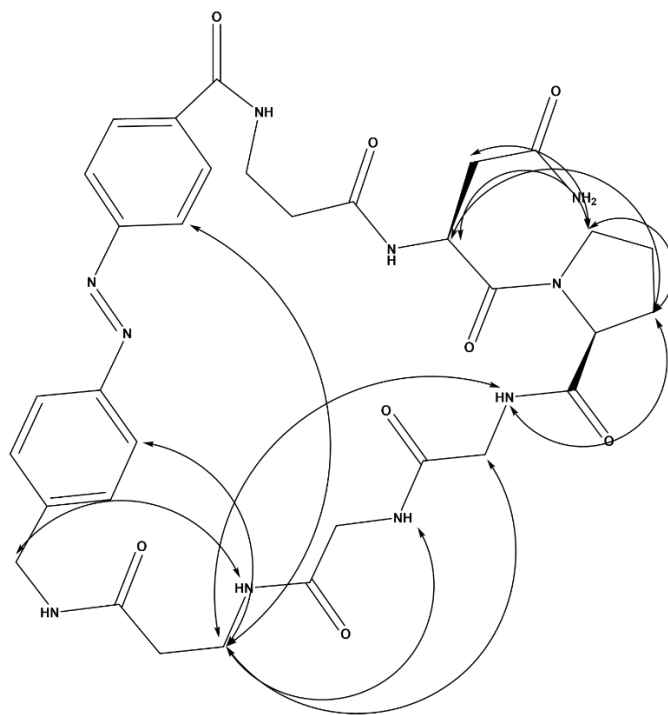
Figure A21. NOEs determined for TApβ (trans).
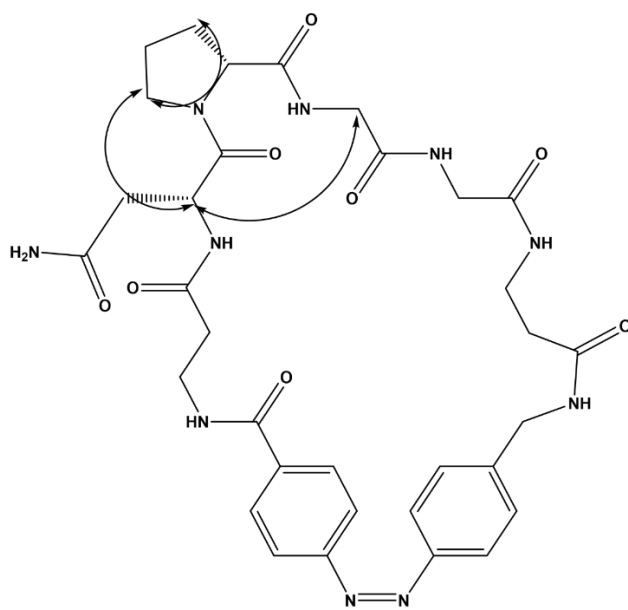
Figure A22. NOEs determined for TApβ (cis).
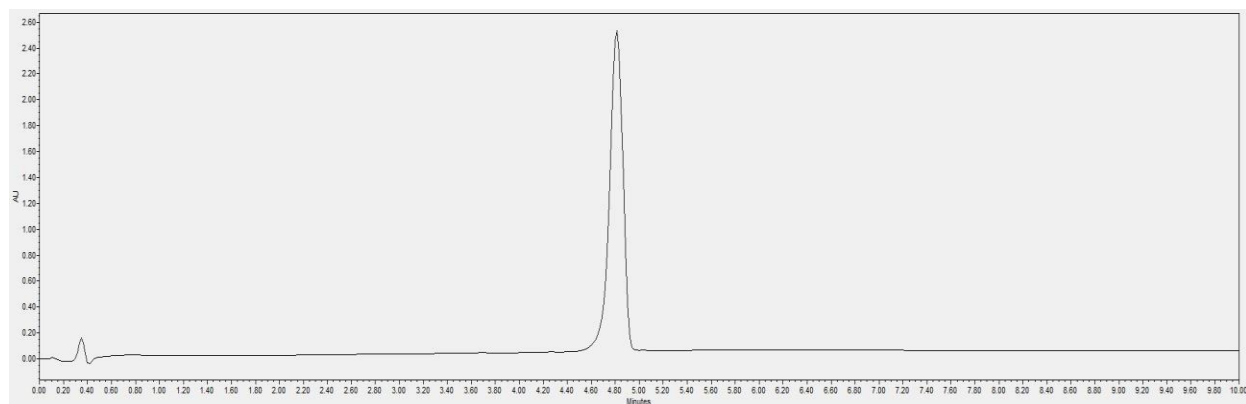
Figure A23. Purity of Bartlett control by UPLC (C18 Waters Acquity column, 0.5 ml/min flowrate, 10-60% Solvent A (CH₃CN/0.1% TFA) in Solvent B (Water/0.1% TFA), 214 nm).
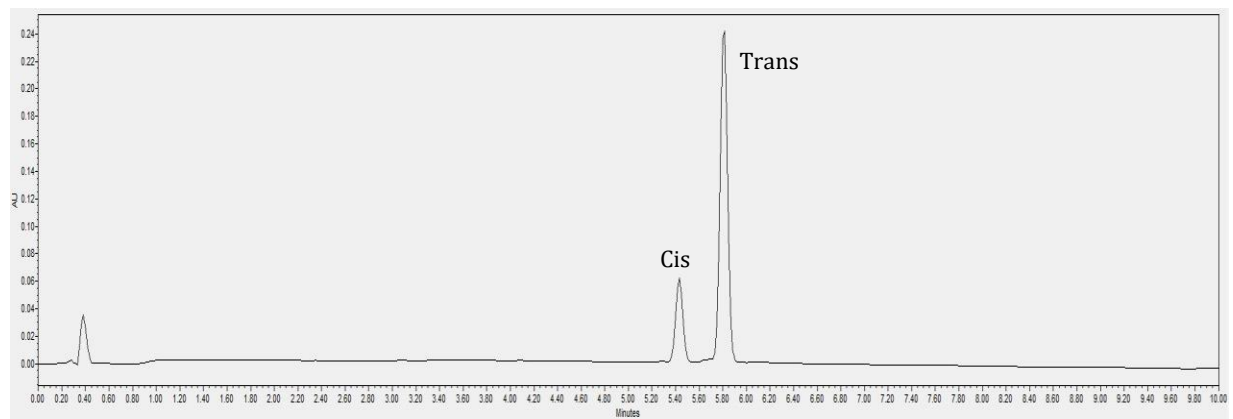
Figure A24. Purity of L-TSβ by UPLC (C18 Waters Acquity column 0.5 ml/min flowrate, 15-35% Solvent A (CH₃CN/0.1% TFA) in Solvent B (Water/0.1% TFA), 214 nm).
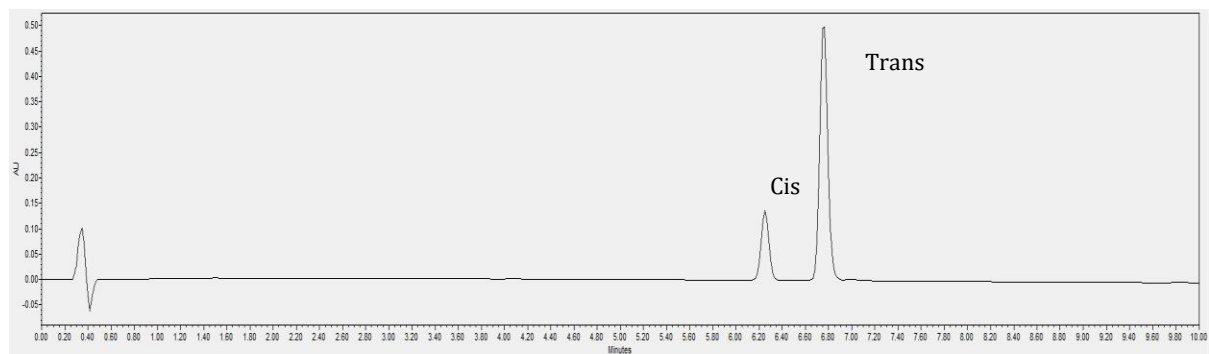
Figure A25. Purity of TSβ by UPLC (C18 Waters Acquity column, 0.5 ml/min flowrate, 10-40% Solvent A (CH$_3$CN/0.1% TFA) in Solvent B (Water/0.1% TFA), 214 nm).
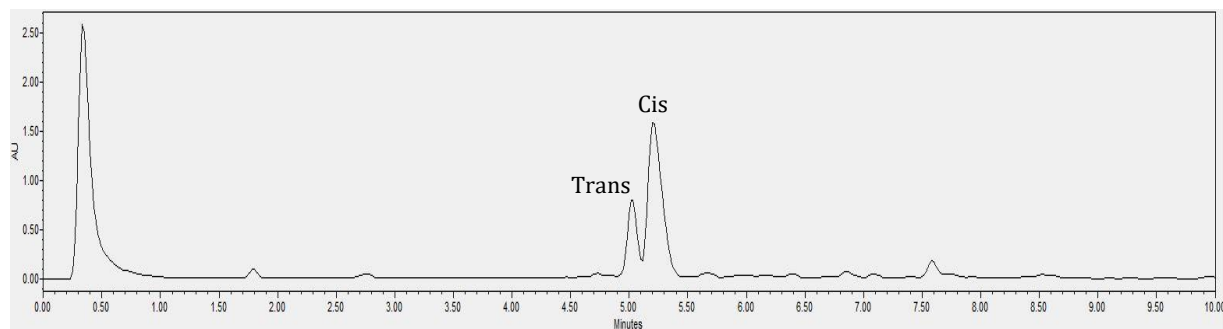
Figure A26. UPLC chromatogram of L-TSβ (protected) isomers after photoexcitation at 365 nm, (C18 Waters Acquity column, 0.5 ml/min flowrate, 10-25% Solvent A (CH$_3$CN/0.1% TFA) in Solvent B (Water/0.1% TFA), 214 nm).

VITA

Corey Johnson was born in Brooklyn, New York, where he grew up and went to Abraham Lincoln high school. He pursued his undergraduate studies first in Animal science before switching to biotechnology at the State University of New York at Cobleskill. There he did a semester of research with Dr. Lynda McMaster-Schuyler on the genetic modification of hops plants to resist local environmental fungi. After receiving his bachelor's degree in biotechnology in 2016, he began his graduate studies within the chemistry department at Purdue University in the fall of 2017. Shortly thereafter, he joined the Chmielewski research lab where he investigated the effect of a more rigid photo-switchable peptide scaffold for β-turn manipulation, where he learned chemical biology, organic synthesis and peptide design. After he obtains his Ph.D. in March 2023 he will pursue a postdoctoral fellowship at the Mass General Hospital in Boston, MA

PUBLICATIONS

ARTICLE

A refined photo-switchable cyclic peptide scaffold for use in β-turn activation

Corey Johnson | John S. Harwood | Mark Lipton ® | Jean Chmielewski ®

Department of Chemistry, Purdue University, West Lafayette, Indiana, USA

Correspondence
Mark Lipton and Jean Chmielewski, Department of Chemistry, Purdue University, West Lafayette, IN 47906, USA.
Email: lipton@purdue.edu; chml@purdue.edu

Funding information
National Science Foundation

Abstract

The ability to reversibly modulate peptide secondary structures, such as the β-turn, allows for precise control of biological function, including protein interactions. Herein, we describe the design of two scaffolds containing an azobenzene moiety with flanking alanine or β-alanine residues to probe essential features for photo-control of a β-turn within a cyclic peptide. To efficiently cyclize the designed linear peptides, prior isomerization of the azobenzene-containing amino acid from the trans to the cis form was necessary. The two cyclic peptides (TAp and TApβ) were found to undergo rapid photochemical conversion to the cis isomer of the azobenzene, with a more gradual thermal reversion to the trans isomer over the course of a week at 37 °C. Spectroscopic analysis and restrained molecular dynamics simulation of the cis form of TAp and TApβ revealed type II and type II' β-turns within the cyclic peptides, respectively. The trans isomer of the TAp cyclic peptide was found to have a kink within the peptide structure, whereas the longer trans-TApβ contained a more extended conformation. TApβ, therefore, demonstrates a clearer difference in the cyclic peptide conformations when in the cis versus trans form, a feature that may prove beneficial for use with biologically active β-turn sequences.

KEYWORDS
azobenzene, cyclic peptide, photoisomerization

1 | INTRODUCTION

Photo-controlled compounds represent an important class of molecules that have been shown to be useful in chemical biology and medicinal chemistry.[1–6] The azobenzene group represents an important portion of these photo-controlled compounds that are highly tunable, and can be multipurpose for various applications.[7–10] These molecules undergo cis-trans isomerization of the azobenzene in a controlled fashion via ultraviolet (UV) light. The azobenzene moiety has been used for α-helix stabilization,[11–15] β-turn formation,[16–18] β-sheet formation,[19–21] protein binding and activation,[22–24] cell-mediated binding,[25–27] and within DNA.[28–32] More specifically,

an azobenzene-containing amino acid, (4-aminomethyl)phenylazobenzoic acid (azo), and its derivatives can be used to promote light mediated conformational switching that can selectively initiate a range of chemical responses.[16,17,33–38]

The β-turn motif is an important component in biological signaling, and mediates a number of peptide- and protein–protein interactions.[39] This motif consists of four amino acid residues that form a hydrogen bond between the i and $i + 3$ residues in the sequence. β-turn mimetics have been used for a variety of applications,[39–49] including targeting β-turn-mediated G-protein coupled receptors.[39,46] While these mimetics are active against their specified targets, controlled activation is difficult to achieve. There is great interest, therefore, in developing

(a)

Trans   Cis

FLAp X= Ala-Ala
TAp X= Ala
TApβ X= β-Ala

(b)

NH₂—Ala Ala Azo Ala Ala Asn Pro Gly Gly—COOH

L-FLAp

NH₂—Ala Azo Ala Asn Pro Gly Gly—COOH

L-TAp

NH₂—β-Ala Azo β-Ala Asn Pro Gly Gly—COOH
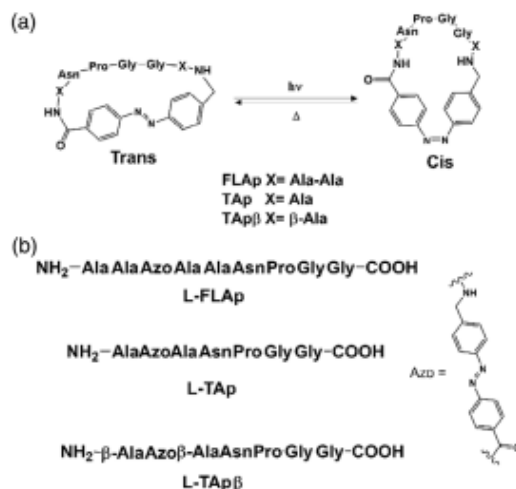
L-TApβ

A_{ZD} =

FIGURE 1 (a) The tetrapeptide, Asn-Pro-Gly-Gly, is a part of a cyclic peptide containing an azobenzene moiety flanked by either Ala-Ala, Ala, or β-Ala to investigate the rigidity of the scaffold. The cyclic peptides can be isomerized to the cis and trans versions using either UV light or elevated temperature, respectively. (b) The pre-cyclized linear peptide sequences containing the azobenzene amino acid (Azo)

tools to modulate the binding of therapeutics. In this regard, cyclic azobenzene-containing peptides have demonstrated photo-control in receptor binding,[17] cell surface signaling,[27] antimicrobial clearance,[18] nanotube formation,[50] and affinity labeling.[51]

Previously, cyclic peptides incorporating Azo were investigated for controlled β-turn formation.[16,17] In one example, a model peptide sequence with a propensity to form a β-turn, Asn-Pro-Gly-Gly, was used with two di-alanine spacers flanking the azobenzene moiety (Figure 1a, FLAp).[16] In another instance, the Ala₂-Azo-Ala₂ portion of FLAp was used with a β-turn sequence known to bind the somatotropin release-inhibiting factor (SRIF) receptor, Thr-Lys-Phe-Trp, all within a cyclic peptide.[17] In this latter case, the photo-induced trans to cis switch of the azobenzene achieved a β-turn within the macrocycle. However, the trans-Azo form of the cyclic peptide also maintained some turn character. This residual turn structure may account for the similarities in SRIF binding with the cis and trans isomers of the cyclic peptide, with the cis-form 2.6-fold more potent than the trans.[17] From these data, it was hypothesized that increasing the rigidity of the peptide scaffold may provide more effective control of the β-turn conformation (Figure 1a).

2 | MATERIALS AND METHODS

2.1 | Materials

All Fmoc-protected amino acids, the glycine p-alkoxybenzyl alcohol resin, HATU and PyOAP were purchased from Chem-Impex

International. All solvents were purchased from Fisher Scientific. HPLC columns were the Luna C18 (250 × 21.20 mm, 100 Å pore size, particle size 10 μm, Phenomenex) for Semi-preparative purification and Luna 5u C18 (250 × 4.60 mm, 100 Å pore size, particle size 5 μm, Phenomenex). Traces for Semi-prep were run for 60 min at 12 ml/min flowrate and analytical traces were run for 30 min at 1.2 ml/min flowrate. The UPLC column was a C18, Waters Acquity, (50.0 × 2.1 mm, particle size 1.7 μm). Traces on the UPLC were run for 10 min at 0.5 ml/min flowrate. All spectra were monitored at 214 nm. All normal precautions for handling organic compounds, reagents and solvents were used, including proper personal protective equipment for all experiments.

2.2 | General procedure for synthesis of FLAp, TAp, and TApβ peptides

2.2.1 | Linear peptide synthesis

Synthesis of the L-FLAp, L-TAp, L-TApβ peptides was carried out starting with a glycine p-alkoxybenzyl alcohol resin (500 mg) using fluorenylmethyloxycarbonyl- (Fmoc) based solid phase peptide synthesis. The N-terminal Fmoc was deprotected using a 20% piperidine/DMF solution for 25 min. The peptides were elongated using the desired Fmoc-AA-OH (4 eq), 1-[bis(dimethylamino)methylene]-1H-1,2,3-triazolo[4,5-b] pyridinium 3-oxide hexafluorophosphate (HATU) (4 eq) and diisopropylethylamine (DIEA) (8 eq) in DMF for 2 h. Once the peptide sequence was complete, the resin was treated with a trifluoroacetic acid cocktail consisting of trifluoroacetic acid, triisopropylsilane and water (95:2.5:2.5) and the peptide was precipitated with cold diethyl ether. The crude peptide was purified on reverse phase HPLC (RP-HPLC) with an eluent of Solvent A (CH₃CN/0.1% TFA) and Solvent B (water/0.1% TFA). L-FLAp was purified to homogeneity using a gradient of 10–30% Solvent A over 60 min with 214 nm detection and a 12 ml/min flowrate, while L-TAp and L-TApβ were purified at 10%–25% Solvent A over 60 min with 214 nm detection and a 12 ml/min flowrate. After lyophilization, the purified peptides were obtained as orange solids. The purified peptides were characterized by matrix assisted laser desorption ionization- time of flight (MALDI-TOF) mass spectrometry: L-FLAp (expected mass 865.4 m/z, observed mass 866.1 m/z.) L-TAp (expected mass 723.2 m/z, observed mass 723.4 m/z). L-TApβ (expected mass 723.2 m/z, observed mass 723.4 m/z) (Figures S1–S3).

2.2.2 | Cyclization

The L-FLAp peptide (1 mM) was dissolved in DMSO (5 ml) and treated with (7-azabenzotriazol-1-yloxy) tripyrrolidino-phosphonium hexafluorophosphate (PyAOP) (35 μmol, 18 mg) and DIEA (70 μmol, 12 μl) in a 50 ml Falcon tube for 2 h at room temperature. The resulting reaction mixture was purified using RP-HPLC with an

eluent of Solvent A (CH₃CN/0.1% TFA) and Solvent B (water/0.1% TFA), with a gradient of 5–50% Solvent A over 60 min with 214 nm detection and a 12 ml/min flowrate. The purified peptide was characterized by MALDI-TOF mass spectrometry: FLAp (Expected mass 847.5 m/z, observed mass 847.8 m/z.) (Figure S4).

2.2.3 | Isomerization prior to cyclization

L-TAp, and L-TApβ peptides (1 mM) were isomerized in DMSO for 15 mins in the Miniature Cyclonic Ultraviolet Photochemical Reactor (Mini-CUPR) in a Quartz glass screw cap vial (5 ml). The resulting solution of predominantly cis azobenzene-containing peptide (80%–90%) was stirred with PyAOP (35 μmol, 18 mg) and DIEA (70 μmol, 12 μl) in a 50 ml Falcon tube for 2 h at room temperature.[52] The resulting reaction mixtures were purified to homogeneity using RP HPLC with an eluent of Solvent A (CH₃CN/0.1% TFA) and Solvent B (Water/0.1% TFA), with a gradient of 5%–50% Solvent A over 60 min with 214 nm detection and a 12 ml/min flowrate. The purified peptides were characterized by MALDI-TOF mass spectrometry: TAp (Expected mass 705.3 m/z, observed mass 705.7 m/z). TApβ (Expected mass 705.3 m/z, observed mass 705.7 m/z) (Figures S5, S6).

2.3 | Isomerization of TAp and TApβ peptides

For isomerization to the cis forms, the cyclic peptides were solubilized (1 mM) in DMSO in a Quartz glass screw cap vial (5 mL), then placed in the Mini-CUPR for 15 min to 2 h. The predominantly cis solutions were analyzed by RP UPLC to determine the percentage of cis and trans isomers using a 5%–25% Solvent A gradient. For isomerization to the trans isomer, the two peptides were incubated in a 37 °C water bath with RP-UPLC measurements performed once a day for a week. The ratio of cis to trans isomers was quantified using RP-UPLC as described above (Figure S7–S10).

2.4 | NMR characterization of cyclic TAp and TApβ peptides

NMR spectra of the cis and trans forms of TAp and TApβ were obtained using a Bruker AV-III-800 spectrometer operating at 800 MHz for ¹H and 201 MHz for ¹³C and equipped with a 5 mm QCI Z-gradient cryoprobe. Bruker TopSpin 3.2 software was used for both data acquisition and processing. Samples were prepared in DMSO-d6 at 1 mM concentration in conventional 5 mm NMR tubes and were run at ca. 300 K with shielding from the light. Spectra were referenced to the chemical shift of the residual DMSO-d6 solvent peak (2.49 ppm for 1H, 39.5 ppm for 13C). Specific techniques, their corresponding spectra and chemical shifts are in the Supporting Information (Figure S11–S18) and (Table S1–S4).

2.5 | Restrained molecular dynamics simulations of cis and trans forms of TAp and TApβ

Restrained Molecular Dynamics simulations were performed using the Macromodel software package (Schrodinger, Inc). NOE interactions obtained from NOESY spectra were implemented as distance constraints using flat-bottomed harmonic pseudopotentials. H–H distances were constrained to 3 Å (±1 Å) for those. NOE's observed to methylenes in which the diastereotopic protons could not be resolved, employed an H–C restraint of 4 Å (±1.5 Å) (Figure S19–S22). Stochastic dynamic simulations were performed using a modified AMBER force field at 300 K with an equilibration time of 50 ps and an evolution time of 200 ps, with sampling every 10 ps. The 20 conformers thus obtained formed a single cluster for each of the four structures studied, with 10 overlays shown in Figure 3.[53-56]

3 | RESULTS AND DISCUSSION

3.1 | Design of cyclic peptide scaffolds

The design of more rigid cyclic azobenzene-containing peptides was based on a previously described photo-switchable peptide, FLAp (Figure 1a).[16] It was hypothesized that a more constrained cyclic peptide would show greater differentiation in forming the β-turn when in the cis versus the trans azobenzene conformations. To rigidify the original scaffold, second generation peptides were envisaged in which the two di-alanine spacers of FLAp were replaced with either two alanine (TAp) or two of the somewhat longer β-alanine residues (TApβ). This reduction in the number of atoms between the Azo residue and the β-turn tetrapeptide should allow for investigation of the role that rigidity of the scaffold plays on the photo-control of the β-turn (Figure 1a).

3.2 | Synthesis of cyclic azo-containing peptides using a cyclonic photoreactor

To accomplish these above goals, therefore, two peptides were synthesized, one with an alanine residue on each side of the Azo residue (TAp) and another with flanking β-alanines (TApβ). Synthesis of the linear versions of the known FLAp and the newly designed TAp and Tapβ (L-FLAp, L-TAp, L-Tapβ) (Figure 1b) was performed on a glycine p-alkoxybenzyl alcohol resin using standard Fmoc-based solid phase peptide synthesis with HATU. Once the linear sequences were complete, the resin was treated with a trifluoroacetic acid cocktail to concomitantly remove the protecting groups and cleave the peptides from the resin. The linear peptides were purified to homogeneity on reverse phase HPLC to afford the three peptides in 40–50% yield (Figures S1–S3).

Once the linear peptides were obtained, these peptides were subjected to cyclization at a concentration of 1 mM using PyAOP and DIEA in DMSO (Scheme 1).[52] The L-FLAp peptide was successfully
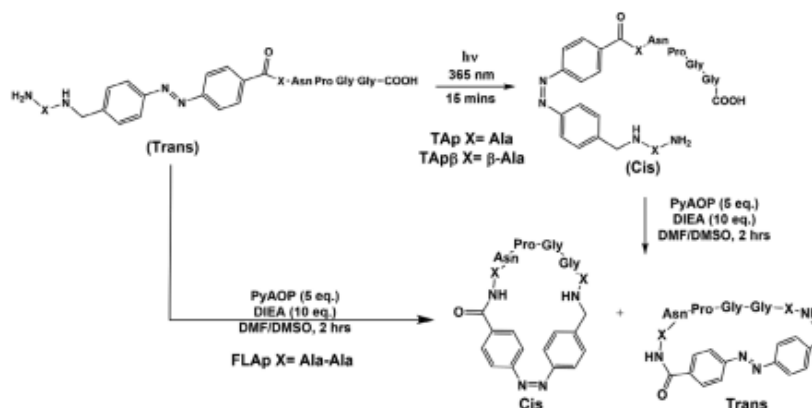
SCHEME 1 Synthesis of cyclic peptides with (TAp and Tapβ) and without (FLAp) initial photo-isomerization of the azobenzene

cyclized with the azobenzene in its trans conformation, to provide FLAp in 15% yield (Figure S4). In contrast, cyclization of L-TApβ with the trans azobenzene provided a lower 5% yield of the cyclic peptide, whereas L-TAp produced only its corresponding cyclic dimer in 10% yield (Table 1). To improve the cyclization yields, we investigated using the cis form of the azobenzene in the linear peptides to bring the C-and N-termini into closer proximity for the reaction. With this in mind, the peptides were isomerized to the cis conformation using a cyclonic ultraviolet photochemical reactor (Mini-CUPR) before cyclization using above conditions.[57] The cyclic peptides were purified to homogeneity by RP-HPLC (Figures S5, S6) and characterized by MALDI-TOF mass spectrometry (see Supplementary Information). In this way, the TAp and TApβ peptides were obtained in 35% and 60% yields, respectively (Table 1).

3.3 | Isomerization of cyclic azobenzene-containing peptides

After purification of TAp and Tapβ, the macrocycles were found to have a 60:40 and 70:30 ratio of trans:cis azobenzene, respectively, presumably due to some heating of the sample during solvent removal. These mixtures of the cyclic peptides (1 mM) were irradiated from 15 mins to 2 h in the Mini-CUPR to photo-isomerize the trans to the cis isomer. Both TAp and TApβ reached their optimal conversion after 15 min, providing 90% and 86% of the cis form, respectively (Figures S7 and S9). TAp and Tapβ were subjected to thermal isomerization to determine the rate at which the cis conformation of the Azo residue reverts to the trans isomer at 37 °C. The cis to trans ratio was quantified by RP-UPLC over the course of 7 days (Figure 2). These data demonstrate that both cyclic peptides have similar rates of thermal isomerization, and the peptides were converted to their maximum trans form (97% and 98%, respectively) after 7 days at 37 °C (Figures S8 and S10). Together, these data indicate that both peptides can be

TABLE 1 Yields of cyclic azobenzene-containing peptides with and without photoexcitation at 365 nm for isomerization

Peptide	No isomerization yield (%)	Isomerization yield (%)
FLAp	15	N/A
TAp	10 (dimer)	35
TApβ	5	60

photo-isomerized to mostly the cis form, and the cis form persists as the major isomer for about 1 day, with almost complete conversion to the trans isomer in a week. Thereby demonstrating the potential to control the cyclic peptide conformation with both light and heat.

3.4 | Structural elucidation of the cis and trans isomers of the cyclic azobenzene-containing peptides

We hypothesized that having a cis-Azo residue within the macrocycles would effectively promote a β-turn conformation within the attached tetrapeptide. In addition, the design sought to limit turn structures within the macrocycle when the Azo residue was in the trans conformation. We turned to two-dimensional NMR and molecular dynamics to probe if those features were obtained. NOESY spectroscopy was performed on both the cis and trans TAp and TApβ peptides to determine if a β-turn was present. Samples of the cis versions of each peptide were obtained by photo-isomerization for 15 mins in the Mini-CUPR as described above, and then shielded from ambient light. For samples of the trans isomers of TAp and TApβ, mixtures were used that contained 70% and 95% of the trans, respectively. NMR samples of the cyclic peptides were prepared at a 10 mM concentration in deuterated dimethylsulfoxide (DMSO-d_6).

The data from the resulting 2D spectra (NOESY, TOCSY, HMBC, and HMQC) were used to model the cis and trans conformations of
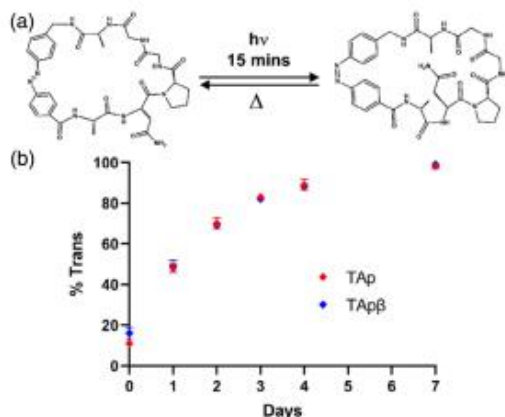
FIGURE 2 (a) The use of heat and light to interconvert the cis and trans isomers of TAP. (b) Thermal relaxation of cis-TAp and cis-TApβ to their trans isomer at 37 °C. Cis and trans percentages were determined by RP-UPLC measurements
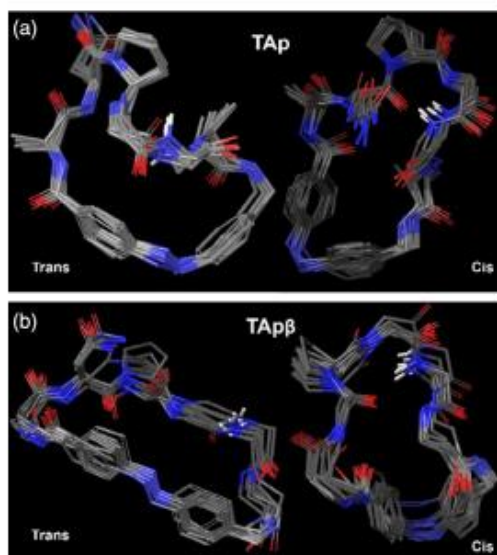

FIGURE 3 (a) Overlay of 10 time-sampled structures of the trans-TAp and cis-TAp macrocycles as obtained from restrained molecular dynamics simulations using NOESY data (top). (b) Ten overlaid time-sampled structures of trans-TApβ and cis-TApβ macrocycles (bottom) using the same methodology as in a) (Asn sidechain is hidden in cis-TApβ to facilitate visualization)

the cyclic peptides using restrained molecular dynamics as implemented in the Macromodel molecular modeling suite (Schrodinger) (see Supplementary Information and Figures S11–

S22).[53] According to our design, it was anticipated that the cis conformation of TAp and TApβ would exhibit a β-turn motif within the central tetrapeptide, while the trans isomer should have these residues in a more extended conformation. Distances were measured from the backbone carbonyl of the asparagine residue (C=O) to the amide proton of the $i + 3$ glycine (H—N) to probe for a β-turn.

For TAp, the cis version was found to contain a type II β-turn with an average C=O⋯H—N distance of 2.2 Å (Figure 3a). These same atoms in the trans isomer had a distance of 6.8 Å, indicating that no β-turn was present. The Asn-Pro-Gly-Gly tetrapeptide with trans-TAp, however, displayed a kinked structure instead of an extended conformation (Figure 3a). Additionally, the azobenzene showed distortion from planarity when in the trans form. Within the cis version of TApβ the average C=O⋯H—N distance was found to be 3.2 Å, which is within an acceptable distance for the hydrogen bond in a β-turn, and the dihedral angles are consistent with a type II' β-turn. In this case, the tetrapeptide within the trans form of TApβ was found to exist in an extended conformation. This extended conformation lacks intramolecular hydrogen bonding, whereas the kinked structure of trans-TAp has one transannular hydrogen bond and a γ-turn at the expense of a planar azobenzene. In comparison, the known trans-FLAp (Figure 1a) has a turn within the tetrapeptide and maintains the planarity of the azobenzene, while cis-FLAp forms a type II β-turn within the tetrapeptide.[16] Overall, when comparing these three macrocyclic designs, TApβ may be optimum as there is a clear structural distinction in the central tetrapeptide when the macrocycle contains a trans versus cis azobenzene isomer.

4 | CONCLUSION

Herein we describe the design and synthesis of two cyclic peptides, TAp and Tapβ, that incorporate a photo-isomerizable azobenzene moiety flanked by either alanine or β-alanine residues with a central tetrapeptide (Asn-Pro-Gly-Gly). Interestingly, the cyclization of the linear forms of these peptides was not successful when the azobenzene was in the trans form, with formation of a cyclic dimer or low yield of the macrocycle, respectively. These data suggest that the trans form of the Azo residue imparts some amount of ring strain to the macrocycle. This is in contrast to the previously described FLAp peptide that provided a modest yield for the cyclization even in the trans form. However, isomerization of the azobenzene to the cis conformation allowed for facile cyclization of both linear peptides in good to very good yields. The trans conformation of the Azo residue within these peptides was efficiently isomerized with light to the cis conformation. These cyclic peptides also showed steady thermal relaxation from the cis to trans form at 37 °C over the course of a week. Importantly, the cis and trans conformations of the peptides show clear structural differences by 2D NMR spectroscopy in conjunction with restrained molecular dynamics. The cis isomers of both TAp and TApβ demonstrated β-turn conformations. Conversely, the trans isomers do not exhibit

a β-turn structure; the tetrapeptide within TAp adopts a kinked structure, whereas this sequence within TApβ exists in a more extended conformation. The higher cyclization yield and greater structural distinction between the cis and trans forms for TApβ suggest that the βAla-Azo-βAla scaffold appears to be more promising for future use with biologically active β-turn sequences where control of receptor binding is desired.

CONFLICT OF INTEREST

Jean Chmielewski serves as an Advisory Board member of *Peptide Science*, and was excluded from the peer-review process and all editorial decisions related to the publication of this article.

DATA AVAILABILITY STATEMENT

The data that supports the findings of this study are available in the supplementary material of this article.

ORCID

Mark Lipton https://orcid.org/0000-0003-0034-0243
Jean Chmielewski https://orcid.org/0000-0003-4958-7175

REFERENCES

[1] S. Jia, W. K. Fong, B. Graham, B. J. Boyd, *Chem. Mater.* **2018**, *30*, 2873.

[2] R. Liu, Y. Yang, Q. Cui, W. Xu, R. Peng, L. Li, *Chem. Eur. J.* **2018**, *24*, 17756.

[3] S. Helmy, F. A. Leibfarth, S. Oh, J. E. Poelma, C. J. Hawker, J. R. De Alaniz, *J. Am. Chem. Soc.* **2014**, *136*, 8169.

[4] K. E. Maly, M. D. Wand, R. P. Lemieux, *J. Am. Chem. Soc.* **2002**, *124*, 7898.

[5] M. Blanco-Lomas, S. Samanta, P. J. Campos, G. A. Woolley, D. Sampedro, *J. Am. Chem. Soc.* **2012**, *134*, 6960.

[6] S. Wiedbrauk, H. Dube, *Tetrahedron Lett.* **2015**, *56*, 4266.

[7] M. Dong, A. Babalhavaeji, C. V. Collins, K. Jarrah, O. Sadovski, Q. Dai, G. A. Woolley, *J. Am. Chem. Soc.* **2017**, *139*, 13483.

[8] M. Dong, A. Babalhavaeji, S. Samanta, A. A. Beharry, G. A. Woolley, *Acc. Chem. Res.* **2015**, *48*, 2662.

[9] S. Samanta, A. A. Beharry, O. Sadovski, T. M. McCormick, A. Babalhavaeji, V. Tropepe, G. A. Woolley, *J. Am. Chem. Soc.* **2013**, *135*, 9777.

[10] A. A. Beharry, G. A. Woolley, *Chem. Soc. Rev.* **2011**, *40*, 4422.

[11] J. R. Kumita, O. S. Smart, G. A. Woolley, *Proc. Natl. Acad. Sci. USA* **2000**, *97*, 3803.

[12] J. R. Kumita, D. G. Flint, G. A. Woolley, O. S. Smart, *Faraday Discuss.* **2002**, *122*, 89.

[13] J. R. Kumita, D. G. Flint, O. S. Smart, G. A. Woolley, *Protein Eng.* **2002**, *15*, 561.

[14] D. G. Flint, J. R. Kumita, O. S. Smart, G. A. Woolley, *Chem. Biol.* **2002**, *9*, 391.

[15] E. Chen, J. R. Kumita, G. A. Woolley, D. S. Kliger, *J. Am. Chem. Soc.* **2003**, *125*, 12443.

[16] L. Ulysse, J. Cubillos, J. Chmielewski, *J. Am. Chem. Soc.* **1995**, *117*, 8466.

[17] L. G. Ulysse, J. Chmielewski, *Chem. Biol. Drug Des.* **2006**, *67*, 127.

[18] Y. Q. Yeoh, J. Yu, S. W. Polyak, J. R. Horsley, A. D. Abell, *ChemBioChem* **2018**, *19*, 2591.

[19] C. Hoppmann, S. Seedorff, A. Richter, H. Fabian, P. Schmieder, K. Rück-Braun, M. Beyermann, *Angew. Chem. Int. Ed.* **2009**, *48*, 6636.

[20] T. M. Doran, B. L. Nilsson, *Methods Mol. Biol.* **2018**, *1777*, 387.

[21] F. Nuti, C. Gellini, M. Larregola, L. Squillantini, R. Chelli, P. R. Salvi, O. Lequin, G. Pietraperzia, A. M. Papini, *Front. Chem.* **2019**, *7*, 180.

[22] M. Gascón-Moya, A. Pejoan, M. Izquierdo-Serra, S. Pittolo, G. Cabré, J. Hernando, R. Alibés, P. Gorostiza, F. Busqué, *J. Org. Chem.* **2015**, *80*, 9915.

[23] J. Kuil, L. T. M. van Wandelen, N. J. de Mol, R. M. J. Liskamp, *Bioorg. Med. Chem.* **2008**, *16*, 1393.

[24] J. Kuil, L. T. M. Van Wandelen, N. J. De Mol, R. M. J. Liskamp, *J. Pept. Sci.* **2009**, *15*, 685.

[25] M. Schütt, S. S. Krupka, A. G. Milbradt, S. Deindl, E. K. Sinner, D. Oesterhelt, C. Renner, L. Moroder, *Chem. Biol.* **2003**, *10*, 487.

[26] J. Auernheimer, C. Dahmen, U. Hersel, A. Bausch, H. Kessler, *J. Am. Chem. Soc.* **2005**, *127*, 16107.

[27] A. G. Milbradt, M. Löweneck, S. S. Krupka, M. Reif, E. K. Sinner, L. Moroder, C. Renner, *Biopolymers* **2005**, *77*, 304.

[28] K. Yamana, A. Yoshikawa, R. Noda, H. Nakano, *Nucleosides Nucleotides* **1998**, *17*, 233.

[29] K. Yamana, K. Kan, H. Nakano, *Bioorg. Med. Chem.* **1999**, *7*, 2977.

[30] M. Erdélyi, A. Karlén, A. Gogoll, *Chem. Eur. J.* **2005**, *12*, 403.

[31] Y. Zhang, Y. Zhang, G. Song, Y. He, X. Zhang, Y. Liu, H. Ju, *Angew. Chem. Int. Ed.* **2019**, *58*, 18207.

[32] G. M. Murawska, C. Poloni, N. A. Simeth, W. Szymanski, B. L. Feringa, *Chem. Eur. J.* **2019**, *25*, 4965.

[33] L. Ulysse, J. Chmielewski, *Bioorg. Med. Chem. Lett.* **1994**, *4*, 2145.

[34] J. Wachtveitl, S. Spörlein, H. Satzger, B. Fonrobert, C. Renner, R. Behrendt, D. Oesterhelt, L. Moroder, W. Zinth, *Biophys. J.* **2004**, *86*, 2350.

[35] S. Rudolph-Böhner, M. Krüger, D. Oesterhelt, L. Moroder, T. Nägele, J. Wachtveitl, *J. Photochem. Photobiol., A* **1997**, *105*, 235.

[36] R. Behrendt, C. Renner, M. Schenk, F. Wang, J. Wachtveitl, D. Oesterhelt, L. Moroder, *Angew. Chem. Int. Ed.* **1999**, *38*, 2771.

[37] C. Renner, R. Behrendt, S. Spörlein, J. Wachtveitl, L. Moroder, *Biopolymers* **2000**, *54*, 578.

[38] C. Renner, R. Behrendt, N. Heim, L. Moroder, *Biopolymers* **2002**, *63*, 382.

[39] G. Ruiz-Gómez, J. D. A. Tyndall, B. Pfeiffer, G. Abbenante, D. P. Fairlie, *Chem. Rev.* **2010**, *110*, PR1.

[40] L. R. Whitby, D. L. Boger, *Acc. Chem. Res.* **2012**, *45*, 1698.

[41] M. C. Zaccaro, B. L. Hong, M. Pattarawarapan, Z. Xia, A. Caron, P. J. L'Heureux, Y. Bengio, K. Burgess, H. U. Saragovi, *Chem. Biol.* **2005**, *12*, 1015.

[42] B. Eckhardt, W. Grosse, L. O. Essen, A. Geyer, *Proc. Natl. Acad. Sci. USA* **2010**, *107*, 18336.

[43] M. Pelay-Gimeno, A. Glas, O. Koch, T. N. Grossmann, *Angew. Chem. Int. Ed.* **2015**, *54*, 8896.

[44] A. Glas, D. Bier, G. Hahne, C. Rademacher, C. Ottmann, T. N. Grossmann, *Angew. Chem. Int. Ed.* **2014**, *53*, 2489.

[45] K. Suat, S. Jois, *Curr. Pharm. Des.* **2003**, *9*, 1209.

[46] J. Zhang, C. Xiong, J. Ying, W. Wang, V. J. Hruby, *Org. Lett.* **2003**, *5*, 3115.

[47] S. Deike, S. Rothemund, B. Voigt, S. Samantray, B. Strodel, W. H. Binder, *Bioorg. Chem.* **2020**, *101*, 104012.

[48] F. Brahimi, A. Malakhov, H. B. Lee, M. Pattarawarapan, L. Ivanisevic, K. Burgess, H. U. Saragovi, *Peptides* **2009**, *30*, 1833.

[49] F. Brahimi, E. Ko, A. Malakhov, K. Burgess, H. U. Saragovi, *PLoS One* **2014**, *9*, e89617.

[50] T. Shimizu, *Bull. Chem. Soc. Jpn.* **2018**, *91*, 623.

[51] K. Day, J. D. Schneible, A. T. Young, V. A. Pozdin, G. Van Den Driessche, L. A. Gaffney, R. Prodromou, D. O. Freytes, D. Fourches, M. Daniele, S. Menegatti, *J. Mater. Chem. B* **2020**, *8*, 7413.

[52] F. Albericio, M. Cases, J. Alsina, S. A. Triolo, L. A. Carpino, S. A. Kates, *Tetrahedron Lett.* **1997**, *38*, 4853.

[53] F. Mohamadi, N. G. J. Richards, W. C. Guida, R. Liskamp, M. Lipton, C. Caufield, G. Chang, T. Hendrickson, W. C. Still, *J. Comput. Chem.* **1990**, *11*, 440.

[54] W. F. Van Gunsteren, H. J. C. Berendsen, *Mol. Simul.* **1988**, *1*, 173.

[55] S. J. Weiner, P. A. Kollman, U. C. Singh, D. A. Case, C. Ghio, G. Alagona, S. Profeta, P. Weiner, *J. Am. Chem. Soc.* **1984**, *106*, 765.

[56] S. J. Weiner, P. A. Kollman, D. T. Nguyen, D. A. Case, *J. Comput. Chem.* **1986**, *7*, 230.

[57] G. S. Eakins, M. L. Niedrauer, M. A. Lipton, U.S. *Patent.* **2020**, *63*, 491.

SUPPORTING INFORMATION

Additional supporting information may be found in the online version of the article at the publisher's website.